arXiv:1601.06393v1 [hep-ph] 24 Jan 2016

Lepton Mixing Predictions from Infinite Group Series $D^{(1)}_{9n,3n}$ with Generalized CP

Cai-Chang Li*, Chang-Yuan Yao†, Gui-Jun Ding‡

Department of Modern Physics, University of Science and Technology of China, Hefei, Anhui 230026, China

Abstract

We have performed a comprehensive analysis of the type D group $D^{(1)}_{9n,3n}$ as flavor symmetry and the generalized CP symmetry. All possible residual symmetries and their consequences for the prediction of the mixing parameters are studied. We find that only one type of mixing pattern is able to accommodate the measured values of the mixing angles in both "direct" and "variant of semidirect" approaches, and four types of mixing patterns are phenomenologically viable in the "semidirect" approach. The admissible values of the mixing angles as well as CP violating phases are studied in detail for each case. It is remarkable that the first two smallest $D^{(1)}_{9n,3n}$ groups with $n = 1, 2$ can fits the experimental data very well. The phenomenological predictions for neutrinoless double beta decay are discussed.

*E-mail: lcc0915@mail.ustc.edu.cn
†E-mail: phyman@mail.ustc.edu.cn
‡E-mail: dinggj@ustc.edu.cn

1 Introduction

The precise measurement of the reactor mixing angle θ_{13} [1–5] encourages the pursuit of the still missing results on leptonic CP violation and neutrino mass ordering as well as the characteristic neutrino nature. Some low-significance hints for a maximally CP-violating value of the Dirac phase $\delta_{CP} \simeq 3\pi/2$ have been observed [6]. The global fits to lepton mixing parameters [7–9] also provide weak evidence for the existence of Dirac type CP violation in neutrino oscillation. In the case that neutrinos are Majorana particles, two more Majorana CP phases α_{21} and α_{31} would be present, and they are crucial to the neutrinoless double beta decay process. However, the present experimental data don't impose any constraint on the values of the Majorana phases.

Finite discrete non-abelian flavor symmetries have been widely used to make predictions for lepton flavor mixing. Assuming the original flavor symmetry group is spontaneously broken to distinct abelian residual symmetries in the neutrino and charged lepton sectors at a low energy scale, one can then determine mixing patterns from the residual symmetries and the structure of discrete flavor symmetry groups. Please see Refs. [10–12] for review on discrete flavor symmetries and the application in model building. For Majorana neutrinos, if the residual symmetries of the charged lepton and neutrino mass matrices originate from a finite flavor group, the lepton mixing matrix would be fully determined by residual symmetries up to independent row and column permutations. It turns out that the possible forms of the PMNS matrix are strongly constrained in this scenario such that the mixing patterns compatible with the data are of trimaximal form, and the Dirac CP phase is predicted to be 0 or π [13]. The same conclusion is reached for neutrinos being Dirac particles [14]. We note that the neutrino masses are not constrained in this approach and consequently the both Majorana phases α_{21} and α_{31} are undetermined. Their values can be fixed by considering a specific model. If the residual flavor symmetries of the neutrino and charged lepton mass matrix are partially contained in the underlying flavor group, the PMNS matrix would contains at least two free continuous parameters. As a result, the predictivity of the model would be lessened to a certain extent.

Besides the extensively discussed residual flavor symmetries, the neutrino and charged lepton mass matrices also admit residual CP transformations, and the residual CP symmetries can be generated by performing two residual CP transformations [15–17]. Analogous to residual flavor symmetries, the residual CP transformations can also constraint the lepton flavor mixing in particular the CP violating phases [15]. The simplest nontrivial CP transformation is known as $\mu - \tau$ reflection which gives rise to maximal atmospheric mixing and maximal Dirac phase [18–20]. The deviation from maximal atmospheric mixing and non-maximal Dirac CP violation can be naturally obtained from the so-called generalized $\mu - \tau$ reflection [21].

Recently the flavor symmetry has been extended to combine with the generalized CP symmetry [22,23]. This can lead to rather predictive scenario where both mixing angles and CP phases determined by a small number of (frequently only one) input parameters [22]. In this case, the CP transformation matrix is generally non-diagonal and it is also called generalized CP. The generalized CP symmetry and the corresponding constraints on quark mass matrices have been exploited about thirty year ago [24, 25]. In this case the interplay between CP and flavor symmetries has to be carefully treated in order to make the theory consistent [22, 23, 26]. There have been some models and model independent analysis of CP and flavor symmetries, such as A_4 [27], S_4 [22, 28–32], $\Delta(27)$ [33], $\Delta(48)$ [34], A_5 [35–37], $\Delta(96)$ [38], and the group series $\Delta(3n^2)$ [39, 40] and $\Delta(6n^2)$ [39, 41, 42] for general integer n. It is notable that smaller group for instance A_4 [27], S_4 [22, 28–32] and A_5 [35–37] can already describe the experimentally measured values of the mixing angles, and the Dirac CP

phase is predicted to be conserved or maximal while the Majorana phases are trivial. On the other hand, all the three CP violating phases generally depend on the free real parameter θ for $\Delta(3n^2)$ [39, 40] and $\Delta(6n^2)$ [39, 41, 42] flavor symmetries.

In the present work, we shall thoroughly analyze the lepton mixing patterns which can be obtained from the breaking of $D^{(1)}_{9n,3n}$ flavor symmetry and generalized CP. All possible residual symmetries in the "direct", "semidirect" and "variant of semidirect" approaches and their consequences for the prediction of the mixing parameters are studied. We shall perform a detailed numerical analysis for all the possible mixing patterns. The admissible values of the mixing parameters for each n and the possible values of the effective mass $|m_{ee}|$ will be explored.

The outline of this paper is as follows. In section 2 we find the class-inverting automorphism of the $D^{(1)}_{9n,3n}$ group and the corresponding physically well-defined generalized CP transformations are determined by solving the consistency condition. In section 3 we review the approach to determining the lepton flavor mixing from residual flavor and CP symmetries of the neutrino and the charged lepton sectors. All possible residual symmetries and the consequences for the prediction of the flavor mixing are studied in the method of the direct approach in section 4. The PMNS matrix is determined to be of the trimaximal form, both Dirac phase δ_{CP} and the Majorana phase α_{31} are conserved, and the values of α_{21} are integer multiple of $2\pi/(3n)$. We investigate the possible mixing patterns which can be derived from the semidirect approach and variant of semidirect approach in section 5 and section 6. The analytical expressions of the PMNS matrices, mixing angles and CP invariants are presented, the admissible values of the mixing angles and CP violation phases are analyzed numerically in detail, and phenomenological predictions for neutrinoless double beta decay are studied. For the lowest order $D^{(1)}_{9n,3n}$ group with $n = 1, 2$, we find all the mixing patterns that can describe the experimentally measured values of the mixing angles, and a χ^2 analysis is performed. Finally we summarize and present our conclusions in section 7. The group theory of $D^{(1)}_{9n,3n}$ is presented in Appendix A including the conjugacy classes, the irreducible representations, the character table, the Kronecker products and the Clebsch-Gordan coefficients.

2 Generalized CP consistent with $D^{(1)}_{9n,3n}$ family symmetry

The finite subgroups of $SU(3)$ have been systematically classified by mathematicians [43] (see Refs. [44–46] for recent work). It is well-established that all discrete subgroups of $SU(3)$ can be divided into five categories: type A, type B, type C, type D, and type E [45, 46]. The type D group turns out to be particularly significant in flavor symmetry theory [13, 47]. Type D group is isomorphic to $(Z_m \times Z_n) \rtimes S_3$, and it can be generated by four generators a, b, c and d subject to the following rules [45]:

$$\begin{aligned} a^3 = b^2 = (ab)^2 = c^m = d^n = 1, \quad cd = dc, \\ aca^{-1} = c^k d, \quad ada^{-1} = c^{-m/n} d^{-(k+1)}, \\ bcb^{-1} = cd, \quad bdb^{-1} = d^{-1}\,. \end{aligned} \tag{2.1}$$

It is found that the type D group exists only for [45]

$$k = 0, m = n \qquad \text{or} \qquad k = 1, m = 3n\,. \tag{2.2}$$

In the case of $k = 0$, $m = n$, the corresponding group denoted as $D^{(0)}_{n,n}$ is exactly the well-known $\Delta(6n^2)$ group [48]. For another case of $k = 1$, $m = 3n$, the corresponding

n	G_f	GAP-Id	Inn(G_f)	Out(G_f)
1	$D^{(1)}_{9,3}$	[162,14]	$((Z_3 \times Z_3) \rtimes Z_3) \rtimes Z_2$	Z_6
2	$D^{(1)}_{18,6}$	[648,259]	$((Z_6 \times Z_6) \rtimes Z_3) \rtimes Z_2$	Z_6
3	$D^{(1)}_{27,9}$	[1458,659]	$((Z_9 \times Z_9) \rtimes Z_3) \rtimes Z_2$	Z_{18}

Table 1: The automorphism groups of the $D^{(1)}_{9n,3n}$ group with $n = 1, 2, 3$, where Inn(G_f) and Out(G_f) denote inner automorphism group and outer automorphism group of G_f respectively. Note that each of these three groups has a unique class-inverting outer automorphism.

type D group denoted as $D^{1)}_{3n,n}$ is isomorphic to $Z_3 \times \Delta(6n^2)$ if n is not divisible by 3 [45]. Therefore the representation of $D^{(1)}_{3n,n}$ can be obtained by multiplying the representation matrices of $\Delta(6n^2)$ with 1, $e^{2\pi i/3}$ and $e^{4\pi i/4}$ for $3 \nmid n$. As a consequence, the $D^{(1)}_{3n,n}$ group for $3 \nmid n$ would give rise to the same set of lepton flavor mixing as $\Delta(6n^2)$ group no matter whether the generalized CP symmetry is considered or not. The $\Delta(6n^2)$ as flavor symmetry group has been comprehensively explored in the literature [39, 41, 47], we shall focus on the second independent type D infinite series of groups $D^{(1)}_{9n,3n}$ where n is any positive integer. It is remarkable that $D^{(1)}_{9n,3n}$ can generate experimentally viable lepton and quark mixing simultaneously [14]. In the present work, we shall include the generalized CP symmetry compatible with $D^{(1)}_{9n,3n}$ and investigate its predictions for lepton mixing angles and CP violating phases. The group theory of $D^{(1)}_{9n,3n}$, its irreducible representations and the Clebsch-Gordan coefficients are presented in Appendix A.

It is highly nontrivial to introduce the generalized CP symmetry in the presence of a discrete flavor symmetry G_f. In order to consistently combine the generalized CP symmetry with flavor symmetry, the following consistency condition has to be fulfilled [22, 23, 26],

$$X_{\mathbf{r}} \rho^*_{\mathbf{r}}(g) X^\dagger_{\mathbf{r}} = \rho_{\mathbf{r}}(g'), \quad g, g' \in G_f \,, \tag{2.3}$$

where $\rho_{\mathbf{r}}(g)$ is the representation matrix of the element g in the irreducible representation $\mathbf{r}$ of G_f, and $X_{\mathbf{r}}$ is the generalized CP transformation. Obviously the CP transformation $X_{\mathbf{r}}$ maps g into another group element g'. Therefore the generalized CP symmetry corresponds the automorphism group of G_f. Moreover, it was shown that the physically well-defined CP transformations should be given by class-inverting automorphism of G_f [26]. We have exploited the computer algebra system GAP [49] to calculate the automorphism group of the first three $D^{(1)}_{9n,3n}$ groups with $n = 1, 2, 3$, the results are listed in table 1. Notice that larger $D^{(1)}_{9n,3n}$ group for $n \geq 4$ is not stored in GAP at present. We see that the automorphism group of $D^{(1)}_{9n,3n}$ is quite complex but each one of $D^{(1)}_{9,3}$, $D^{(1)}_{18,6}$ and $D^{(1)}_{27,9}$ has a unique class-inverting outer automorphism. Furthermore, we find a generic class-inverting automorphism u of the $D^{(1)}_{9n,3n}$ group, and its actions on the generators a, b, c, d are as follows

$$a \overset{u}{\longmapsto} a, \quad b \overset{u}{\longmapsto} b, \quad c \overset{u}{\longmapsto} c^{-1}, \quad d \overset{u}{\longmapsto} d^{-1} \,. \tag{2.4}$$

It is easy to check that u indeed maps each element into the class of its inverse element for any value of the parameter n. We denote the physical CP transformation corresponding to the automorphism u as $X_{\mathbf{r}}(u)$, and its explicit form is determined by the following consistency equations:

$$X_{\mathbf{r}}(u)\, \rho^*_{\mathbf{r}}(a) X^\dagger_{\mathbf{r}}(u) = \rho_{\mathbf{r}}(u(a)) = \rho_{\mathbf{r}}(a) \,,$$

$$
\begin{aligned}
&X_{\mathbf{r}}\left(u\right)\rho^{*}_{\mathbf{r}}(b)X^{\dagger}_{\mathbf{r}}\left(u\right)=\rho_{\mathbf{r}}\left(u\left(b\right)\right)=\rho_{\mathbf{r}}\left(b\right)\,,\\
&X_{\mathbf{r}}\left(u\right)\rho^{*}_{\mathbf{r}}(c)X^{\dagger}_{\mathbf{r}}\left(u\right)=\rho_{\mathbf{r}}\left(u\left(c\right)\right)=\rho_{\mathbf{r}}\left(c^{-1}\right)\,,\\
&X_{\mathbf{r}}\left(u\right)\rho^{*}_{\mathbf{r}}(d)X^{\dagger}_{\mathbf{r}}\left(u\right)=\rho_{\mathbf{r}}\left(u\left(d\right)\right)=\rho_{\mathbf{r}}\left(d^{-1}\right)\,.
\end{aligned}
\tag{2.5}
$$

In our working basis shown in Appendix A, the representation matrices of a and b are real while the representation matrices of c and d are complex and diagonal for any irreducible representations of $D^{(1)}_{9n,3n}$. Therefore the CP transformation $X_{\mathbf{r}}(u)$ is a unit matrix, i.e.

$$
X_{\mathbf{r}}\left(u\right)=\mathbb{1}_{\mathbf{r}}\,. \tag{2.6}
$$

Given this CP transformation $X_{\mathbf{r}}(u)$, the matrix $\rho_{\mathbf{r}}(g)X_{\mathbf{r}}(u)=\rho_{\mathbf{r}}(g)$ is also an admissible CP transformation for any $g\in D^{(1)}_{9n,3n}$. It corresponds to performing a conventional CP transformation followed by a group transformation $\rho_{\mathbf{r}}(g)$. As a consequence, we conclude that the generalized CP transformation compatible with the $D^{(1)}_{9n,3n}$ family symmetry is of the same form as the flavor symmetry transformation in our basis, i.e.

$$
X_{\mathbf{r}}=\rho_{\mathbf{r}}(g),\quad g\in D^{(1)}_{9n,3n}\,. \tag{2.7}
$$

Note that other possible CP transformations can also be defined if a model contains only a subset of irreducible representations. Lepton mixing can be derived from the remnant symmetries in the charged lepton and neutrino mass matrices, while the mechanism of symmetry breaking is irrelevant. The basic procedure and the resulting master formulae are given in Refs. [15, 16, 27, 28, 41]. In the following, we shall consider all possible remnant symmetries of the neutrino and charged lepton sectors and discuss the predictions for the PMNS matrix and the lepton mixing parameters.

3 Framework

In the present work, the family symmetry is taken to be $D^{(1)}_{9n,3n}$, and the generalized CP symmetry is considered in order to predict the lepton mixing parameters including the CP violating phases. Without loss of generality, we assume that the three left-handed leptons transform as a triplet $\mathbf{3}_{1,0}$ under $D^{(1)}_{9n,3n}$. For brevity we shall denote the faithful irreducible representation $\mathbf{3}_{1,0}$ as $\mathbf{3}$. The representation matrices of the generators a, b, c and d in $\mathbf{3}_{1,0}$ are given in Eq. (A.35). The light neutrinos are assumed to be Majorana particles. From the bottom-up perspective, the most general symmetry of a generic charged lepton mass matrices is $U(1)\times U(1)\times U(1)$, which has finite subgroups isomorphic to a cyclic group Z_m for any integer m or a direct product of several cyclic groups [14–16]. On the other hand, the largest possible symmetry of the neutrino mass matrix is $Z_2\times Z_2$ [14–16, 50]. Moreover the neutrino and charged lepton mass matrices are invariant under a set of CP transformations, and both the $U(1)\times U(1)\times U(1)$ symmetry group of the charged-lepton mass term and the $Z_2\times Z_2$ symmetry of the neutrino mass terms can be generated by performing two CP symmetry transformations [15, 16]. Conversely, the lepton mass matrices are strongly constrained by the postulated remnant symmetry such that the lepton mixing matrix can be derived from the remnant symmetries in the charged lepton and neutrino sectors, while the mechanism of dynamically realizing the assumed remnant symmetries is irrelevant [15, 16]. From the view of the top-down method, the remnant flavor and CP symmetries of the neutrino and charged lepton mass matrices may originate from certain symmetry group implemented at high energy scales. In the present work, both flavor symmetry $D^{(1)}_{9n,3n}$ and the generalized CP are imposed, i.e., the parent symmetry is $D^{(1)}_{9n,3n}\rtimes H_{CP}$, where H_{CP} denotes the generalized

CP transformations consistent with $D^{(1)}_{9n,3n}$ and it is given by Eq. (2.7). $D^{(1)}_{9n,3n} \rtimes H_{CP}$ is assumed to be broken down into $G_l \rtimes H^l_{CP}$ and $G_\nu \times H^\nu_{CP}$ in the charged lepton and neutrino sectors respectively. The allowed forms of the neutrino and charged lepton mass matrices are constrained by the remnant symmetries, and subsequently we can diagonalize them to get the PMNS matrix.

The requirement that a subgroup $G_l \rtimes H^l_{CP}$ is preserved at low energies entails that the combination $m_l^\dagger m_l$ has to fulfill

$$\begin{aligned} &\rho^\dagger_{\mathbf{3}}(g_l) m_l^\dagger m_l \rho_{\mathbf{3}}(g_l) = m_l^\dagger m_l, \quad g_l \in G_l, \\ &X^\dagger_{l\mathbf{3}} m_l^\dagger m_l X_{l\mathbf{3}} = \left(m_l^\dagger m_l\right)^*, \quad X_{l\mathbf{3}} \in H^l_{CP}\,, \end{aligned} \tag{3.1}$$

where the charged lepton mass matrix m_l is given in the convention $l^c m_l l$. The hermitian combination $m_l^\dagger m_l$ is diagonalized by the unitary transformation U_l with $U_l^\dagger m_l^\dagger m_l U_l = \mathrm{diag}(m_e^2, m_\mu^2, m_\tau^2)$. The three charged leptons have distinct masses $m_e \neq m_\mu \neq m_\tau$. From Eq. (3.1), it is straightforward to derive that the remnant symmetry $G_l \rtimes H^l_{CP}$ leads to the following constraints on U_l

$$\begin{aligned} &U_l^\dagger \rho_{\mathbf{3}}(g_l) U_l = \rho^{diag}_{\mathbf{3}}(g_l), \quad g_l \in G_l, \\ &U_l^\dagger X_{l\mathbf{3}} U_l^* = X^{diag}_{l\mathbf{3}}, \quad X_{l\mathbf{3}} \in H^l_{CP}\,, \end{aligned} \tag{3.2}$$

where both $\rho^{diag}_{\mathbf{3}}(g_l)$ and $X^{diag}_{l\mathbf{3}}$ are diagonal phase matrices. As a consequence, we see that U_l also diagonalizes the residual flavor symmetry transformation matrix $\rho_{\mathbf{3}}(g_l)$, the residual CP transformation $X_{l\mathbf{3}}$ is a symmetric matrix, and the following restricted consistency condition should be satisfied [32],

$$X_{l\mathbf{r}} \rho^*_{\mathbf{r}}(g_l) X^{-1}_{l\mathbf{r}} = \rho_{\mathbf{r}}(g_l^{-1}), \qquad g_l \in G_l,\ X_{l\mathbf{r}} \in H^l_{CP}\,. \tag{3.3}$$

In the same fashion, the neutrino mass matrix is invariant under the action of the elements of the residual subgroup $G_\nu \times H^\nu_{CP}$:

$$\begin{aligned} &\rho^T_{\mathbf{3}}(g_\nu) m_\nu \rho_{\mathbf{3}}(g_\nu) = m_\nu, \qquad g_\nu \in G_\nu, \\ &X^T_{\nu\mathbf{3}} m_\nu X_{\nu\mathbf{3}} = m_\nu^*, \qquad\quad X_{\nu\mathbf{3}} \in H^\nu_{CP}\,. \end{aligned} \tag{3.4}$$

We denote the unitary diagonalization matrix of m_ν as U_ν fulfilling $U_\nu^T m_\nu U_\nu = \mathrm{diag}\,(m_1, m_2, m_3)$. Then U_ν would be subject to the following constraints from the postulated residual symmetry [15–17]:

$$\begin{aligned} &U_\nu^\dagger \rho_{\mathbf{3}}(g_\nu) U_\nu = \mathrm{diag}(\pm 1, \pm 1, \pm 1), \\ &U_\nu^\dagger X_{\nu\mathbf{3}} U_\nu^* = \mathrm{diag}(\pm 1, \pm 1, \pm 1)\,, \end{aligned} \tag{3.5}$$

where the "$\pm$" signs can be chosen independently. Therefore the residual CP transformation $X_{\nu\mathbf{3}}$ is a symmetric unitary matrix as well, and the restricted consistency condition on the neutrino sector takes the form [15–17, 22]:

$$X_{\nu\mathbf{r}} \rho^*_{\mathbf{r}}(g_\nu) X^{-1}_{\nu\mathbf{r}} = \rho_{\mathbf{r}}(g_\nu), \qquad g_\nu \in G_\nu,\ X_{\nu\mathbf{r}} \in H^\nu_{CP}\,. \tag{3.6}$$

Obviously $X_{\nu\mathbf{r}}$ maps any element g_ν of the neutrino residual flavor symmetry G_ν into itself. Hence the mathematical structure of the remnant subgroup comprising G_ν and H^ν_{CP} is generally a direct product instead of a semidirect product. Given a pair of well-defined remnant symmetries $G_l \rtimes H^l_{CP}$ and $G_\nu \times H^\nu_{CP}$ for which the consistency equations in Eqs. (3.3, 3.6) are fulfilled, the allowed forms of the mass matrices $m_l^\dagger m_l$ and m_ν can be determined

from Eqs. (3.1, 3.4), and subsequently the prediction for the PMNS matrix $U_{\rm PMNS}=U_l^\dagger U_\nu$ can be obtained by diagonalizing $m_l^\dagger m_l$ and m_ν.

For two pair of remnant symmetry subgroups $\left\{G_l \rtimes H_{CP}^l, G_\nu \times H_{CP}^\nu\right\}$ and $\left\{G_l' \rtimes H_{CP}^{l'}, G_\nu' \times H_{CP}^{\nu'}\right\}$, if G_l, G_ν and G_l', G_ν' are related by a similarity transformation, for example if they are conjugate,

$$G_l'=hG_lh^{-1}, \qquad G_\nu'=hG_\nu h^{-1}, \qquad h\in D_{9n,3n}^{(1)}\,. \tag{3.7}$$

The remnant CP would also be related by

$$H_{CP}^{l'}=\rho_{\mathbf{r}}(h)H_{CP}^l\rho_{\mathbf{r}}^T(h), \qquad H_{CP}^{\nu'}=\rho_{\mathbf{r}}(h)H_{CP}^\nu\rho_{\mathbf{r}}^T(h) \tag{3.8}$$

in order to fulfill the consistency conditions in Eqs. (3.3, 3.6). That is to say the elements of $H_{CP}^{l'}$ and $H_{CP}^{\nu'}$ are given by $\rho_{\mathbf{r}}(h)X_{l\mathbf{r}}\rho_{\mathbf{r}}^T(h)$ and $\rho_{\mathbf{r}}(h)X_{\nu\mathbf{r}}\rho_{\mathbf{r}}^T(h)$ respectively, where $X_{\nu\mathbf{r}}\in H_{CP}^\nu$ and $X_{l\mathbf{r}}\in H_{CP}^l$. Notice that all the possible remnant CP transformations compatible with the remnant flavor symmetry have been considered in this work. Hence if $G_l \rtimes H_{CP}^l$ and $G_\nu \times H_{CP}^\nu$ fix the charged lepton and neutrino mass matrices to be $m_l^\dagger m_l$ and m_ν, then $m_l'^\dagger m_l' \equiv \rho_{\mathbf{3}}(h)m_l^\dagger m_l\rho_{\mathbf{3}}^\dagger(h)$ and $m_\nu' \equiv \rho_{\mathbf{3}}^*(h)m_\nu\rho_{\mathbf{3}}^\dagger(h)$ would be invariant under the remnant symmetries $G_l'\rtimes H_{CP}^{l'}$ and $G_\nu'\times H_{CP}^{\nu'}$ respectively. As a result, two pair of remnant symmetries $\left\{G_l \rtimes H_{CP}^l, G_\nu \times H_{CP}^\nu\right\}$ and $\left\{G_l' \rtimes H_{CP}^{l'}, G_\nu' \times H_{CP}^{\nu'}\right\}$ would yield the same results for the PMNS matrix $U_{\rm PMNS}$. In this work, we shall perform a comprehensive analysis of the mixing patterns which can be derived from the group $D_{9n,3n}^{(1)}\rtimes H_{CP}$. It is sufficient to only analyze a few representative remnant symmetries which give rise to different results for $U_{\rm PMNS}$ and lepton mixing parameters, as other possible choices for the remnant symmetry groups are related to the representative ones by similarity transformation and consequently no new results are obtained.

4 Lepton mixing from direct approach

In the direct approach, the residual flavor symmetry G_ν is a Klein four subgroup, and the residual flavor symmetry G_l is a cyclic group Z_m with index $m\geq 3$ or a product of cyclic groups. We assume that the residual flavor symmetry group G_l can distinguish the three generations of charged lepton. In other words, the restricted representation of the triplet representation $\mathbf{3}$ on G_l should decompose into three inequivalent 1-dimensional representations of G_l. From Eq. (3.1) and Eq. (3.2), we see that U_l not only diagonalizes the mass matrix $m_l^\dagger m_l$ but also the residual flavor symmetry transformation matrix $\rho_{\mathbf{3}}(g_l)$ with $g_l\in G_l$. As a result, the requirement that $U_l^\dagger\rho_{\mathbf{3}}(g_l)U_l=\rho_{\mathbf{3}}^{diag}(g_l)$ is diagonal allows us to determine U_l and no knowledge of $m_l^\dagger m_l$ is necessary. Notice that the remnant CP invariant condition in Eq. (3.1) is automatically satisfied, the reason is that the residual CP transformation $X_{l\mathbf{3}}$ has to be compatible with residual flavor symmetry and its allowed form is strongly constrained by the restricted consistency condition of Eq. (3.3).

As shown in the Appendix A, the group structure of the $D_{9n,3n}^{(1)}$ has been studied in detail. The residual subgroup G_l is an abelian subgroup, and it can be generated by the generator c^sd^t, bc^sd^t, ac^sd^t, $a^2c^sd^t$, abc^sd^t or $a^2bc^sd^t$ with $s=0,1,\ldots,9n-1, t=0,1,\ldots,3n-1$. The diagonalization of $\rho_{\mathbf{3}}(g_l)$ determines the unitary transformation U_l up to permutations and phases of the column vectors if $\rho_{\mathbf{3}}(g_l)$ has non-degenerate eigenvalues, where g_l can be taken to be the generator of G_l. The explicit form of U_l for different G_l and the corresponding remnant CP transformations compatible with G_l are summarized in table 2. If the eigenvalues of $\rho_{\mathbf{3}}(g_l)$ are degenerate so that its diagonalization matrix U_l can not be determined uniquely, we would extend G_l from a single cyclic subgroup to a product of cyclic groups,

G_l	U_l	Constraints	H^l_{CP}
$\langle c^s d^t\rangle$	$U_l^{(1)}=\begin{pmatrix}1&0&0\\0&1&0\\0&0&1\end{pmatrix}$	$t\neq 0$ $s-t\neq 0 \bmod(3n)$ $s-2t\neq 0 \bmod(3n)$	$\{c^\gamma d^\delta\}$
$\langle bc^s d^t\rangle$	$U_l^{(2)}=\frac{1}{\sqrt{2}}\begin{pmatrix}\sqrt{2}&0&0\\0&-e^{\frac{i\pi(2t-s)}{3n}}&e^{\frac{i\pi(2t-s)}{3n}}\\0&1&1\end{pmatrix}$	$s\neq 0,3n,6n$	$\{c^{2t-s+2\delta+3n\tau}d^\delta,$ $bc^{2\delta+3n\tau}d^\delta\}$
$\langle ac^s d^t\rangle$	$U_l^{(3)}=\frac{1}{\sqrt{3}}\begin{pmatrix}e^{-\frac{2i\pi s}{9n}}&\omega^2 e^{-\frac{2i\pi s}{9n}}&\omega e^{-\frac{2i\pi s}{9n}}\\e^{\frac{2i\pi(3t-2s)}{9n}}&\omega e^{\frac{2i\pi(3t-2s)}{9n}}&\omega^2 e^{\frac{2i\pi(3t-2s)}{9n}}\\1&1&1\end{pmatrix}$	—	$\{bc^{-2t+3n\tau}d^{-t},$ $abc^{s-2t+3n\tau}d^{s-2t},$ $a^2bc^{t-s+3n\tau}\}$
$\langle a^2c^s d^t\rangle$	$U_l^{(3')}=\frac{1}{\sqrt{3}}\begin{pmatrix}e^{\frac{2i\pi(3t-2s)}{9n}}&\omega e^{\frac{2i\pi(3t-2s)}{9n}}&\omega^2 e^{\frac{2i\pi(3t-2s)}{9n}}\\e^{\frac{2i\pi(3t-s)}{9n}}&\omega^2 e^{\frac{2i\pi(3t-s)}{9n}}&\omega e^{\frac{2i\pi(3t-s)}{9n}}\\1&1&1\end{pmatrix}$	—	$\{bc^{2(t-s)+3n\tau}d^{t-s},$ $abc^{-t+3n\tau}d^{-t},$ $a^2bc^{2t-s+3n\tau}\}$
$\langle abc^s d^t\rangle$	$U_l^{(4)}=\frac{1}{\sqrt{2}}\begin{pmatrix}e^{\frac{i\pi(t-s)}{3n}}&0&-e^{\frac{i\pi(t-s)}{3n}}\\0&\sqrt{2}&0\\1&0&1\end{pmatrix}$	$s-3t\neq 0,3n,6n$	$\{c^\gamma d^{\gamma+s-t}, abc^\gamma d^\gamma\}$
$\langle a^2bc^s d^t\rangle$	$U_l^{(5)}=\frac{1}{\sqrt{2}}\begin{pmatrix}-e^{-\frac{i\pi t}{3n}}&e^{-\frac{i\pi t}{3n}}&0\\1&1&0\\0&0&\sqrt{2}\end{pmatrix}$	$2s-3t\neq 0,3n,6n$	$\{c^\gamma d^{-t}, a^2bc^\gamma\}$

Table 2: The form of U_l for different residual subgroup G_l generated by a single element g, and here we denote $G_l=\langle g\rangle$. H^l_{CP} is the residual CP transformations consistent with G_l. The allowed values of the parameters s, t, γ, δ and τ are $t,\delta=0,1,...3n-1$, $s,\gamma=0,1,...,9n-1$ and $\tau=0,1,2$. The parameter ω is the cube root of unit with $\omega=e^{2\pi i/3}$. Note that because $\left(ac^{2s-3t}d^{s-t}\right)^2=a^2c^sd^t$ holds, the U_l for $G_l=\langle a^2c^sd^t\rangle$ can be obtained from the that corresponding to $G_l=\langle ac^sd^t\rangle$ by the replacement $s\to 2s-3t$ and $t\to s-t$. The constraints on the parameters s and t is to remove the degeneracy among the eigenvalues.

for example $G_l=G_1\times G_2$ where the generators of G_1 and G_2 should be commutable with each other. If G_1 (or G_2) is sufficient to distinguish among the generations such that its eigenvalues are not degenerate, then another subgroup G_2 (or G_1) would not impose any new constraint on the lepton mixing. On the other hand, if the three eigenvalues of the generator of either G_1 or G_2 are completely degenerate, e.g. $G_1($ or $G_2)=\langle c^{3n}\rangle$, its three-dimensional representation matrix would be proportional to a unit matrix. As a result, we shall concentrate on the case that the representation matrices of both G_1 and G_2 have two degenerate eigenvalues, therefore either G_1 or G_2 alone fixes only a column of U_l and the third column can be determined by unitary condition. The possible extension of remnant flavor symmetry group G_l, the corresponding remnant CP transformations and the unitary transformations U_l are collected in table 3. We see that the diagonalization matrix U_l can only take five distinct forms $U_l^{(1)}$, $U_l^{(2)}$, $U_l^{(3)}$, $U_l^{(4)}$ or $U_l^{(5)}$ such that the constraints on s and t shown in table 2 are relaxed.

In the direct approach, the flavor symmetry group $D^{(1)}_{9n,3n}$ group is broken down to a Klein four subgroup in the neutrino sector. From Appendix A, we see that $D^{(1)}_{9n,3n}$ for even n has only four Klein four subgroups:

$$K_4^{(c^{9n/2},d^{3n/2})}\equiv\left\{1,c^{9n/2},d^{3n/2},c^{9n/2}d^{3n/2}\right\},\quad K_4^{(d^{3n/2},bd^x)}\equiv\left\{1,d^{3n/2},bd^x,bd^{x+3n/2}\right\},$$
$$K_4^{(c^{9n/2}d^{3n/2},abc^{3y}d^y)}\equiv\left\{1,c^{9n/2}d^{3n/2},abc^{3y}d^y,abc^{3y+9n/2}d^{y+3n/2}\right\},$$

$\mathcal{G}_1$	$\mathcal{G}_2$	Constraints on group parameters	Form of U_l	H^l_{CP}
$\langle c^s d^t \rangle$	$\langle c^{s'} d^{t'} \rangle$	$\begin{cases} s-2t=0 \pmod{3n} \\ s'-t'=0 \pmod{3n} \end{cases}$ or $\begin{cases} s-2t=0 \pmod{3n} \\ t'=0 \pmod{3n} \end{cases}$ or $\begin{cases} s-t=0 \pmod{3n} \\ t'=0 \pmod{3n} \end{cases}$ $(s \leftrightarrow s',\ \ t \leftrightarrow t')$	$U_l^{(1)}$	$\{c^\gamma d^\delta\}$
$\langle bc^s d^t \rangle$	$\langle c^{s'} d^{t'} \rangle$	$s'-2t'=0 \pmod{3n}$ $s=0 \pmod{3n}$	$U_l^{(2)}$	$\{c^{2t+2\delta+3n\tau} d^\delta,$ $bc^{2\delta+3n\tau} d^\delta\}$
	$\langle bc^{s'} d^{t'} \rangle$	$(s-s')-2(t-t')=3l_1 n \pmod{6n}$ $s=3l_2 n \pmod{6n}, \quad s'=3l_3 n \pmod{6n}$		
$\langle abc^s d^t \rangle$	$\langle c^{s'} d^{t'} \rangle$	$s'-t'=0 \pmod{3n}$ $3t-s=0 \pmod{3n}$	$U_l^{(4)}$	$\{c^\gamma d^{\gamma+2t},$ $abc^\gamma d^\gamma\}$
	$\langle abc^{s'} d^{t'} \rangle$	$(s-s')-(t-t')=3l_1 n \pmod{6n}$ $3t-s=3l_2 n \pmod{6n}$ $3t'-s'=3l_3 n \pmod{6n}$		
$\langle a^2 bc^s d^t \rangle$	$\langle c^{s'} d^{t'} \rangle$	$t'=0 \pmod{3n}$ $2s-3t=0 \pmod{3n}$	$U_l^{(5)}$	$\{c^\gamma d^{-t},$ $a^2 bc^\gamma\}$
	$\langle a^2 bc^{s'} d^{t'} \rangle$	$t-t'=3l_1 n \pmod{6n}$ $2s-3t=3l_2 n \pmod{6n}$ $2s'-3t'=3l_3 n \pmod{6n}$		

Table 3: The product extension of the remnant flavor symmetry $G_l = G_1 \times G_2$, the remnant CP transformation compatible with G_l, and the corresponding unitary transformation U_l. We require the column vectors fixed by $\mathcal{G}_1$ and $\mathcal{G}_2$ be different. Consequently we have the parameters $l_{1,2,3} = 0, 1$ and $l_1 + l_2 + l_3 = 1, 3$. The values of parameters s, t, s', t', γ, δ and τ are $s, s', \gamma = 0, 1, \cdots, 9n-1$, $t, t', \delta = 0, 1, \cdots, 3n-1$ and $\tau = 0, 1, 2$.

G_ν	X_ν
$K_4^{(c^{9n/2}, d^{3n/2})}$	$\rho_{\mathbf{r}}(c^\gamma d^\delta)$
$K_4^{(d^{3n/2}, bd^x)}$	$\rho_{\mathbf{r}}(c^{2\delta+2x+3n\tau} d^\delta), \rho_{\mathbf{r}}(bc^{2\delta+3n\tau} d^\delta)$
$K_4^{(c^{9n/2} d^{3n/2}, abc^{3y} d^y)}$	$\rho_{\mathbf{r}}(c^{\delta-2y-3n\tau} d^\delta), \rho_{\mathbf{r}}(abc^{\delta-3n\tau} d^\delta)$
$K_4^{(c^{9n/2}, a^2 bc^{3z} d^{2z})}$	$\rho_{\mathbf{r}}(c^\gamma d^{-2z}), \rho_{\mathbf{r}}(a^2 bc^\gamma)$

Table 4: The K_4 subgroups of the $D^{(1)}_{9n,3n}$ group and eligible remnant CP transformations, where the superscript of the K_4 subgroup denotes its generators. The allowed values of the parameters are $\gamma = 0, 1, \ldots, 9n-1$, $x, y, z, \delta = 0, 1, \ldots, 3n-1$, and $\tau = 0, 1, 2$.

$$K_4^{(c^{9n/2},a^2bc^{3z}d^{2z})} \equiv \left\{1, c^{9n/2}, a^2bc^{3z}d^{2z}, a^2bc^{3z+9n/2}d^{2z}\right\}\,, \tag{4.1}$$

where $x, y, z = 0, 1, \ldots, 3n-1$. We note that $K_4^{(c^{9n/2},d^{3n/2})}$ is a normal subgroup of $D_{9n,3n}^{(1)}$, and the remaining three K_4 subgroups are conjugate:

$$\begin{aligned}
&(a^2c^{y-x+2\delta}d^{\delta})K_4^{(d^{3n/2},bd^x)}(a^2c^{y-x+2\delta}d^{\delta})^{-1} = K_4^{(c^{9n/2}d^{3n/2},abc^{3y}d^y)}\,,\\
&(ac^{-z-x+2\delta}d^{\delta})K_4^{(d^{3n/2},bd^x)}(ac^{-z-x+2\delta}d^{\delta})^{-1} = K_4^{(c^{9n/2},a^2bc^{3z}d^{2z})}\,,
\end{aligned} \tag{4.2}$$

with $\delta = 0, 1, \ldots, 3n-1$. Furthermore, the residual CP symmetry H_{CP}^{ν} in the neutrino sector has to be compatible with the remnant K_4 symmetry, and the following restricted consistency condition must be fulfilled,

$$X_{\nu\mathbf{r}}\rho_{\mathbf{r}}^*(g)X_{\nu\mathbf{r}}^{-1} = \rho_{\mathbf{r}}(g), \qquad g \in K_4\,. \tag{4.3}$$

Solving this equation, we can straightforwardly find the eligible remnant CP transformations for different K_4 subgroups. The results are collected in table 4. Then we proceed to determine the neutrino mass matrix m_ν invariant under the action of both remnant CP and remnant flavor symmetry for each case, i.e., m_ν is subject to the constraints in Eq. (3.4).

- $G_\nu = K_4^{(c^{9n/2},d^{3n/2})}$, $X_{\nu\mathbf{r}} = \rho_{\mathbf{r}}(c^{\gamma}d^{\delta})$

  In our working basis, the representation matrices for both a and c are diagonal with

$$\rho_{\mathbf{3}}(c^{9n/2}) = \begin{pmatrix} -1 & 0 & 0 \\ 0 & -1 & 0 \\ 0 & 0 & 1 \end{pmatrix}, \quad \rho_{\mathbf{3}}(d^{3n/2}) = \begin{pmatrix} 1 & 0 & 0 \\ 0 & -1 & 0 \\ 0 & 0 & -1 \end{pmatrix}. \tag{4.4}$$

  Consequently the residual flavor symmetry enforces the neutrino mass matrix to be diagonal as well. Taking into account the remnant CP symmetry further, we find

$$m_\nu = \begin{pmatrix} m_{11}e^{-2i\pi\frac{\gamma}{9n}} & 0 & 0 \\ 0 & m_{22}e^{-2i\pi\frac{\gamma-3\delta}{9n}} & 0 \\ 0 & 0 & m_{33}e^{2i\pi\frac{2\gamma-3\delta}{9n}} \end{pmatrix}, \tag{4.5}$$

  where m_{11}, m_{22} and m_{33} are real parameters. We can read out the neutrino diagonalization matrix U_ν as

$$U_\nu = \text{diag}\left(e^{i\pi\frac{\gamma}{9n}}, e^{i\pi\frac{\gamma-3\delta}{9n}}, e^{-i\pi\frac{2\gamma-3\delta}{9n}}\right)Q_\nu\,, \tag{4.6}$$

  where Q_ν is a diagonal phase matrix with entry being ± 1 or $\pm i$, and it encodes the CP parity of the neutrino states. The light neutrino mass eigenvalues are

$$m_1 = |m_{11}|\,, \qquad m_2 = |m_{22}|\,, \qquad m_3 = |m_{33}|\,. \tag{4.7}$$

  Obviously the light neutrino masses depend on only three real parameters, and the order of the light neutrino masses can not be fixed by remnant symmetries. Therefore the unitary transformation U_ν is determined up to independent row and column permutations in the present framework, and the neutrino mass spectrum can be wither normal ordering (NO) or inverted ordering (IO).

- $G_\nu = K_4^{(d^{3n/2},bd^x)}$, $X_{\nu\mathbf{r}} = \left\{\rho_{\mathbf{r}}(c^{2\delta+2x+3n\tau}d^{\delta}), \rho_{\mathbf{r}}(bc^{2\delta+3n\tau}d^{\delta})\right\}$

In the same fashion as previous case, we find that the light neutrino mass matrix takes the following form:

$$m_\nu = \begin{pmatrix} m_{11}e^{-2i\pi\frac{2x+2\delta+3n\tau}{9n}} & 0 & 0 \\ 0 & m_{22}e^{-2i\pi\frac{2x-\delta+3n\tau}{9n}} & m_{23}e^{i\pi\frac{2x+2\delta+3n\tau}{9n}} \\ 0 & m_{23}e^{i\pi\frac{2x+2\delta+3n\tau}{9n}} & m_{22}e^{2i\pi\frac{4x+\delta-3n\tau}{9n}} \end{pmatrix}, \tag{4.8}$$

where m_{11}, m_{22} and m_{23} are real. It is diagonalized by the unitary transformation U_ν with

$$U_\nu = \frac{1}{\sqrt{2}} \begin{pmatrix} \sqrt{2}e^{i\pi\frac{2x+2\delta+3n\tau}{9n}} & 0 & 0 \\ 0 & e^{i\pi\frac{2x-\delta+3n\tau}{9n}} & -e^{i\pi\frac{2x-\delta+3n\tau}{9n}} \\ 0 & e^{-i\pi\frac{4x+\delta-3n\tau}{9n}} & e^{-i\pi\frac{4x+\delta-3n\tau}{9n}} \end{pmatrix}, \tag{4.9}$$

where the matrix Q_ν is omitted for simplicity and we will also not explicitly write out this factor hereafter. The light neutrino masses are

$$m_1 = |m_{11}|\,, \qquad m_2 = |m_{22} + (-1)^\tau m_{23}|\,, \qquad m_3 = |m_{22} - (-1)^\tau m_{23}|\,. \tag{4.10}$$

- $G_\nu = K_4^{(c^{9n/2}d^{3n/2}, abc^{3y}d^y)}$, $X_{\nu\mathbf{r}} = \left\{\rho_\mathbf{r}(c^{\delta-2y-3n\tau}d^\delta), \rho_\mathbf{r}(abc^{\delta-3n\tau}d^\delta)\right\}$

  In this case, we find that the light neutrino mass matrix takes the form

$$m_\nu = \begin{pmatrix} m_{11}e^{2i\pi\frac{2y-\delta+3n\tau}{9n}} & 0 & m_{13}e^{-i\pi\frac{2y+2\delta+3n\tau}{9n}} \\ 0 & m_{22}e^{2i\pi\frac{2y+2\delta+3n\tau}{9n}} & 0 \\ m_{13}e^{-i\pi\frac{2y+2\delta+3n\tau}{9n}} & 0 & m_{11}e^{-2i\pi\frac{4y+\delta+6n\tau}{9n}} \end{pmatrix}, \tag{4.11}$$

where m_{11}, m_{13} and m_{22} are real. Consequently the unitary transformation U_ν is

$$U_\nu = \frac{1}{\sqrt{2}} \begin{pmatrix} -e^{i\pi\frac{-2y+\delta+6n\tau}{9n}} & 0 & e^{i\pi\frac{-2y+\delta+6n\tau}{9n}} \\ 0 & \sqrt{2}e^{-i\pi\frac{2y+2\delta+3n\tau}{9n}} & 0 \\ e^{i\pi\frac{4y+\delta+6n\tau}{9n}} & 0 & e^{i\pi\frac{4y+\delta+6n\tau}{9n}} \end{pmatrix}. \tag{4.12}$$

The light neutrino masses are

$$m_1 = |m_{11} - (-1)^\tau m_{13}|\,, \qquad m_2 = |m_{22}|\,, \qquad m_3 = |m_{11} + (-1)^\tau m_{13}|\,. \tag{4.13}$$

- $G_\nu = K_4^{(c^{9n/2}, a^2bc^{3z}d^{2z})}$, $X_{\nu\mathbf{r}} = \{\rho_\mathbf{r}(c^\gamma d^{-2z}), \rho_\mathbf{r}(a^2bc^\gamma)\}$

  The light neutrino mass matrix m_ν is constrained by the remnant symmetry to be of the form

$$m_\nu = \begin{pmatrix} m_{11}e^{-2i\pi\frac{\gamma}{9n}} & m_{12}e^{-2i\pi\frac{3z+\gamma}{9n}} & 0 \\ m_{12}e^{-2i\pi\frac{3z+\gamma}{9n}} & m_{11}e^{-2i\pi\frac{6z+\gamma}{9n}} & 0 \\ 0 & 0 & m_{33}e^{4i\pi\frac{3z+\gamma}{9n}} \end{pmatrix}, \tag{4.14}$$

where m_{11}, m_{12} and m_{33} are real. The unitary matrix U_ν diagonalizing the above neutrino mass matrix is determined to be

$$U_\nu = \frac{1}{\sqrt{2}} \begin{pmatrix} -e^{i\pi\frac{\gamma}{9n}} & e^{i\pi\frac{\gamma}{9n}} & 0 \\ e^{i\pi\frac{6z+\gamma}{9n}} & e^{i\pi\frac{6z+\gamma}{9n}} & 0 \\ 0 & 0 & \sqrt{2}e^{-2i\pi\frac{3z+\gamma}{9n}} \end{pmatrix}. \tag{4.15}$$

The neutrino masses are given by

$$m_1 = |m_{11} - m_{12}|\,, \qquad m_2 = |m_{11} + m_{22}|\,, \qquad m_3 = |m_{33}|\,. \tag{4.16}$$

Then we proceed to discuss the possible mixing patterns achievable in direct approach by combining the different remnant symmetries of the charged lepton sector with those of the neutrino sector. As shown in section 3, two pairs of subgroups $\{G_l, G_\nu\}$ and $\{G'_l, G'_\nu\}$ would yield the same results for the PMNS matrix after considering all the eligible residual CP transformations, if these two pairs of groups are conjugate. Notice the conjugate relations between distinct K_4 subgroups in Eq. (4.1) and the identities $(bc^{2\epsilon}d^{2\epsilon})(abc^sd^t)(bc^{2\epsilon}d^{2\epsilon})^{-1} = a^2bc^sd^{s-t}$, $(bc^{2\epsilon}d^{2\epsilon})K_4^{(c^{9n/2},d^{3n/2})}(bc^{2\epsilon}d^{2\epsilon})^{-1} = K_4^{(c^{9n/2},d^{3n/2})}$ and $(bc^{2\epsilon}d^{2\epsilon})K_4^{(d^{3n/2},bd^x)}(bc^{2\epsilon}d^{2\epsilon})^{-1} = K_4^{(d^{3n/2},bd^x)}$ for any integer ϵ, we find it is sufficient to only consider eight kinds of remnant symmetries with $G_l = \langle c^sd^t\rangle$, $\langle bc^sd^t\rangle$, $\langle ac^sd^t\rangle$, $\langle abc^sd^t\rangle$ and $G_\nu = K_4^{(c^{9n/2},d^{3n/2})}$, $K_4^{(d^{3n/2},bd^x)}$. In this scenarios, all mixing parameters including Majorana phases are completely fixed by remnant symmetries.

(i) $G_l = \langle c^sd^t\rangle$, $G_\nu = K_4^{(c^{9n/2},d^{3n/2})}$, $X_{\nu\mathbf{r}} = \{\rho_{\mathbf{r}}(c^\gamma d^\delta)\}$
In this case, the unitary transformation U_l is a unit matrix, as shown in table 2. U_ν is a diagonal phase matrix and it is given by Eq. (4.6). As a result, the PMNS matrix is also a diagonal matrix up to row and column permutations, and obviously it doesn't agree with the present neutrino oscillation data [7–9].

(ii) $G_l = \langle bc^sd^t\rangle$, $G_\nu = K_4^{(c^{9n/2},d^{3n/2})}$, $X_{\nu\mathbf{r}} = \{\rho_{\mathbf{r}}(c^\gamma d^\delta)\}$
In this case, the postulated residual subgroups lead to the mixing pattern

$$U_{\rm PMNS} = \frac{1}{\sqrt{2}}\begin{pmatrix}\sqrt{2} & 0 & 0\\ 0 & 1 & -e^{i\varphi_1}\\ 0 & 1 & e^{i\varphi_1}\end{pmatrix}\,, \tag{4.17}$$

with

$$\varphi_1 = -\frac{\pi(\gamma-2\delta+s-2t)}{3n}\,. \tag{4.18}$$

The lepton mixing angles are $\theta_{13} = \theta_{12} = 0$, $\theta_{23} = 45^\circ$, and therefore large corrections to both θ_{12} and θ_{13} are necessary in order to be compatible with experimental data.

(iii) $G_l = \langle ac^sd^t\rangle$, $G_\nu = K_4^{(c^{9n/2},d^{3n/2})}$, $X_{\nu\mathbf{r}} = \{\rho_{\mathbf{r}}(c^\gamma d^\delta)\}$
This residual symmetry allows us to pin down the lepton mixing matrix as:

$$U_{\rm PMNS} = \frac{1}{\sqrt{3}}\begin{pmatrix}e^{i\varphi_1} & 1 & e^{i\varphi_2}\\ \omega e^{i\varphi_1} & 1 & \omega^2 e^{i\varphi_2}\\ \omega^2 e^{i\varphi_1} & 1 & \omega e^{i\varphi_2}\end{pmatrix}\,, \tag{4.19}$$

where

$$\varphi_1 = \frac{\pi(3\gamma-3\delta+2s)}{9n}, \qquad \varphi_2 = \frac{\pi(3\gamma-6\delta+4s-6t)}{9n}\,. \tag{4.20}$$

This pattern leads to $\sin^2\theta_{12} = \sin^2\theta_{23} = 1/2$, $\sin^2\theta_{13} = 1/3$ and a maximal Dirac CP phase $|\delta_{CP}| = \pi/2$. The solar as well as the reactor mixing angle have to acquire appropriate corrections in order to be in accordance with experimental data.

(iv) $G_l = \langle abc^sd^t\rangle$, $G_\nu = K_4^{(c^{9n/2},d^{3n/2})}$, $X_{\nu\mathbf{r}} = \{\rho_{\mathbf{r}}(c^\gamma d^\delta)\}$
In this case we find the lepton mixing matrix is

$$U_{\rm PMNS} = \frac{1}{\sqrt{2}}\begin{pmatrix}\sqrt{2} & 0 & 0\\ 0 & 1 & e^{i\varphi_1}\\ 0 & -1 & e^{i\varphi_1}\end{pmatrix}\,, \quad \text{with} \quad \varphi_1 = -\frac{\pi(\gamma-\delta+s-t)}{3n}\,, \tag{4.21}$$

which leads to $\theta_{12} = \theta_{13} = 0$, $\theta_{23} = 45^\circ$. Large corrections to θ_{12} and θ_{13} are needed to be compatible with experimental data.

(v) $G_l = \langle c^s d^t \rangle$, $G_\nu = K_4^{(d^{3n/2}, bd^x)}$, $X_{\nu\mathbf{r}} = \{\rho_{\mathbf{r}}(c^{2\delta+2x+3n\tau} d^\delta), \rho_{\mathbf{r}}(bc^{2\delta+3n\tau} d^\delta)\}$
The unitary transformation U_ν is fixed by residual subgroup to be Eq. (4.9), and the PMNS matrix takes the form

$$U_{\rm PMNS} = \begin{pmatrix} 1 & 0 & 0 \\ 0 & \frac{1}{\sqrt{2}} & -\frac{1}{\sqrt{2}} \\ 0 & \frac{1}{\sqrt{2}} & \frac{1}{\sqrt{2}} \end{pmatrix} , \tag{4.22}$$

which lead to $\theta_{12} = \theta_{13} = 0$, $\theta_{23} = 45^\circ$. Again θ_{12} and θ_{13} require large corrections in order to be in the experimentally preferred range.

(vi) $G_l = \langle bc^s d^t \rangle$, $G_\nu = K_4^{(d^{3n/2}, bd^x)}$, $X_{\nu\mathbf{r}} = \{\rho_{\mathbf{r}}(c^{2\delta+2x+3n\tau} d^\delta), \rho_{\mathbf{r}}(bc^{2\delta+3n\tau} d^\delta)\}$
Using these residual symmetries, we can derive the lepton mixing matrix

$$U_{\rm PMNS} = \begin{pmatrix} 1 & 0 & 0 \\ 0 & -\sin\varphi_1 & \cos\varphi_1 \\ 0 & \cos\varphi_1 & \sin\varphi_1 \end{pmatrix} , \quad \text{with} \quad \varphi_1 = \frac{\pi(s-2t+2x)}{6n} . \tag{4.23}$$

The mixing angles are $\theta_{12} = \theta_{13} = 0$, $\sin^2\theta_{23} = \cos^2\varphi_1$ which is strongly disfavored by the experimental data [7–9].

(vii) $G_l = \langle ac^s d^t \rangle$, $G_\nu = K_4^{(d^{3n/2}, bd^x)}$, $X_{\nu\mathbf{r}} = \{\rho_{\mathbf{r}}(c^{2\delta+2x+3n\tau} d^\delta), \rho_{\mathbf{r}}(bc^{2\delta+3n\tau} d^\delta)\}$
In this case, the lepton mixing matrix is determined to be of the trimaximal form, i.e., the second column of the PMNS matrix is $(1,1,1)^T/\sqrt{3}$ with

$$U_{\rm PMNS} = \frac{1}{\sqrt{3}} \begin{pmatrix} -\sqrt{2}e^{i\varphi_2}\cos\varphi_1 & 1 & \sqrt{2}e^{i\varphi_2}\sin\varphi_1 \\ \sqrt{2}e^{i\varphi_2}\sin\left(\frac{\pi}{6}+\varphi_1\right) & 1 & \sqrt{2}e^{i\varphi_2}\cos\left(\frac{\pi}{6}+\varphi_1\right) \\ \sqrt{2}e^{i\varphi_2}\sin\left(\frac{\pi}{6}-\varphi_1\right) & 1 & -\sqrt{2}e^{i\varphi_2}\cos\left(\frac{\pi}{6}-\varphi_1\right) \end{pmatrix} , \tag{4.24}$$

where

$$\varphi_1 = \frac{2s-3t+3x}{9n}\pi, \qquad \varphi_2 = -\frac{\delta+t+x}{3n}\pi . \tag{4.25}$$

These two parameters φ_1 and φ_2 are independent from each other, and they can take the following discrete values

$$\begin{aligned} \varphi_1 \ (\text{mod}\ 2\pi) &= 0, \frac{1}{9n}\pi, \frac{2}{9n}\pi, \ldots, \frac{18n-1}{9n}\pi , \\ \varphi_2 \ (\text{mod}\ 2\pi) &= 0, \frac{1}{3n}\pi, \frac{2}{3n}\pi, \ldots, \frac{6n-1}{3n}\pi . \end{aligned} \tag{4.26}$$

We can read out the mixing angles as

$$\sin^2\theta_{13} = \frac{2}{3}\sin^2\varphi_1, \quad \sin^2\theta_{12} = \frac{1}{2+\cos 2\varphi_1}, \quad \sin^2\theta_{23} = \frac{1+\cos(\frac{\pi}{6}+2\varphi_1)}{2+\cos 2\varphi_1} .$$

All possible predictions of $\sin\theta_{13}$ for each $D^{(1)}_{9n,3n}$ of even n are displayed in figure 1. It is remarkable that viable reactor mixing angle θ_{13} can always be achieved for each n. Moreover, the three mixing angles are closely related as follows

$$3\sin^2\theta_{12}\cos^2\theta_{13} = 1, \quad \sin^2\theta_{23} = \frac{1}{2} \pm \frac{1}{2}\tan\theta_{13}\sqrt{2-\tan^2\theta_{13}} . \tag{4.27}$$

Inputting the experimentally preferred 3σ range $0.0176 \leq \sin^2\theta_{13} \leq 0.0295$ [7], we obtain predictions for solar as well as atmospheric mixing angles:

$$0.339 \leq \sin^2\theta_{12} \leq 0.343, \qquad 0.378 \leq \sin^2\theta_{23} \leq 0.406, \ \text{or} \ 0.594 \leq \sin^2\theta_{23} \leq 0.622 . \tag{4.28}$$

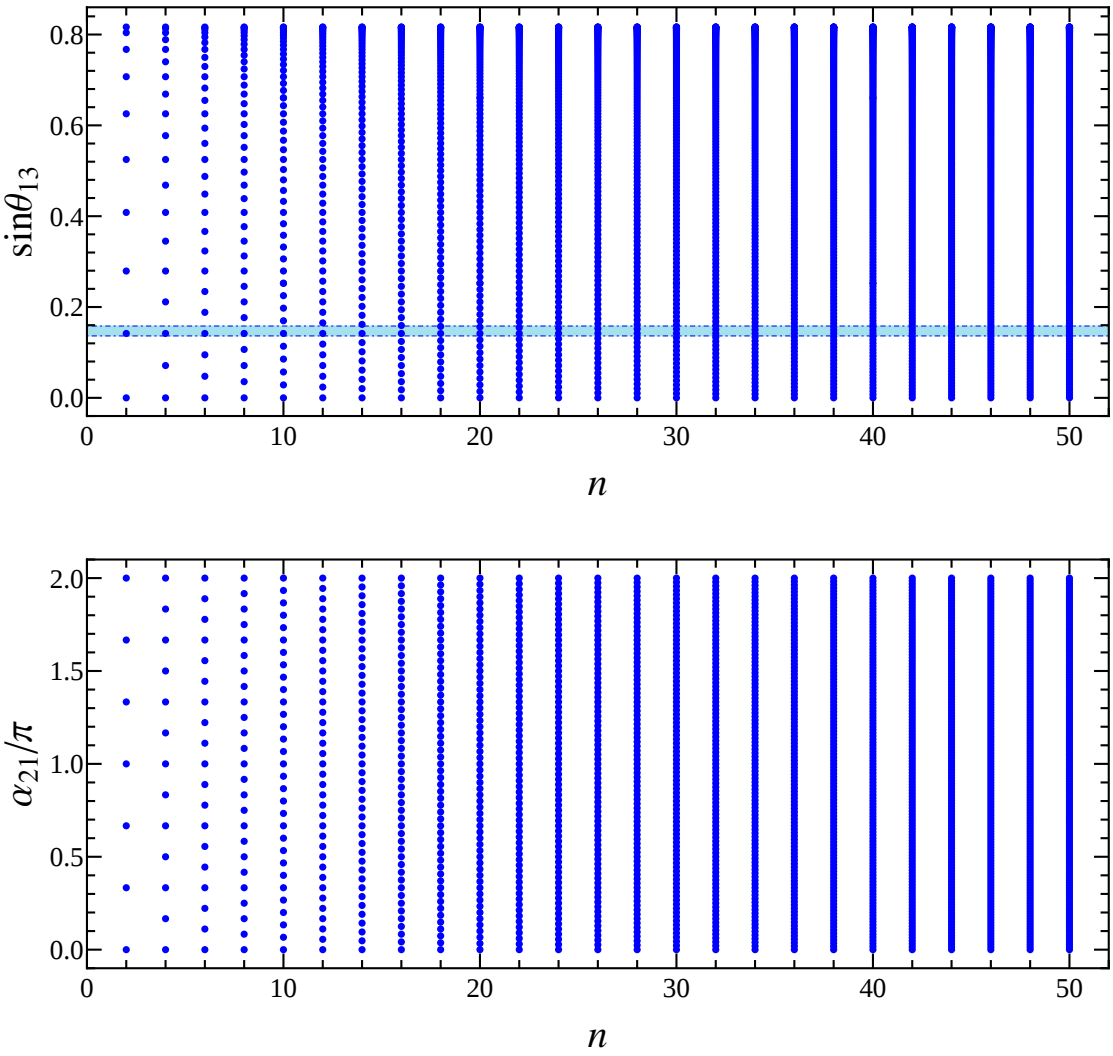

Figure 1: The possible values of the mixing angle $\sin\theta_{13}$ and the Majorana phase α_{21} for each $D^{(1)}_{9n,3n}$ group with even n when the remnant symmetries are $G_l = \langle ac^s d^t \rangle$, $G_\nu = K_4^{(d^{3n/2}, bd^x)}$, $X_{\nu\mathbf{r}} = \{\rho_{\mathbf{r}}(c^{2\delta+2x+3n\tau}d^\delta), \rho_{\mathbf{r}}(bc^{2\delta+3n\tau}d^\delta)\}$. The light blue region denotes the 3σ bound of $\sin\theta_{13}$, which is taken from Ref. [7].

From the PMNS matrix of Eq. (4.24), we can also extract the CP violating phases

$$\sin\delta_{CP} = \sin\alpha_{31} = 0, \quad \tan\alpha_{21} = -\tan 2\varphi_2\,, \tag{4.29}$$

where the contribution of the CP parity matrix Q_ν is considered. We see that both Dirac phase δ_{CP} and the Majorana phase α_{31} are trivial, and another Majorana phase α_{21} is

$$\alpha_{21} = -2\varphi_2 \;\; \text{or} \;\; \alpha_{21} = \pi - 2\varphi_2\,. \tag{4.30}$$

The admissible values of α_{21} are

$$\alpha_{21} = 0, \frac{2}{3n}\pi, \frac{4}{3n}\pi, \ldots, \frac{6n-2}{3n}\pi\,, \tag{4.31}$$

which are plotted in figure 1. Note that here the predictions for the CP phases are consistent with the general results of Ref. [16].

(viii) $G_l = \langle abc^s d^t \rangle$, $G_\nu = K_4^{(d^{3n/2}, bd^x)}$, $X_{\nu\mathbf{r}} = \{\rho_\mathbf{r}(c^{2\delta+2x+3n\tau}d^\delta), \rho_\mathbf{r}(bc^{2\delta+3n\tau}d^\delta)\}$
In this case, we find the lepton mixing matrix is the well-known bimaximal pattern

$$U_{\rm PMNS} = \frac{1}{2}\begin{pmatrix} -\sqrt{2} & \sqrt{2} & 0 \\ 1 & 1 & \sqrt{2}e^{i\varphi_1} \\ 1 & 1 & -\sqrt{2}e^{i\varphi_1} \end{pmatrix}, \quad \text{with} \quad \varphi_1 = \frac{\pi(s-2t+2x)}{6n}\,. \tag{4.32}$$

The bimaximal mixing can be a valid first approximation in a model where corrections of order of the Cabibbo angle can naturally arise [32, 51].

5 Lepton mixing from semidirect approach

In the semidirect approach, the original symmetry $D^{(1)}_{9n,3n} \rtimes H_{CP}$ is broken at low energies into $G_l \rtimes H^l_{CP}$ in the charged lepton sector and to $Z_2 \times H^\nu_{CP}$ in the neutrino sector. The PMNS matrix turns out to depend on only a single real parameter in this scenario. It is generally assumed that the residual flavor symmetry G_l is able to distinguish the three generations of charged leptons such that the unitary matrix U_l can be determined from the requirement that all the generators of G_l should be simultaneously diagonalized by U_l. The possible candidates for the subgroup G_l, the remnant CP transformations compatible with G_l and the corresponding unitary transformation U_l are summarized in table 2 and table 3. Then we turn to the neutrino sector. From the multiplication rules given in Eq. (A.1), we see that the order 2 elements of the $D^{(1)}_{9n,3n}$ group are

$$bd^x, \quad abc^{3y}d^y, \quad a^2bc^{3z}d^{2z}, \quad x, y, z = 0, 1 \ldots 3n-1\,, \tag{5.1}$$

and additionally

$$c^{9n/2}, \quad d^{3n/2}, \quad c^{9n/2}d^{3n/2}\,, \tag{5.2}$$

for even n. The residual CP transformation $X_{\nu\mathbf{r}}$ is a symmetric unitary matrix, and it should map the element of the neutrino residual flavor symmetry to itself,

$$X_{\nu\mathbf{r}}\rho^*_\mathbf{r}(g_\nu)X^{-1}_{\nu\mathbf{r}} = \rho_\mathbf{r}(g_\nu), \quad g_\nu \in G_\nu\,. \tag{5.3}$$

The eligible residual CP transformations for different Z_2 subgroups are collected in table 5. Furthermore, we notice that all the Z_2 elements in Eq. (5.1) are conjugate:

$$\begin{aligned}
&\left(c^\gamma d^\delta\right) bd^x \left(c^\gamma d^\delta\right)^{-1} = bd^{x'}, && \left(bc^\gamma d^\delta\right) bd^x \left(bc^\gamma d^\delta\right)^{-1} = bd^{-x'}\,, \\
&\left(ac^\gamma d^\delta\right) bd^x \left(ac^\gamma d^\delta\right)^{-1} = a^2bc^{-3x'}d^{-2x'}, && \left(a^2c^\gamma d^\delta\right) bd^x \left(a^2c^\gamma d^\delta\right)^{-1} = abc^{3x'}d^{x'}\,, \\
&\left(abc^\gamma d^\delta\right) bd^x \left(abc^\gamma d^\delta\right)^{-1} = a^2bc^{3x'}d^{2x'}, && \left(a^2bc^\gamma d^\delta\right) bd^x \left(a^2bc^\gamma d^\delta\right)^{-1} = abc^{-3x'}d^{-x'}\,,
\end{aligned} \tag{5.4}$$

where $x' = x + \gamma - 2\delta$. Similarly the three elements in Eq. (5.2) are also conjugate to each other:

$$\begin{aligned}
&\left(c^\gamma d^\delta\right) c^{9n/2} \left(c^\gamma d^\delta\right)^{-1} = c^{9n/2}, && \left(bc^\gamma d^\delta\right) c^{9n/2} \left(bc^\gamma d^\delta\right)^{-1} = c^{9n/2}d^{3n/2}\,, \\
&\left(ac^\gamma d^\delta\right) c^{9n/2} \left(ac^\gamma d^\delta\right)^{-1} = c^{9n/2}d^{3n/2}, && \left(a^2c^\gamma d^\delta\right) c^{9n/2} \left(a^2c^\gamma d^\delta\right)^{-1} = d^{3n/2}\,, \\
&\left(abc^\gamma d^\delta\right) c^{n/2} \left(abc^\gamma d^\delta\right)^{-1} = d^{3n/2}, && \left(a^2bc^\gamma d^\delta\right) c^{9n/2} \left(a^2bc^\gamma d^\delta\right)^{-1} = c^{9n/2}\,.
\end{aligned} \tag{5.5}$$

As a result, it is sufficient to consider the representative residual symmetry $G_\nu = Z_2^{bd^x}$, $Z_2^{c^{9n/2}}$ and $G_l = \langle c^s d^t \rangle$, $\langle bc^s d^t \rangle$, $\langle ac^s d^t \rangle$, $\langle abc^s d^t \rangle$ and $\langle a^2bc^s d^t \rangle$. Since only a Z_2 subgroup instead of a full Klein subgroup is preserved by the neutrino mass matrix, the postulated remnant flavor symmetries can only fix one column of the PMNS matrix. We list the explicit

G_ν	X_ν
$Z_2^{bd^x}$	$\rho_{\mathbf{r}}(c^{2\delta+2x+3n\tau}d^{\delta}),\ \rho_{\mathbf{r}}(bc^{2\delta+3n\tau}d^{\delta})$
$Z_2^{abc^{3y}d^y}$	$\rho_{\mathbf{r}}(c^{\delta-2y-3n\tau}d^{\delta}),\ \rho_{\mathbf{r}}(abc^{\delta-3n\tau}d^{\delta})$
$Z_2^{a^2bc^{3z}d^{2z}}$	$\rho_{\mathbf{r}}(c^{\gamma}d^{-2z}),\ \rho_{\mathbf{r}}(a^2bc^{\gamma})$
$Z_2^{c^{9n/2}}$	$\rho_{\mathbf{r}}(c^{\gamma}d^{\delta}),\ \rho_{\mathbf{r}}(a^2bc^{\gamma})$
$Z_2^{d^{3n/2}}$	$\rho_{\mathbf{r}}(c^{\gamma}d^{\delta}),\ \rho_{\mathbf{r}}(bc^{2\delta+3n\tau}d^{\delta})$
$Z_2^{c^{9n/2}d^{3n/2}}$	$\rho_{\mathbf{r}}(c^{\gamma}d^{\delta}),\ \rho_{\mathbf{r}}(abc^{\delta+3n\tau}d^{\delta})$

Table 5: Different types of remnant Z_2 subgroup G_ν and viable remnant CP transformations, where the superscript of the Z_2 subgroup denotes its generators. The allowed values of the parameters are $\gamma = 0, 1, \ldots, 9n-1$, $x, y, z, \delta = 0, 1, \ldots, 3n-1$, and $\tau = 0, 1, 2$.

form of the determined columns for different remnant flavor symmetry in table 6. Global analysis of the neutrino oscillation data gives the 3σ ranges on the absolute values of the elements of the PMNS matrix [7]:

$$||U_{\rm PMNS}|| = \begin{pmatrix} 0.789 \sim 0.853 & 0.501 \sim 0.594 & 0.133 \sim 0.172 \\ 0.194 \sim 0.558 & 0.408 \sim 0.735 & 0.602 \sim 0.784 \\ 0.194 \sim 0.558 & 0.408 \sim 0.735 & 0.602 \sim 0.784 \end{pmatrix} , \tag{5.6}$$

It is obvious that none entry of the PMNS matrix is vanishing [7–9]. Therefore if one element of the fixed column is predicted to be zero, it would be excluded by the experimental data. From table 6 we see that only three independent cases are viable with the residual flavor symmetries $(G_\nu, G_l) = (Z_2^{bd^x}, \langle ac^s d^t\rangle)$, $(Z_2^{c^{9n/2}}, \langle ac^s d^t\rangle)$ and $(Z_2^{bd^x}, \langle abc^s d^t\rangle)$. In the following, the contribution of all admissible remnant CP transformations will be included further. We shall find the neutrino mass matrix invariant under the residual flavor and CP symmetries, and then the unitary transformation U_ν as well as the PMNS matrix $U_{\rm PMNS}$ will be presented for each case.

(I) $G_l = \langle ac^s d^t\rangle$, $G_\nu = Z_2^{bd^x}$, $X_{\nu\mathbf{r}} = \left\{\rho_{\mathbf{r}}(c^{2\delta+2x+3n\tau}d^{\delta}), \rho_{\mathbf{r}}(bc^{2\delta+2x+3n\tau}d^{\delta+x})\right\}$

The residual symmetry transformation $G_\nu \times H_{CP}^\nu$ of the neutrino fields leaves the neutrino mass term invariant. Therefore the neutrino mass matrix m_ν must satisfy

$$\begin{aligned} &\rho_{\mathbf{3}}^T(g_\nu) m_\nu \rho_{\mathbf{3}}(g_\nu) = m_\nu, \qquad g_\nu \in G_\nu, \\ &X_{\nu\mathbf{3}}^T m_\nu X_{\nu\mathbf{3}} = m_\nu^*, \qquad\quad X_{\nu\mathbf{3}} \in H_{CP}^\nu \,. \end{aligned} \tag{5.7}$$

In our working basis, it is straightforward to find that the neutrino mass matrix is constrained to take the form

$$m_\nu = \begin{pmatrix} e^{-\frac{4i\pi(x+\delta)}{9n}} m_{11} & e^{-\frac{i\pi(4x+\delta)}{9n}} m_{12} & e^{\frac{i\pi(2x-\delta)}{9n}} m_{12} \\ e^{-\frac{i\pi(4x+\delta)}{9n}} m_{12} & e^{-\frac{2i\pi(2x-\delta)}{9n}} m_{22} & e^{\frac{2i\pi(x+\delta)}{9n}} m_{23} \\ e^{\frac{i\pi(2x-\delta)}{9n}} m_{12} & e^{\frac{2i\pi(x+\delta)}{9n}} m_{23} & e^{\frac{2i\pi(4x+\delta)}{9n}} m_{22} \end{pmatrix} , \tag{5.8}$$

where m_{11}, m_{12}, m_{22} and m_{23} are real. It follows that the neutrino mass matrix m_ν can be diagonalized by

$$U_\nu^T m_\nu U_\nu = {\rm diag}\,(m_1, m_2, m_3) \,, \tag{5.9}$$

	$G_\nu = Z_2^{bd^x}$	$G_\nu = Z_2^{c^{9n/2}}$
$G_l = \langle c^s d^t \rangle$	$\frac{1}{\sqrt{2}} \begin{pmatrix} 0 \\ -1 \\ 1 \end{pmatrix}$ ✗	$\begin{pmatrix} 0 \\ 0 \\ 1 \end{pmatrix}$ ✗
$G_l = \langle bc^s d^t \rangle$	$\begin{pmatrix} 0 \\ \cos\left(\frac{s-2t+2x}{6n}\pi\right) \\ \sin\left(\frac{s-2t+2x}{6n}\pi\right) \end{pmatrix}$ ✗	$\frac{1}{\sqrt{2}} \begin{pmatrix} 0 \\ -1 \\ 1 \end{pmatrix}$ ✗
$G_l = \langle ac^s d^t \rangle$	$\sqrt{\frac{2}{3}} \begin{pmatrix} \sin\left(\frac{2s-3t+3x}{9n}\pi\right) \\ \cos\left(\frac{\pi}{6}+\frac{2s-3t+3x}{9n}\pi\right) \\ \cos\left(\frac{\pi}{6}-\frac{2s-3t+3x}{9n}\pi\right) \end{pmatrix}$ ✓	$\frac{1}{\sqrt{3}} \begin{pmatrix} 1 \\ 1 \\ 1 \end{pmatrix}$ ✓
$G_l = \langle abc^s d^t \rangle$	$\frac{1}{2} \begin{pmatrix} 1 \\ 1 \\ \sqrt{2} \end{pmatrix}$ ✓	$\frac{1}{\sqrt{2}} \begin{pmatrix} 0 \\ -1 \\ 1 \end{pmatrix}$ ✗
$G_l = \langle a^2 bc^s d^t \rangle$	$\frac{1}{2} \begin{pmatrix} 1 \\ 1 \\ \sqrt{2} \end{pmatrix}$ ✓	$\begin{pmatrix} 0 \\ 0 \\ 1 \end{pmatrix}$ ✗

Table 6: The column vector of the PMNS matrix determined by the residual flavor symmetries G_ν and G_l. If one (or two) element of the fixed column is vanishing, we would use the notation "✗" to indicate that it is disfavored by the present experimental data otherwise the notation "✓" is labelled to indicate that agreement with the experimental data could be achieved. Notice that two pair of subgroups $(G_\nu, G_l) = (Z_2^{bd^x}, \langle abc^s d^t \rangle)$ and $(Z_2^{bd^x}, \langle a^2 bc^s d^{s-t} \rangle)$ are conjugate under the element $bc^{2x}d^{2x}$.

with the unitary transformation

$$U_\nu = \frac{1}{\sqrt{2}} \begin{pmatrix} \sqrt{2}e^{\frac{2i\pi(x+\delta)}{9n}} \cos\theta & 0 & \sqrt{2}e^{\frac{2i\pi(x+\delta)}{9n}} \sin\theta \\ -e^{\frac{i\pi(2x-\delta)}{9n}} \sin\theta & -e^{\frac{i\pi(2x-\delta)}{9n}} & e^{\frac{i\pi(2x-\delta)}{9n}} \cos\theta \\ -e^{-\frac{i\pi(4x+\delta)}{9n}} \sin\theta & e^{-\frac{i\pi(4x+\delta)}{9n}} & e^{-\frac{i\pi(4x+\delta)}{9n}} \cos\theta \end{pmatrix} Q_\nu \,, \tag{5.10}$$

where the angle θ is

$$\tan 2\theta = \frac{2\sqrt{2}m_{12}}{m_{22}+m_{23}-m_{11}} \,. \tag{5.11}$$

The factor Q_ν is a diagonal phase matrix with elements equal to ± 1 and $\pm i$ and it is necessary to make the light neutrino masses positive definite. The neutrino mass eigenvalues are given by

$$\begin{aligned} m_1 &= \frac{1}{2}\left| m_{11}+m_{22}+m_{23}-\frac{m_{22}+m_{23}-m_{11}}{\cos 2\theta} \right| , \\ m_2 &= \left| m_{22}-m_{23} \right| , \\ m_3 &= \frac{1}{2}\left| m_{11}+m_{22}+m_{23}+\frac{m_{22}+m_{23}-m_{11}}{\cos 2\theta} \right| . \end{aligned}$$

We see that the neutrino masses depend on four parameters m_{11}, m_{12}, m_{22} and m_{23}, the experimentally measured mass squared differences could be easily accommodated. The order of the three neutrino masses m_1, m_2 and m_3 can not be pinned down in the present framework, hence the unitary matrix U_ν is determined up to permutations of the columns (the same holds true in the following cases), and the neutrino mass spectrum can be either normal ordering (NO) or inverted ordering (IO). Taking into account the corresponding

charged lepton diagonalization matrix U_l listed in table 2 and table 3, we find the PMNS matrix $U_{\rm PMNS} \equiv U_l^\dagger U_\nu$ up to row and column permutations is

$$U^I_{\rm PMNS} = \frac{1}{\sqrt{3}} \begin{pmatrix} e^{i\varphi_2}\cos\theta - \sqrt{2}\cos\varphi_1 \sin\theta & \sqrt{2}\sin\varphi_1 & e^{i\varphi_2}\sin\theta + \sqrt{2}\cos\theta\cos\varphi_1 \\ -e^{i\varphi_2}\cos\theta - \sqrt{2}\sin\theta\sin\left(\frac{\pi}{6}-\varphi_1\right) & \sqrt{2}\cos\left(\frac{\pi}{6}-\varphi_1\right) & -e^{i\varphi_2}\sin\theta + \sqrt{2}\cos\theta\sin\left(\frac{\pi}{6}-\varphi_1\right) \\ e^{i\varphi_2}\cos\theta + \sqrt{2}\sin\theta\sin\left(\frac{\pi}{6}+\varphi_1\right) & \sqrt{2}\cos\left(\frac{\pi}{6}+\varphi_1\right) & e^{i\varphi_2}\sin\theta - \sqrt{2}\cos\theta\sin\left(\frac{\pi}{6}+\varphi_1\right) \end{pmatrix} Q_\nu \,,$$

with

$$\varphi_1 = \frac{2s-3t+3x}{9n}\pi, \qquad \varphi_2 = \frac{\delta+t+x}{3n}\pi \,. \tag{5.12}$$

Both φ_1 and φ_2 are determined by the postulated remnant symmetries, they are independent of each other, and their values can be multiple of $\frac{\pi}{9n}$ and $\frac{\pi}{3n}$ respectively

$$\begin{aligned} &\varphi_1 \ (\text{mod}\ 2\pi) = 0, \frac{1}{9n}\pi, \frac{2}{9n}\pi, \ldots, \frac{18n-1}{9n}\pi \,, \\ &\varphi_2 \ (\text{mod}\ 2\pi) = 0, \frac{1}{3n}\pi, \frac{2}{3n}\pi, \ldots, \frac{6n-1}{3n}\pi \,. \end{aligned} \tag{5.13}$$

We see that one column of the PMNS matrix is determined to be

$$\sqrt{\frac{2}{3}} \begin{pmatrix} \sin\varphi_1 \\ \cos\left(\pi/6-\varphi_1\right) \\ \cos\left(\pi/6+\varphi_1\right) \end{pmatrix} \tag{5.14}$$

in this case. As the neutrino mass ordering isn't constrained in the present framework, this column vector can be any of the three column of the PMNS matrix. As a consequence, the PMNS matrix can take the following three possible forms:

$$\begin{aligned} U^{I,1}_{\rm PMNS} &= \frac{1}{\sqrt{3}} \begin{pmatrix} \sqrt{2}\sin\varphi_1 & e^{i\varphi_2}\cos\theta - \sqrt{2}\cos\varphi_1\sin\theta & e^{i\varphi_2}\sin\theta + \sqrt{2}\cos\theta\cos\varphi_1 \\ \sqrt{2}\cos\left(\frac{\pi}{6}-\varphi_1\right) & -e^{i\varphi_2}\cos\theta - \sqrt{2}\sin\theta\sin\left(\frac{\pi}{6}-\varphi_1\right) & -e^{i\varphi_2}\sin\theta + \sqrt{2}\cos\theta\sin\left(\frac{\pi}{6}-\varphi_1\right) \\ \sqrt{2}\cos\left(\frac{\pi}{6}+\varphi_1\right) & e^{i\varphi_2}\cos\theta + \sqrt{2}\sin\theta\sin\left(\frac{\pi}{6}+\varphi_1\right) & e^{i\varphi_2}\sin\theta - \sqrt{2}\cos\theta\sin\left(\frac{\pi}{6}+\varphi_1\right) \end{pmatrix} , \\ U^{I,2}_{\rm PMNS} &= \frac{1}{\sqrt{3}} \begin{pmatrix} e^{i\varphi_2}\cos\theta - \sqrt{2}\cos\varphi_1\sin\theta & \sqrt{2}\sin\varphi_1 & e^{i\varphi_2}\sin\theta + \sqrt{2}\cos\theta\cos\varphi_1 \\ -e^{i\varphi_2}\cos\theta - \sqrt{2}\sin\theta\sin\left(\frac{\pi}{6}-\varphi_1\right) & \sqrt{2}\cos\left(\frac{\pi}{6}-\varphi_1\right) & -e^{i\varphi_2}\sin\theta + \sqrt{2}\cos\theta\sin\left(\frac{\pi}{6}-\varphi_1\right) \\ e^{i\varphi_2}\cos\theta + \sqrt{2}\sin\theta\sin\left(\frac{\pi}{6}+\varphi_1\right) & \sqrt{2}\cos\left(\frac{\pi}{6}+\varphi_1\right) & e^{i\varphi_2}\sin\theta - \sqrt{2}\cos\theta\sin\left(\frac{\pi}{6}+\varphi_1\right) \end{pmatrix} , \\ U^{I,3}_{\rm PMNS} &= \frac{1}{\sqrt{3}} \begin{pmatrix} e^{i\varphi_2}\sin\theta + \sqrt{2}\cos\theta\cos\varphi_1 & e^{i\varphi_2}\cos\theta - \sqrt{2}\cos\varphi_1\sin\theta & \sqrt{2}\sin\varphi_1 \\ -e^{i\varphi_2}\sin\theta + \sqrt{2}\cos\theta\sin\left(\frac{\pi}{6}-\varphi_1\right) & -e^{i\varphi_2}\cos\theta - \sqrt{2}\sin\theta\sin\left(\frac{\pi}{6}-\varphi_1\right) & \sqrt{2}\cos\left(\frac{\pi}{6}-\varphi_1\right) \\ e^{i\varphi_2}\sin\theta - \sqrt{2}\cos\theta\sin\left(\frac{\pi}{6}+\varphi_1\right) & e^{i\varphi_2}\cos\theta + \sqrt{2}\sin\theta\sin\left(\frac{\pi}{6}+\varphi_1\right) & \sqrt{2}\cos\left(\frac{\pi}{6}+\varphi_1\right) \end{pmatrix} . \end{aligned}$$

The effect of row permutation is equivalent to redefinitions of the parameters θ, φ_1 and φ_2, and no new possible values of φ_1 and φ_2 beyond those in Eq. (5.13) are obtained. Then we proceed to discuss the phenomenological predictions of each mixing pattern. For $U^{I,1}_{\rm PMNS}$ the three lepton mixing angles read as

$$\begin{aligned} \sin^2\theta_{13} &= \frac{1}{3}\left(1+\cos^2\theta\cos 2\varphi_1 + \sqrt{2}\sin 2\theta\cos\varphi_1\cos\varphi_2\right) , \\ \sin^2\theta_{12} &= \frac{1+\sin^2\theta\cos 2\varphi_1 - \sqrt{2}\sin 2\theta\cos\varphi_1\cos\varphi_2}{2-\cos^2\theta\cos 2\varphi_1 - \sqrt{2}\sin 2\theta\cos\varphi_1\cos\varphi_2} , \\ \sin^2\theta_{23} &= \frac{1-\cos^2\theta\sin\left(\pi/6+2\varphi_1\right) - \sqrt{2}\sin 2\theta\cos\varphi_2\sin\left(\pi/6-\varphi_1\right)}{2-\cos^2\theta\cos 2\varphi_1 - \sqrt{2}\sin 2\theta\cos\varphi_1\cos\varphi_2} \,, \end{aligned} \tag{5.15}$$

which yield the correlation

$$3\cos^2\theta_{12}\cos^2\theta_{13} = 2\sin^2\varphi_1 \,, \tag{5.16}$$

In order to accommodate the experimentally favored 3σ ranges $0.259 \leq \sin^2\theta_{12} \leq 0.359$ and $0.0176 \leq \sin^2\theta_{13} \leq 0.0295$ from the global fit [7], we find the allowed region of the parameter φ_1 is

$$\varphi_1 \in [0.417\pi, 0.583\pi] \cup [1.417\pi, 1.583\pi] \ . \tag{5.17}$$

Obviously φ_1 should be around $\pi/2$ or $3\pi/2$. Furthermore, the three CP rephasing invariants J_{CP}, I_1 and I_2 are predicted to be

$$\begin{aligned}
|J_{CP}| &= \frac{1}{6\sqrt{6}} \left|\sin 2\theta \sin 3\varphi_1 \sin\varphi_2\right| \ , \\
|I_1| &= \frac{2\sqrt{2}}{9} \left|\sin^2\varphi_1 \sin\varphi_2 \left(\sqrt{2}\cos^2\theta\cos\varphi_2 - \sin 2\theta \cos\varphi_1\right)\right| \ , \\
|I_2| &= \frac{2\sqrt{2}}{9} \left|\sin^2\varphi_1 \sin\varphi_2 \left(\sqrt{2}\sin^2\theta\cos\varphi_2 + \sin 2\theta \cos\varphi_1\right)\right| \ ,
\end{aligned} \tag{5.18}$$

where J_{CP} is well-known Jarlskog invariant, and I_1 and I_2 are defined for the Majorana phases with

$$\begin{aligned}
J_{CP} &= \mathrm{Im}\left[(U_{\rm PMNS})_{11} (U_{\rm PMNS})_{33} (U^*_{\rm PMNS})_{13} (U^*_{\rm PMNS})_{31}\right] \\
&= \frac{1}{8}\sin 2\theta_{12}\sin 2\theta_{13}\sin 2\theta_{23}\cos\theta_{13}\sin\delta_{CP} \ , \\
I_1 &= \mathrm{Im}\left[(U_{\rm PMNS})^{*2}_{11} (U_{\rm PMNS})^2_{12}\right] = \frac{1}{4}\sin^2 2\theta_{12}\cos^4\theta_{13}\sin\alpha_{21} \ , \\
I_2 &= \mathrm{Im}\left[(U_{\rm PMNS})^{*2}_{11} (U_{\rm PMNS})^2_{13}\right] = \frac{1}{4}\sin^2 2\theta_{13}\cos^2\theta_{12}\sin\alpha'_{31} \ ,
\end{aligned} \tag{5.19}$$

where $\alpha'_{31} \equiv \alpha_{31} - 2\delta_{CP}$, δ_{CP} is the Dirac CP violating phase, α_{21} and α_{31} are the Majorana CP phases in the standard parameterization of the PMNS matrix [52]. We show the absolute values of J_{CP}, I_1 and I_2 in Eq. (5.18), the reason is because the sign of the J_{CP} depends on the ordering of rows and columns and the sign of I_1 and I_2 could be changed by the CP parity matrix Q_ν. Moreover, if the lepton doublet fields are assigned to the triplet $\mathbf{3}_{9n-1,0}$ instead of $\mathbf{3}_{1,0}$, the prediction for $U_{\rm PMNS}$ would be complex conjugated such that the signs of J_{CP}, I_1 and I_2 are all inversed. We show the possible predictions for the mixing parameters $\sin^2\theta_{12}$, $\sin\theta_{13}$, $\sin^2\theta_{23}$ as well as $|\sin\delta_{CP}|$, $|\sin\alpha_{21}|$ and $|\sin\alpha_{31}|$ for each $D^{(1)}_{9n,3n}$ group in figure 2, where all the admissible values of φ_1 and φ_2 shown in Eq. (5.13) are considered and all the three mixing angles are required to lie in the 3σ allowed regions adapted from [7]. It is notable that the solar mixing angle is predicted to be within the narrow interval of $0.313 \leq \sin^2\theta_{12} \leq 0.344$. The near future medium-baseline reactor neutrino oscillation experiments, such as JUNO [53] and RENO-50 [54] are expected to make very precise, sub-percent measurements of the solar mixing angle θ_{12}. They provide the one of the most significant test of this mixing pattern. The allowed values of the CP violation phases increase with group index n and they are strongly constrained for smaller n. From figure 2 we can read $0 \leq |\sin\delta_{CP}| \leq 0.226$, $0.847 \leq |\sin\alpha_{21}| \leq 0.873$ and $0 \leq |\sin\alpha'_{31}| \leq 0.488$ in the case of $n = 1$. However, almost any values of the CP phases can be achieved for sufficient large value of n.

Then we turn to the second mixing pattern $U^{I,2}_{\rm PMNS}$ in which $\sqrt{\frac{2}{3}}\left(\sin\varphi_1, \cos\left(\frac{\pi}{6}-\varphi_1\right), \cos\left(\frac{\pi}{6}+\varphi_1\right)\right)^T$ is the second column vector. Its predictions for the mixing angles are

$$\begin{aligned}
\sin^2\theta_{13} &= \frac{1}{3}\left(1 + \cos^2\theta\cos 2\varphi_1 + \sqrt{2}\sin 2\theta\cos\varphi_1\cos\varphi_2\right) , \\
\sin^2\theta_{12} &= \frac{2\sin^2\varphi_1}{2 - \cos^2\theta\cos 2\varphi_1 - \sqrt{2}\sin 2\theta\cos\varphi_1\cos\varphi_2} \ ,
\end{aligned}$$

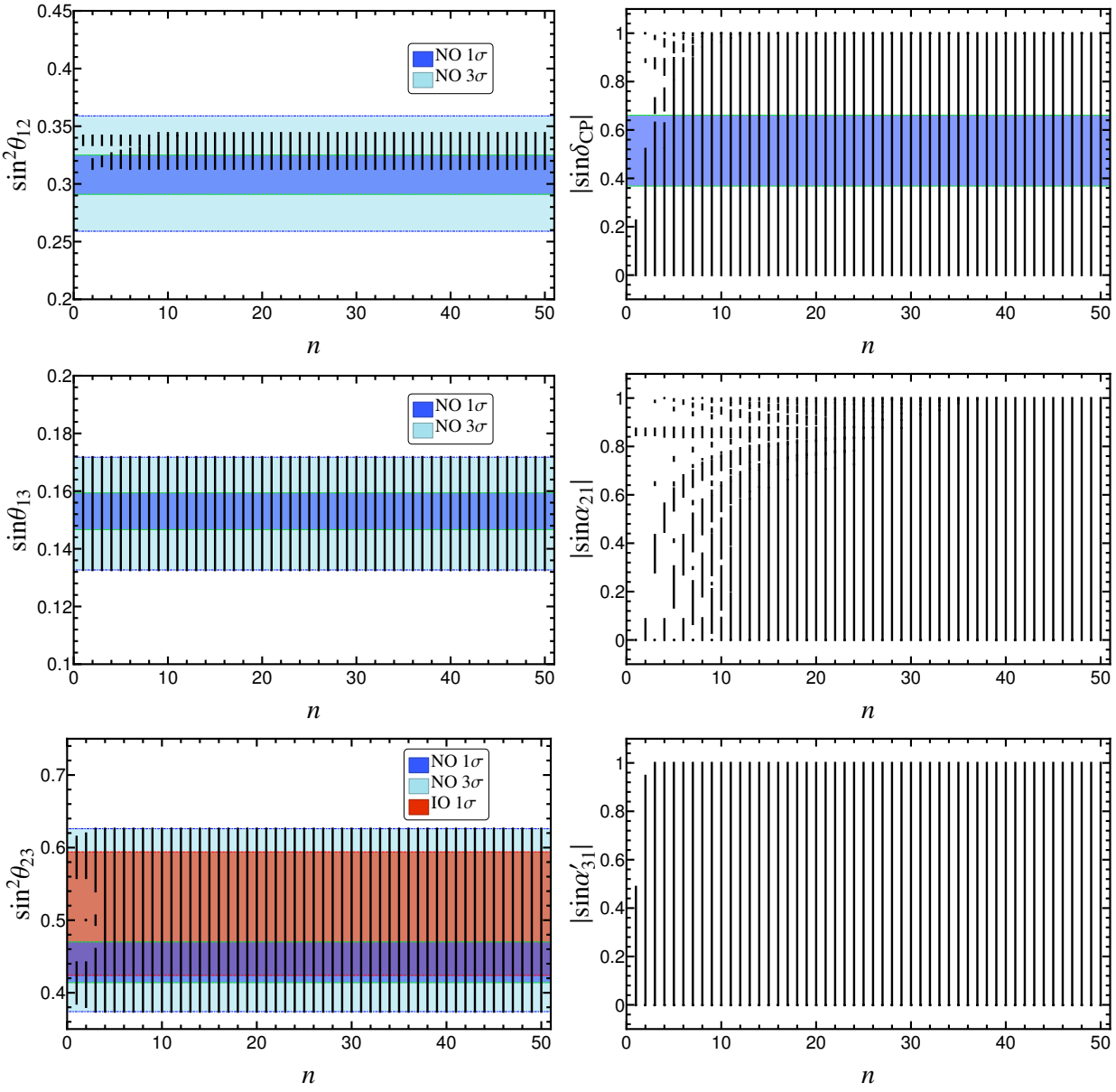

Figure 2: The possible values of $\sin^2\theta_{12}$, $\sin\theta_{13}$, $\sin^2\theta_{23}$, $|\sin\delta_{CP}|$, $|\sin\alpha_{21}|$ and $|\sin\alpha'_{31}|$ with respect to n for the mixing pattern $U^{I,1}_{\rm PMNS}$ in the case I, where the three lepton mixing angles are required to be within the experimentally preferred 3σ ranges. The 1σ and 3σ regions of the three neutrino mixing angles are adapted from global fit [7].

$$\sin^2\theta_{23} = \frac{1-\cos^2\theta\sin\left(\pi/6+2\varphi_1\right)-\sqrt{2}\sin 2\theta\cos\varphi_2\sin\left(\pi/6-\varphi_1\right)}{2-\cos^2\theta\cos 2\varphi_1-\sqrt{2}\sin 2\theta\cos\varphi_1\cos\varphi_2}\,. \tag{5.20}$$

We see that the solar and reactor mixing angles are correlated as

$$3\sin^2\theta_{12}\cos^2\theta_{13} = 2\sin^2\varphi_1\,. \tag{5.21}$$

In order to accommodate the experimental results on θ_{12} and θ_{13}, φ_1 should vary in the interval:

$$\varphi_1 \in [0.210\pi, 0.259\pi]\cup[0.741\pi, 0.790\pi]\cup[1.210\pi, 1.259\pi]\cup[1.741\pi, 1.790\pi]\,. \tag{5.22}$$

Consequently we have

$$|\cos(\varphi_1-\frac{\pi}{6})|, |\cos(\varphi_1+\frac{\pi}{6})| \in [0.230, 0.377]\cup[0.958, 0.991]\,. \tag{5.23}$$

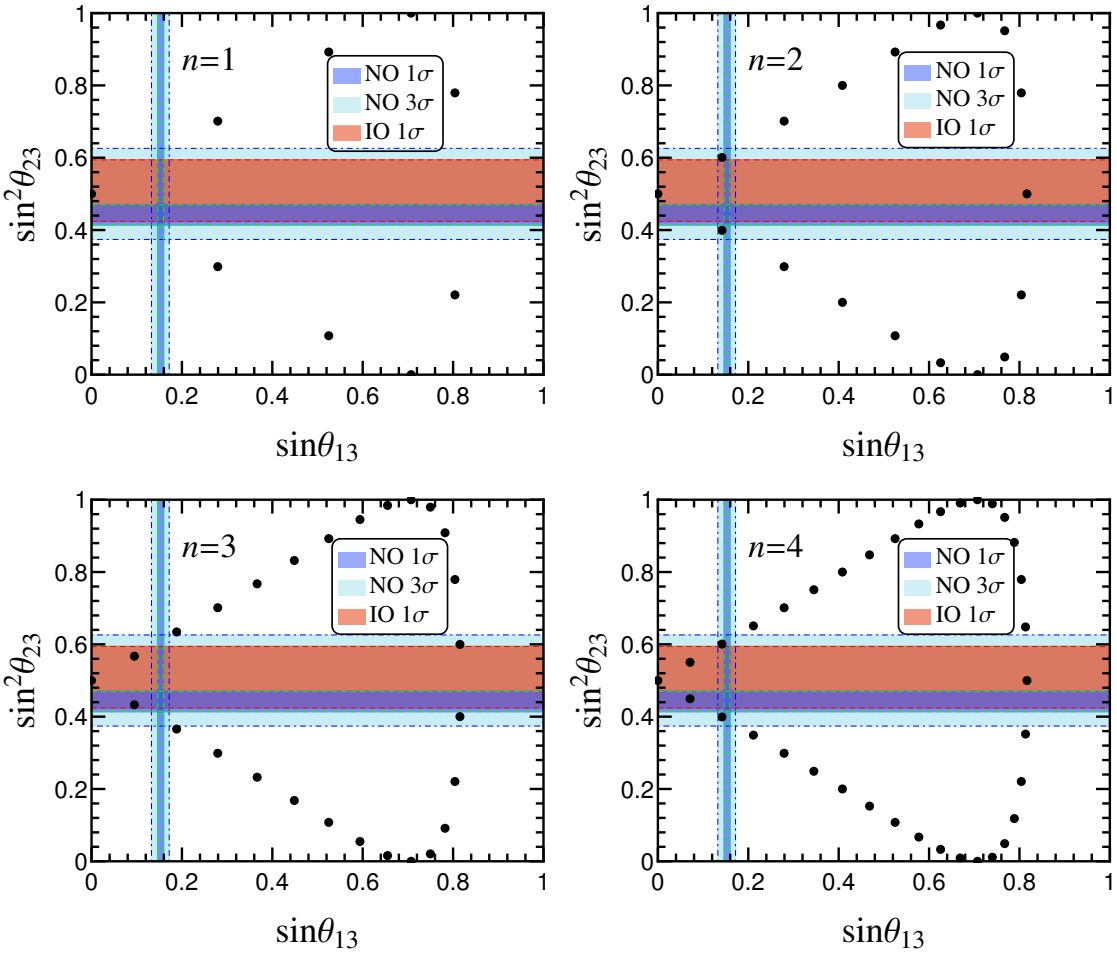

Figure 3: The allowed values of $\sin^2\theta_{23}$ and $\sin\theta_{13}$ for the mixing pattern $U^{I,3}_{\rm PMNS}$ in case I, where the first four smallest $D^{(1)}_{9n,3n}$ group with $n = 1, 2, 3, 4$ are considered. The 1σ and 3σ regions of the three neutrino mixing angles are adapted from global fit [7].

We see that both (22) and (32) entries of $U^{I,2}_{\rm PMNS}$ are not in agreement with the experimental data given by Eq. (5.6). Hence this mixing pattern is phenomenologically disfavored.

For the third possible arrangement of the rows and columns, the PMNS matrix is $U^{I,3}_{\rm PMNS}$. In this case, the third column of the PMNS matrix doesn't depend on the continuous parameter θ and it is completely fixed the remnant CP symmetry. It is straightforward to extract the mixing angles.

$$\sin^2\theta_{13} = \frac{2}{3}\sin^2\varphi_1, \qquad \sin^2\theta_{23} = \frac{1+\sin\left(\pi/6+2\varphi_1\right)}{2+\cos 2\varphi_1}\,,$$
$$\sin^2\theta_{12} = \frac{1+\sin^2\theta\cos 2\varphi_1-\sqrt{2}\sin 2\theta\cos\varphi_1\cos\varphi_2}{2+\cos 2\varphi_1}\,. \tag{5.24}$$

The experimental data $1.76\times10^{-2} \leq \sin^2\theta_{13} \leq 2.95\times10^{-2}$ at 3σ level [7] can be accommodated for the following values of the parameter φ_1:

$$\varphi_1 \in [0.0519\pi, 0.0675\pi]\cup[0.933\pi, 0.948\pi]\cup[1.0519\pi, 1.0675\pi]\cup[1.933\pi, 1.948\pi]\,. \tag{5.25}$$

As both θ_{13} and θ_{23} depend on a single parameter φ_1, we can derive a sum rule between them,

$$2\sin^2\theta_{23} = 1\pm\tan\theta_{13}\sqrt{2-\tan^2\theta_{13}}\,. \tag{5.26}$$

Given the experimental best fitting value of the reactor mixing angle $\sin^2\theta_{13} = 2.34 \times 10^{-2}$ [7], we have

$$\sin^2\theta_{23} \simeq 0.391, \quad \text{or} \quad \sin^2\theta_{23} \simeq 0.609\,, \tag{5.27}$$

which is within the 3σ range although it is non-maximal. For a given $D^{(1)}_{9n,3n}$ group, the atmospheric and reactor mixing angles can only take a set of discrete values. The possible values of $\sin^2\theta_{23}$ and $\sin\theta_{13}$ for the first four smallest $n = 1, 2, 3, 4$ are displayed in figure 3. We see that the values $\varphi_1 = \pm\pi/18, \pm 17\pi/18$ in the case of $n = 2, 4$ lead to $(\theta_{13}, \theta_{23}) = (8.151^\circ, 50.813^\circ)$ or $(8.151^\circ, 39.187^\circ)$ which are compatible with the present experimental data [7]. The next generation of superbeam neutrino oscillation experiments would provide a high-precision determination of θ_{23}. If no significant deviations from maximal mixing of θ_{23} will be detected, our present scheme will be excluded. Furthermore, we find that the CP invariants are

$$\begin{aligned}
|J_{CP}| &= \frac{1}{6\sqrt{6}}\left|\sin 2\theta \sin 3\varphi_1 \sin\varphi_2\right|\,, \\
|I_1| &= \frac{1}{9}\left|\cos\varphi_1 \sin\varphi_2 \left(4\cos 2\theta \cos\varphi_1 \cos\varphi_2 - \sqrt{2}\sin 2\theta \cos 2\varphi_1\right)\right|\,, \\
|I_2| &= \frac{2\sqrt{2}}{9}\left|\sin^2\varphi_1 \sin\varphi_2 \left(\sqrt{2}\sin^2\theta \cos\varphi_2 + \sin 2\theta \cos\varphi_1\right)\right|\,.
\end{aligned} \tag{5.28}$$

Furthermore, we study the admissible values of mixing angles and CP phases for each $D^{(1)}_{9n,3n}$ group. The numerical results are displayed in figure 4. We easily see that the atmospheric mixing angle θ_{23} is not maximal and it is around the 3σ upper or lower bounds. Similar to the $\Delta(6n^2)$ group [41], maximal value of the Majorana phase α'_{31} can not be achieved in this case and it is found to be in the range of $|\sin\alpha'_{31}| \leq 0.910$ while almost any values of δ_{CP} and α_{21} can be possible for large n.

As a concrete example, we shall study the first two smallest $D^{(1)}_{9n,3n}$ group with $n = 1$ and $n = 2$. From the expression of the PMNS matrix, we know that $U^{I,1}_{\rm PMNS}$ has the following symmetry properties:

$$\begin{aligned}
&U^{I,1}_{\rm PMNS}(\theta, \varphi_1, \pi + \varphi_2) = U^{I,1}_{\rm PMNS}(-\theta, \varphi_1, \varphi_2){\rm diag}(1, -1, 1), \\
&U^{I,1}_{\rm PMNS}(\theta, \varphi_1, \pi - \varphi_2) = [U^{I,1}_{\rm PMNS}(-\theta, \varphi_1, \varphi_2)]^*{\rm diag}(1, -1, 1), \\
&U^{I,1}_{\rm PMNS}(\theta, \varphi_1, -\varphi_2) = [U^{I,1}_{\rm PMNS}(\theta, \varphi_1, \varphi_2)]^*, \\
&U^{I,1}_{\rm PMNS}(\theta, \pi + \varphi_1, \varphi_2) = U^{I,1}_{\rm PMNS}(-\theta, \varphi_1, \varphi_2){\rm diag}(-1, 1, -1)\,,
\end{aligned} \tag{5.29}$$

where the diagonal matrix can be absorbed into the matrix Q_ν. Similar relations are satisfied for the PMNS matrix $U^{I,3}_{\rm PMNS}$. Note that the PMNS matrix would become its complex conjugation if the three generations of leptons are assigned to the triplet $\mathbf{3}_{9n-1,0} \cong \mathbf{3}^*_{1,0}$. As a result, without loss of generality, we shall focus on the case of $0 \leq \varphi_1 \leq \pi$ and $0 \leq \varphi_2 \leq \pi/2$. A conventional χ^2 analysis is performed. Notice that we don't include the information of the Dirac CP phase δ_{CP} into the χ^2 function, since the evidence for a preferred value of δ_{CP} coming from both present experiments and the global fitting is rather weak. The numerical results are reported in table 7, where we exclude all patterns that can not accommodate the experimental data at the best fitting point $\theta = \theta_{bf}$ for which the χ^2 function is minimized. Since the global fit results of the mixing angles are slightly distinct for NO and IO neutrino mass spectrums [7], the χ^2 function has been defined for NO and IO respectively. The values in the parentheses are the results for the IO case. Applying the symmetry transformations in Eq. (5.29), we can obtain other values of φ_1 and φ_2 which yield the same best fit values for the mixing angles such that the same χ^2_{min} is

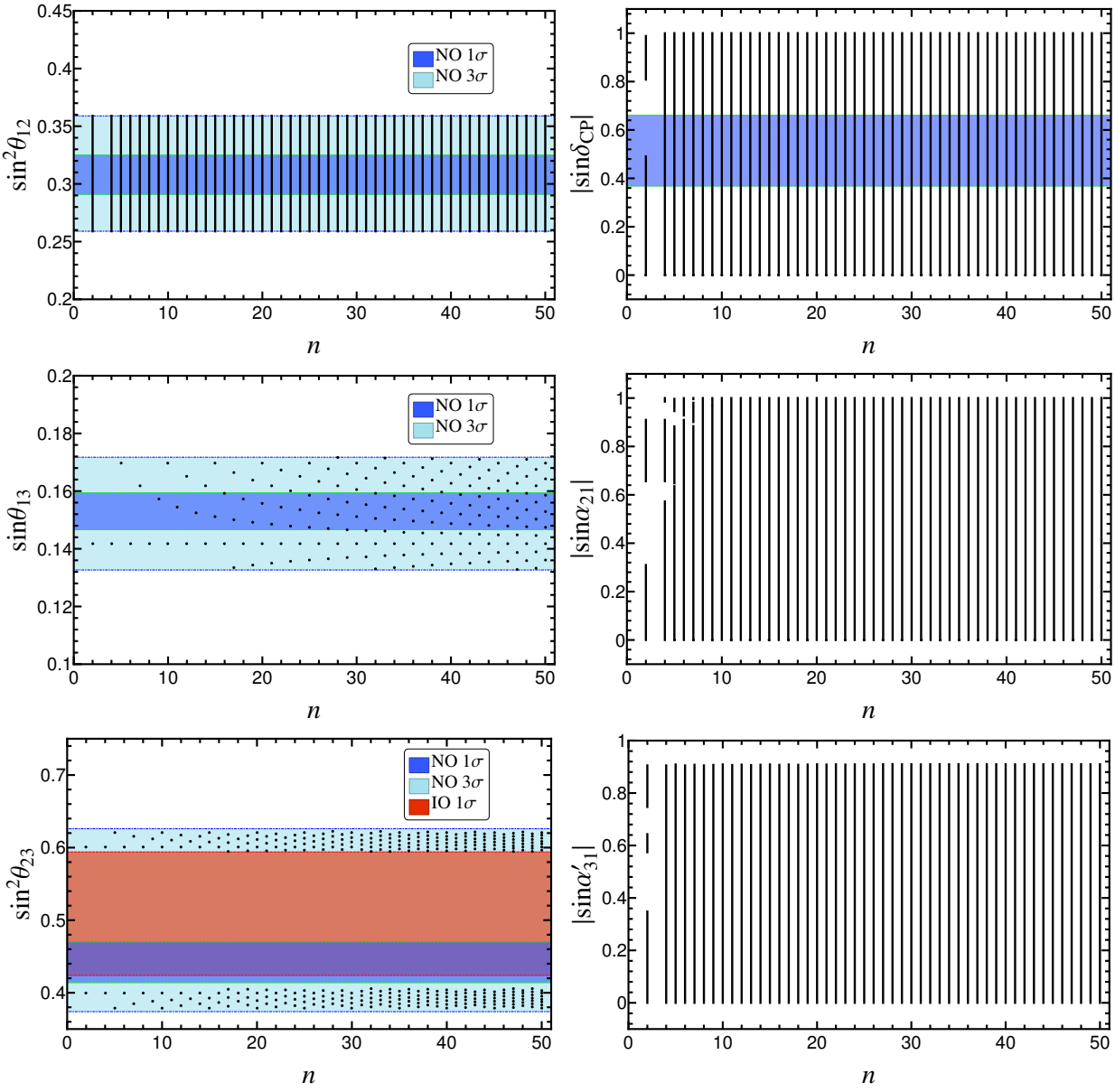

Figure 4: The possible values of $\sin^2\theta_{12}$, $\sin\theta_{13}$, $\sin^2\theta_{23}$, $|\sin\delta_{CP}|$, $|\sin\alpha_{21}|$ and $|\sin\alpha'_{31}|$ with respect to n for the mixing pattern $U^{I,3}_{\rm PMNS}$ in the case I, where the three lepton mixing angles are required to be within the experimentally preferred 3σ ranges. The 1σ and 3σ regions of the three neutrino mixing angles are adapted from global fit [7].

obtained. For both mixing patterns $U^{I,1}_{\rm PMNS}$ and $U^{I,3}_{\rm PMNS}$, we can check that the formulae in Eqs. (5.15,5.24) for the mixing angles $\sin^2\theta_{12}$ and $\sin^2\theta_{13}$ are invariant while $\sin^2\theta_{23}$ turns into $\cos^2\theta_{23}$ under the transformation $\varphi_1 \to \pi-\varphi_1$, $\theta\to\pi-\theta$. As a result, the sum of the best fitting value θ_{bf} for φ_1 and $\pi-\varphi_1$ is approximately equal to π. It is remarkable that even the smallest $D^{(1)}_{9n,3n}$ group with $n=1$ allows a reasonable fit to the experimental data, for instance, the mixing patterns with $(\varphi_1,\varphi_2)=(4\pi/9,0)$, $(4\pi/9,\pi/3)$, $(5\pi/9,0)$ and $(5\pi/9,\pi/3)$ can describe the experimentally measured values of the mixing angles, as can be seen from table 7. In particular, the CP violating phases are neither conserved nor maximal in the case of $(\varphi_1,\varphi_2)=(4\pi/9,\pi/3)$ and $(5\pi/9,\pi/3)$. The PMNS matrix $U^{I,1}_{\rm PMNS}$ for $n=2$ as well as $(\varphi_1,\varphi_2)=(\pi/2,\pi/2)$ give rise to maximal atmospheric mixing and maximal Dirac phase. On the other hand, the group index n should be equal or greater than 2 in order to obtain phenomenologically viable mixing pattern of the form $U^{I,3}_{\rm PMNS}$. Scrutinizing all

Case I										
$n=1$ and $n=2$										
	φ_1	φ_2	θ_{bf}	χ^2_{min}	$\sin^2\theta_{13}$	$\sin^2\theta_{12}$	$\sin^2\theta_{23}$	$\lvert\sin\delta_{CP}\rvert$	$\lvert\sin\alpha_{21}\rvert$	$\lvert\sin\alpha'_{31}\rvert$
$U^{I,1}_{\rm PMNS}$	$\frac{4\pi}{9}$	0	0.0245 (0.0274)	3.789 (4.267)	0.0243 (0.0248)	0.337 (0.337)	0.419 (0.421)	0 (0)	0 (0)	0 (0)
		$\frac{\pi}{3}$	0.0435 (0.0480)	3.928 (4.438)	0.0242 (0.0247)	0.337 (0.337)	0.417 (0.419)	0.125 (0.137)	0.857 (0.856)	0.276 (0.302)
	$\frac{5\pi}{9}$	0	3.108 (3.117)	21.499 (3.822)	0.0259 (0.0244)	0.336 (0.337)	0.574 (0.581)	0 (0)	0 (0)	0 (0)
		$\frac{\pi}{3}$	3.087 (3.097)	22.307 (3.849)	0.0255 (0.0243)	0.337 (0.337)	0.578 (0.583)	0.154 (0.127)	0.854 (0.856)	0.338 (0.281)
$n=2$										
$U^{I,1}_{\rm PMNS}$	$\frac{4\pi}{9}$	$\frac{\pi}{6}$	0.0278 (0.0311)	3.807 (4.289)	0.0243 (0.0248)	0.337 (0.337)	0.419 (0.421)	0.0462 (0.0510)	0.869 (0.870)	0.103 (0.114)
		$\frac{\pi}{2}$	0.108 (0.116)	5.666 (6.131)	0.0237 (0.0243)	0.338 (0.337)	0.400 (0.400)	0.362 (0.384)	0.0532 (0.0572)	0.739 (0.774)
	$\frac{5\pi}{9}$	$\frac{\pi}{6}$	3.104 (3.113)	21.616 (3.826)	0.0258 (0.0244)	0.336 (0.337)	0.575 (0.581)	0.0602 (0.0468)	0.871 (0.869)	0.134 (0.104)
		$\frac{\pi}{2}$	3.033 (3.026)	27.468 (4.087)	0.0238 (0.0243)	0.337 (0.337)	0.600 (0.600)	0.365 (0.383)	0.0537 (0.0569)	0.744 (0.772)
	$\frac{\pi}{2}$	$\frac{\pi}{3}$	0.261 (0.272)	26.399 (1.490)	0.0222 (0.0240)	0.318 (0.317)	0.604 (0.608)	0.885 (0.887)	0.866 (0.866)	0.866 (0.866)
		$\frac{\pi}{3}$	2.877 (2.873)	3.838 (4.352)	0.0228 (0.0234)	0.318 (0.317)	0.394 (0.393)	0.886 (0.887)	0.866 (0.866)	0.866 (0.866)
		$\frac{\pi}{2}$	0.269 (0.272)	3.946 (0.380)	0.0235 (0.0241)	0.317 (0.317)	0.5 (0.5)	1 (1)	0 (0)	0 (0)
$U^{I,3}_{\rm PMNS}$	$\frac{\pi}{18}$	0	0.0344 (0.0344)	27.637 (4.238)	0.0201 (0.0201)	0.308 (0.308)	0.601 (0.601)	0 (0)	0 (0)	0 (0)
		$\frac{\pi}{6}$	0.0399 (0.0399)	27.637 (4.238)				0.0431 (0.0431)	0.881 (0.881)	0.0279 (0.0279)
		$\frac{\pi}{3}$	0.0716 (0.0716)	27.637 (4.238)				0.134 (0.134)	0.815 (0.815)	0.0868 (0.0868)
		$\frac{\pi}{2}$	0(0)	31.219 (7.820)		0.340 (0.340)		0 (0)	0 (0)	0 (0)
	$\frac{17\pi}{18}$	0	3.107 (3.107)	5.707 (6.374)		0.308 (0.308)	0.399 (0.399)	0 (0)	0 (0)	0 (0)
		$\frac{\pi}{6}$	3.102 (3.102)	5.707 (6.374)				0.0431 (0.0431)	0.881 (0.881)	0.0279 (0.0279)
		$\frac{\pi}{3}$	3.070 (3.070)	5.707 (6.374)				0.134 (0.134)	0.815 (0.815)	0.0868 (0.0868)
		$\frac{\pi}{2}$	0 (0)	9.289 (9.955)		0.340 (0.340)		0 (0)	0 (0)	0 (0)

Table 7: Results of the χ^2 analysis for $n=1,2$ in the case I. The χ^2 function has a global minimum χ^2_{min} at the best fit value θ_{bf} for θ. We give the values of the mixing angles and CP violation phases for $\theta=\theta_{bf}$. The values given in parentheses denote the results for the IO neutrino mass spectrum.

the admissible cases listed in table 7, we find that the predictions for θ_{13} are almost the same, nevertheless θ_{12}, θ_{23} and δ_{CP} are predicted to be considerably different. The JUNO experiment will be capable of reducing the error of $\sin^2\theta_{12}$ to about 0.1° or around 0.3% [53]. Future long baseline experiments such as DUNE [55], LBNO [56], T2HK [57] and possibly ESSνSB [58] at the European Spallation Source can make very precise measurements of the oscillation parameters θ_{12}, θ_{23} and δ_{CP}. Therefore future neutrino facilities have the potential to discriminate between the above possible cases, or to rule them out entirely. Furthermore, we expect that a more ambitious facility such as the neutrino factory [59] could provide a more stringent tests of our approach.

Since the Majorana CP violating phases can be predicted in the present framework, we now discuss its phenomenological implications in the neutrinoless double beta ($0\nu\beta\beta$) decay. It is well-known that the $0\nu\beta\beta$ decay process is the most sensitive probe for Majorana neutrinos. Its observation would establish the Majorana nature of neutrinos irrespective of the underlying mass generation mechanism. The $0\nu\beta\beta$ decay rate is proportional to the square of the effective Majorana mass $|m_{ee}|$ which is given by [52]

$$|m_{ee}| = \left| m_1 \cos^2\theta_{12}\cos^2\theta_{13} + m_2 \sin^2\theta_{12}\cos^2\theta_{13} e^{i\alpha_{21}} + m_3 \sin^2\theta_{13} e^{i\alpha'_{31}} \right| . \tag{5.30}$$

The values of $|m_{ee}|$ are dependent on both CP phases α_{21} and $\alpha'_{31} \equiv \alpha_{31} - 2\delta_{CP}$. For the mixing pattern $U^{I,1}_{\rm PMNS}$, $|m_{ee}|$ is of the form

$$\begin{aligned} |m_{ee}| = \frac{1}{3}\Big| & 2m_1 \sin^2\varphi_1 + q_1 m_2 (e^{i\varphi_2}\cos\theta - \sqrt{2}\cos\varphi_1 \sin\theta)^2 \\ & + q_2 m_3 (e^{i\varphi_2}\sin\theta + \sqrt{2}\cos\theta\cos\varphi_1)^2 \Big| , \end{aligned} \tag{5.31}$$

where $q_1, q_2 = \pm 1$ appears due to the undetermined CP parity of the neutrino states encoded in the matrix Q_ν. For another admissible mixing pattern $U^{I,3}_{\rm PMNS}$, $|m_{ee}|$ is given by

$$\begin{aligned} |m_{ee}| = \frac{1}{3}\Big| & 2m_3 \sin^2\varphi_1 + q_1 m_2 (e^{i\varphi_2}\cos\theta - \sqrt{2}\cos\varphi_1 \sin\theta)^2 \\ & + q_2 m_1 (e^{i\varphi_2}\sin\theta + \sqrt{2}\cos\theta\cos\varphi_1)^2 \Big| . \end{aligned} \tag{5.32}$$

The achievable values of the effective mass $|m_{ee}|$ for both $n \to \infty$ and $n = 2$ are plotted in figure 5. Here we require the three mixing angle be within their 3σ allowed values while the neutrino mass-squared splittings are fixed at their best-fit values from Ref. [7]. We see that the majority of the experimentally allowed 3σ region of $|m_{ee}|$ can be reproduced in the limit $n \to \infty$. In the case of $n = 2$, it is remarkable that the effective mass $|m_{ee}|$ obtained from $U^{I,1}_{\rm PMNS}$ is found to be around 0.0155eV, 0.0175eV, 0.0279eV, 0.0423eV, or 0.0484eV for IO neutrino mass spectrum. These predictions are beyond the reach of the present $0\nu\beta\beta$ experiments such as GERDA [60], EXO-200 [61, 62] and KamLAND-ZEN [63]. However, the proposed facilities nEXO and KamLAND2-Zen [64] etc aim to increase the sensitivity to cover the full IO region, such that all of our patterns with this mass spectrum could be tested. For NO the effective mass $|m_{ee}|$ is much smaller than the IO case and it can even vanish for certain values of the lightest neutrino mass because of a cancellation between different terms in Eq. (5.30). Obviously exploring the NH region experimentally is beyond the reach of any planned $0\nu\beta\beta$ experiment. Even if the signals of $0\nu\beta\beta$ decays are not observed and the neutrino masses spectrum are measured to be NO by upcoming neutrino oscillation experiments [53, 54], one can still extract useful information on the Majorana phases α_{21} and α'_{31} by combining the cosmological data on the absolute neutrino mass scale and the improved measurement of θ_{12}, θ_{23} and δ_{CP} from a number of complementary neutrino oscillation experiments.

(II) $G_l = \langle abc^s d^t \rangle$, $G_\nu = Z_2^{bd^x}$, $X_{\nu\mathbf{r}} = \left\{ \rho_{\mathbf{r}}(c^{2\delta+2x+3n\tau} d^\delta), \rho_{\mathbf{r}}(bc^{2\delta+2x+3n\tau} d^{\delta+x}) \right\}$

This case differs from the previous one in the residual flavor symmetry G_l. From table 2 and table 3, we know that the charged lepton diagonalization matrix is exactly $U_l^{(4)}$. Since the neutrino mass matrix preserves the same remnant symmetry as case I, the neutrino mass matrix should take the form of Eq. (5.8), and it is diagonalized by the unitary transformation U_ν in Eq. (5.10). Using the freedom in exchanging rows and columns, we find the

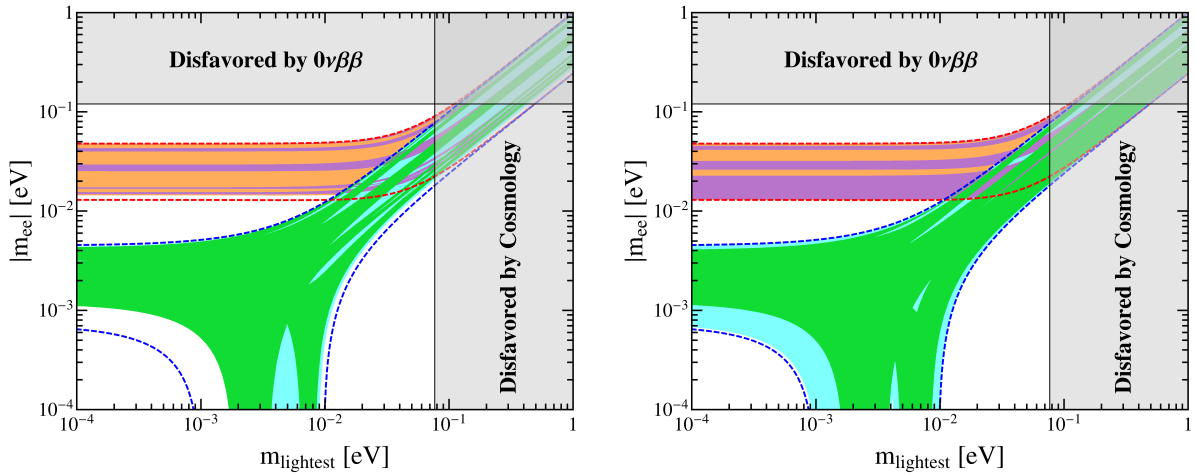

Figure 5: The possible values of the effective Majorana mass $|m_{ee}|$ as a function of the lightest neutrino mass in the case I. The left and right panels are for the mixing patterns $U^{I,1}_{\rm PMNS}$ and $U^{I,3}_{\rm PMNS}$ respectively. The red (blue) dashed lines indicate the most general allowed regions for IO (NO) neutrino mass spectrum obtained by varying the mixing parameters over the 3σ ranges [7]. The orange (cyan) areas denote the achievable values of $|m_{ee}|$ in the limit of $n \to \infty$ assuming IO (NO) spectrum. The purple and green regions are the theoretical predictions for the $D^{(1)}_{9n,3n}$ group with $n = 2$. Notice that the purple (green) region overlaps the orange (cyan) one. The present most stringent upper limits $|m_{ee}| < 0.120$ eV from EXO-200 [61, 62] and KamLAND-ZEN [63] is shown by horizontal grey band. The vertical grey exclusion band represents the current bound coming from the cosmological data of $\sum m_i < 0.230$ eV at 95% confidence level obtained by the Planck collaboration [65].

phenomenologically viable lepton mixing matrix is

$$U^{II,1}_{\rm PMNS} = \frac{1}{2}\begin{pmatrix} -\sin\theta - \sqrt{2}e^{i\varphi_3}\cos\theta & 1 & \cos\theta - \sqrt{2}e^{i\varphi_3}\sin\theta \\ -\sin\theta + \sqrt{2}e^{i\varphi_3}\cos\theta & 1 & \cos\theta + \sqrt{2}e^{i\varphi_3}\sin\theta \\ -\sqrt{2}\sin\theta & -\sqrt{2} & \sqrt{2}\cos\theta \end{pmatrix} Q_\nu \,, \tag{5.33}$$

or

$$U^{II,2}_{\rm PMNS} = \frac{1}{2}\begin{pmatrix} -\sin\theta - \sqrt{2}e^{i\varphi_3}\cos\theta & 1 & \cos\theta - \sqrt{2}e^{i\varphi_3}\sin\theta \\ -\sqrt{2}\sin\theta & -\sqrt{2} & \sqrt{2}\cos\theta \\ -\sin\theta + \sqrt{2}e^{i\varphi_3}\cos\theta & 1 & \cos\theta + \sqrt{2}e^{i\varphi_3}\sin\theta \end{pmatrix} Q_\nu \,, \tag{5.34}$$

where

$$\varphi_3 = \frac{s - t + 2x + \delta}{3n}\pi \,, \tag{5.35}$$

and its possible values are

$$\varphi_3 \ (\text{mod}\ 2\pi) = 0, \frac{1}{3n}\pi, \frac{2}{3n}\pi, \ldots, \frac{6n-1}{3n}\pi \,. \tag{5.36}$$

It is easy to check that $U^{II,1}_{\rm PMNS}$ as well as $U^{II,2}_{\rm PMNS}$ have the symmetry property

$$\begin{aligned} U^{II,1}_{\rm PMNS}(\theta, \varphi_3 + \pi) &= U^{II,1}_{\rm PMNS}(-\theta, \varphi_3)\text{diag}(-1,1,1), \\ U^{II,2}_{\rm PMNS}(\theta, \varphi_3 + \pi) &= U^{II,2}_{\rm PMNS}(-\theta, \varphi_3)\text{diag}(-1,1,1) \,. \end{aligned} \tag{5.37}$$

We see that the second column of the PMNS matrix is $(1, 1, -\sqrt{2})/2$ or $(1, -\sqrt{2}, 1)/2$ in this case. For the mixing pattern $U^{II,1}_{\rm PMNS}$, the three lepton mixing angles are found to be

$$\sin^2\theta_{13} = \frac{1}{8}\left(3 - \cos 2\theta - 2\sqrt{2}\sin 2\theta\cos\varphi_3\right) ,$$

$$\sin^2\theta_{12}=\frac{2}{5+\cos 2\theta+2\sqrt{2}\sin 2\theta\cos\varphi_3},$$
$$\sin^2\theta_{23}=\frac{3-\cos 2\theta+2\sqrt{2}\sin 2\theta\cos\varphi_3}{5+\cos 2\theta+2\sqrt{2}\sin 2\theta\cos\varphi_3}, \tag{5.38}$$

which fulfill the following sum rules

$$4\sin^2\theta_{12}\cos^2\theta_{13}=1,$$
$$\cos^2\theta_{13}\cos^2\theta_{23}=\frac{\cos 2\theta_{13}+2\cos^2\varphi_3\pm 2\cos\varphi_3\sqrt{6\sin^2\theta_{13}-8\sin^4\theta_{13}-\sin^2\varphi_3}}{1+8\cos^2\varphi_3}. \tag{5.39}$$

Given the 3σ range of θ_{13}, the solar mixing angle θ_{12} is determined to lie in the region of $0.254\leq\sin^2\theta_{12}\leq 0.258$ which is rather close to its 3σ lower limit 0.259 [7]. However, this mixing pattern is a good leading order approximation because accordance with the experimental data could be easily achieved in a concrete model after higher order corrections contributions are included. We plot the 1σ, 2σ and 3σ contour regions for $\sin^2\theta_{ij}$ with $ij=12,13,23$ in the $\varphi_3-\theta$ plane in figure 6. Obviously the most stringent constraint comes from the precisely measured reactor angle θ_{13}. Moreover, the three CP rephasing invariants are given by

$$|J_{CP}|=\frac{1}{8\sqrt{2}}\left|\sin 2\theta\sin\varphi_3\right|,$$
$$|I_1|=\frac{1}{8\sqrt{2}}\left|(\sin 2\theta+2\sqrt{2}\cos^2\theta\cos\varphi_3)\sin\varphi_3\right|,$$
$$|I_2|=\frac{1}{8\sqrt{2}}\left|(\sin 2\theta-2\sqrt{2}\cos 2\theta\cos\varphi_3)\sin\varphi_3\right|. \tag{5.40}$$

The three CP violation phases extracted from these invariants depend on θ and φ_3. The predictions for $|\sin\delta_{CP}|$, $|\sin\alpha_{21}|$ and $|\sin\alpha'_{31}|$ are plotted in figure 7, where the black areas represent the regions in which all three lepton mixing angles are in the experimentally preferred 3σ ranges. To accommodate the experimental data of mixing angles [7], both δ_{CP} and α_{21} can not be maximal. The values of $|\sin\delta_{CP}|$ and $|\sin\alpha_{21}|$ are bounded from above with $|\sin\delta_{CP}|\leq 0.895$ and $|\sin\alpha_{21}|\leq 0.545$.

The second PMNS matrix $U^{II,2}_{\rm PMNS}$ can be obtained from $U^{II,1}_{\rm PMNS}$ by exchanging the second and third rows. Therefore $U^{II,2}_{\rm PMNS}$ and $U^{II,1}_{\rm PMNS}$ give rise to the same reactor and solar mixing angles and the Majorana phases, while the atmospheric angle changes from θ_{23} to $\pi/2-\theta_{23}$ and the Dirac phase changes from δ_{CP} to $\pi+\delta_{CP}$. The achievable values of the mixing parameters for each $D^{(1)}_{9n,3n}$ group are displayed in figure 8.

For the first two smallest $D^{(1)}_{9n,3n}$ group with $n=1,2$. The possible values of φ_3 are $0,\frac{\pi}{3},\ldots,\frac{5\pi}{3}$ for $n=1$ and $0,\frac{\pi}{6},\ldots,\frac{11\pi}{6}$ for $n=2$. We find that agreement with experimental data can be achieved for $\varphi_3=0$ or π. Due to symmetry relation in Eq. (5.37), $\varphi_3=0$ and $\varphi_3=\pi$ should give rise to the same predictions for the mixing parameters. Therefore it is sufficient to focus on $\varphi_3=0$, and the best fitting results are listed in table 8. Notice that all the three CP phases are predicted to take CP conserving values $\{\delta_{CP},\alpha_{21},\alpha_{31}\}\subseteq\{0,\pi\}$. The same conclusion can be drawn from figure 8.

As regards the neutrinoless double beta decay, both $U^{II,1}_{\rm PMNS}$ and $U^{II,2}_{\rm PMNS}$ yield the same effective Majorana mass:

$$|m_{ee}|=\frac{1}{4}\left|m_1(\sin\theta+\sqrt{2}e^{i\varphi_3}\cos\theta)^2+q_1m_2+q_2m_3(\cos\theta-\sqrt{2}e^{i\varphi_3}\sin\theta)^2\right| \tag{5.41}$$

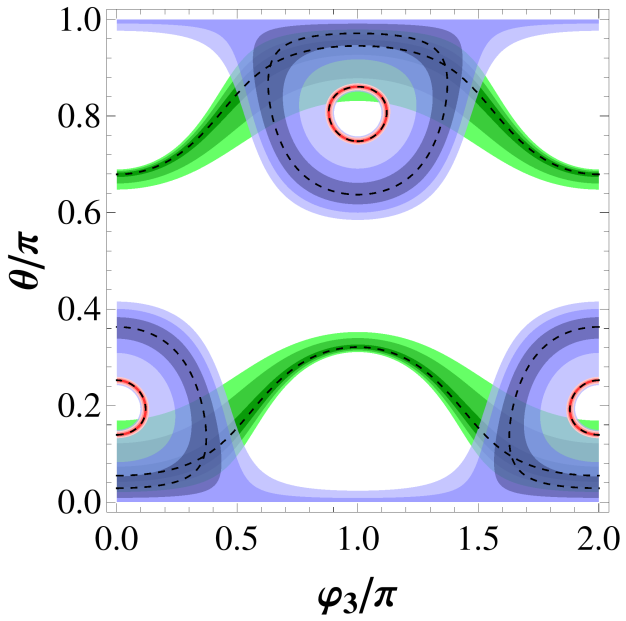

Figure 6: The contour regions of the three mixing angles in the case II. The red, blue and green areas denote the predictions for $\sin^2\theta_{13}$, $\sin^2\theta_{12}$ and $\sin^2\theta_{23}$ respectively. The allowed 1σ, 2σ and 3σ regions of each mixing angle are represented by different shadings. Here we take the 3σ lower limit of $\sin^2\theta_{12}$ to be 0.254 instead of 0.259 given by Ref. [7]. The best fit values of the mixing angles are indicated by dotted lines.

Case II									
$n=1$ and $n=2$									
	φ_3	θ_{bf}	χ^2_{min}	$\sin^2\theta_{13}$	$\sin^2\theta_{12}$	$\sin^2\theta_{23}$	$\lvert\sin\delta_{CP}\rvert$	$\lvert\sin\alpha_{21}\rvert$	$\lvert\sin\alpha'_{31}\rvert$
$U^{II,1}_{\rm PMNS}$	0	0.433 (0.435)	27.807 (10.086)	0.0246 (0.0242)	0.256 (0.256)	0.578 (0.579)	0 (0)	0 (0)	0 (0)
$U^{II,2}_{\rm PMNS}$		0.436 (0.434)	9.865 (10.455)	0.0238 (0.0244)	0.256 (0.256)	0.421 (0.422)			

Table 8: Results of the χ^2 analysis for $n=1,2$ in the case II. The χ^2 function has a global minimum χ^2_{min} at the best fit value θ_{bf} for θ. We give the values of the mixing angles and CP violation phases for $\theta=\theta_{bf}$. The values given in parentheses denote the results for the IO neutrino mass spectrum.

with $q_1, q_2 = \pm 1$. We show the predicted values of $|m_{ee}|$ in figure 9. Notice that for IO spectrum $|m_{ee}|$ can be either 0.0233eV or 0.0483eV which are accessible to the next generation $0\nu\beta\beta$ experiments. In the case of NO spectrum, $|m_{ee}|$ strongly depends on the lightest neutrino mass and CP parity, and it can be vanishing for certain values of the lightest neutrino mass.

(III) $G_l = \langle ac^s d^t\rangle$, $G_\nu = Z_2^{c^{9n/2}}$, $X_{\nu\mathbf{r}} = \left\{\rho_{\mathbf{r}}(c^\gamma d^\delta)\right\}$

In this case, n should be even in order to have a Z_2 subgroup generated by $c^{9n/2}$. The neutrino mass matrix invariant under the assumed residual symmetry is found to take the form

$$m_\nu = \begin{pmatrix} m_{11}e^{-\frac{i2\pi\gamma}{9n}} & m_{12}e^{-\frac{i\pi(2\gamma-3\delta)}{9n}} & 0 \\ m_{12}e^{-\frac{i\pi(2\gamma-3\delta)}{9n}} & m_{22}e^{-\frac{i2\pi(\gamma-3\delta)}{9n}} & 0 \\ 0 & 0 & m_{33}e^{\frac{i2\pi(2\gamma-3\delta)}{9n}} \end{pmatrix}, \tag{5.42}$$

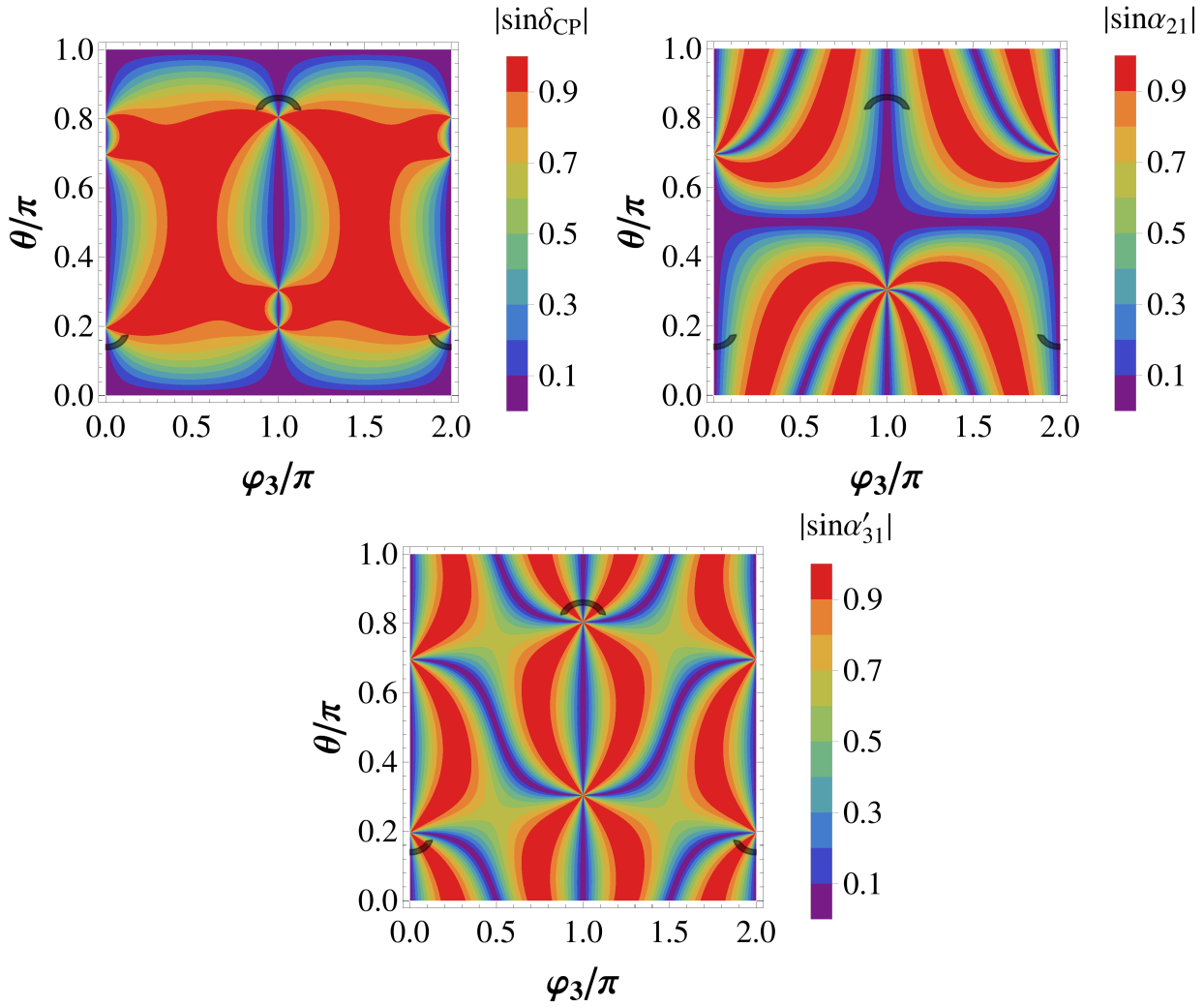

Figure 7: The contour plots of $|\sin\delta_{CP}|$, $|\sin\alpha_{21}|$ and $|\sin\alpha'_{31}|$ in the $\varphi_3-\theta$ plane in the case II. The black areas represent the regions in which the lepton mixing angles are compatible with experimental data at 3σ level, and it can be read out from figure 6.

where m_{11}, m_{12}, m_{13} and m_{22} are real. It is diagonalized by the unitary matrix

$$U_\nu = \begin{pmatrix} e^{\frac{i\pi\gamma}{9n}}\cos\theta & e^{\frac{i\pi\gamma}{9n}}\sin\theta & 0 \\ -e^{\frac{i\pi(\gamma-3\delta)}{9n}}\sin\theta & e^{\frac{i\pi(\gamma-3\delta)}{9n}}\cos\theta & 0 \\ 0 & 0 & e^{-\frac{i\pi(2\gamma-3\delta)}{9n}} \end{pmatrix} Q_\nu \,, \tag{5.43}$$

with the rotation angle θ satisfying

$$\tan 2\theta = \frac{2m_{12}}{m_{22}-m_{11}} \,. \tag{5.44}$$

The light neutrino masses are

$$\begin{aligned} m_1 &= \frac{1}{2}\left| m_{11}+m_{22}-\frac{m_{22}-m_{11}}{\cos 2\theta}\right| , \\ m_2 &= \frac{1}{2}\left| m_{11}+m_{22}+\frac{m_{22}-m_{11}}{\cos 2\theta}\right| , \\ m_3 &= |m_{33}| \,. \end{aligned}$$

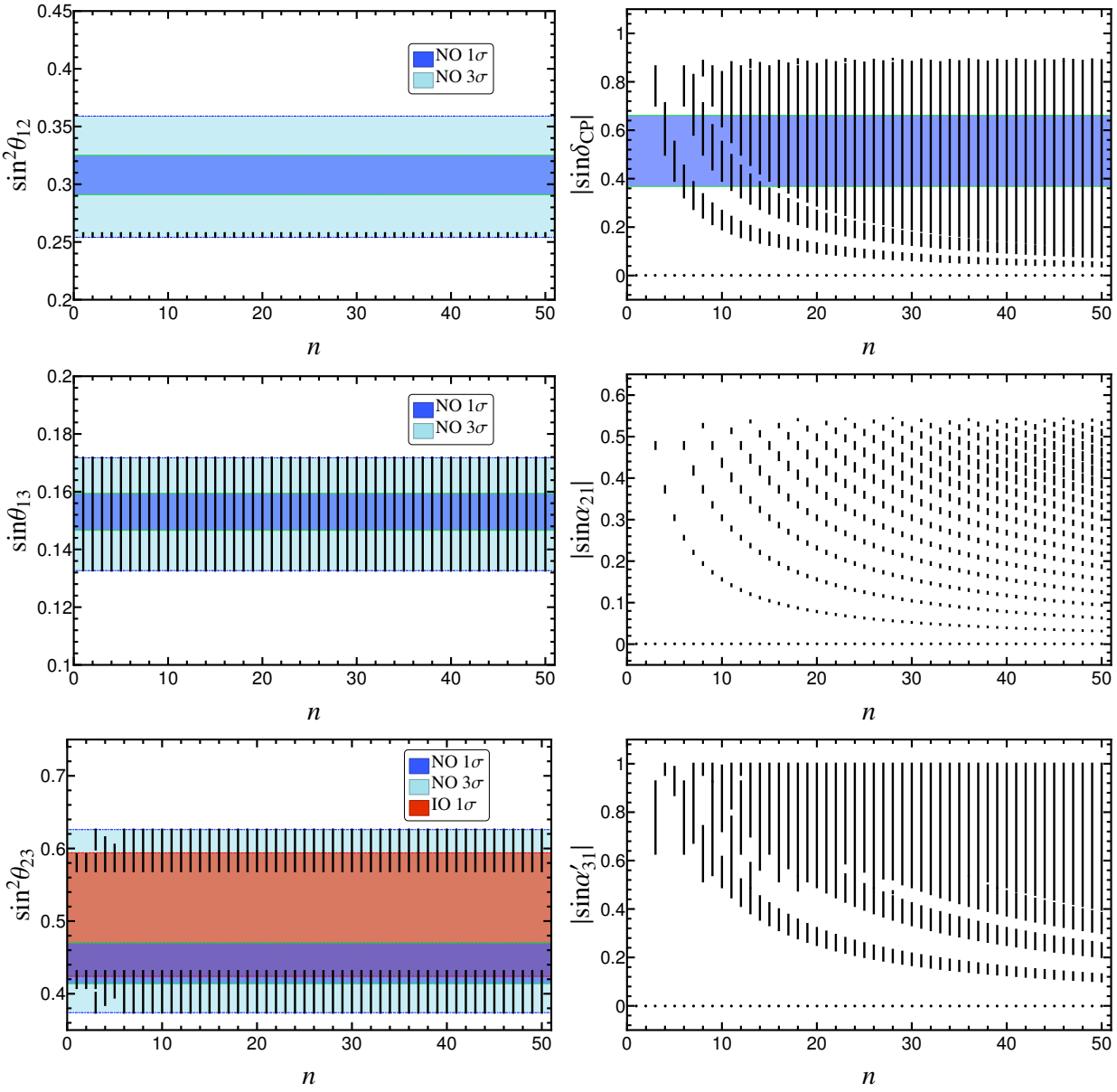

Figure 8: The possible values of $\sin^2\theta_{12}$, $\sin\theta_{13}$, $\sin^2\theta_{23}$, $|\sin\delta_{CP}|$, $|\sin\alpha_{21}|$ and $|\sin\alpha'_{31}|$ with respect to n for the mixing pattern $U^{II,1}_{\rm PMNS}$ and $U^{II,2}_{\rm PMNS}$ in the case II, where the three lepton mixing angles are required to be within the experimentally preferred 3σ ranges. The 1σ and 3σ regions of the three neutrino mixing angles are adapted from global fit [7]. Here we take the 3σ lower limit of $\sin^2\theta_{12}$ to be 0.254 instead of 0.259 given by Ref. [7].

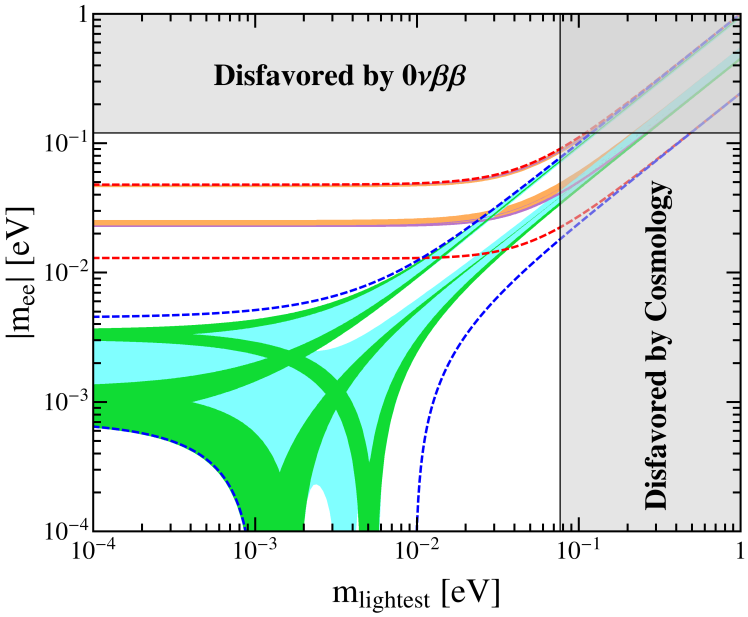

Figure 9: The possible values of the effective Majorana mass $|m_{ee}|$ as a function of the lightest neutrino mass in the case II. The red (blue) dashed lines indicate the most general allowed regions for IO (NO) neutrino mass spectrum obtained by varying the mixing parameters over the 3σ ranges [7]. The orange (cyan) areas denote the achievable values of $|m_{ee}|$ in the limit of $n \to \infty$ assuming IO (NO) spectrum. The purple and green regions are the theoretical predictions for the $D^{(1)}_{9n,3n}$ group with $n = 2$. Notice that the purple (green) region overlaps the orange (cyan) one. The present most stringent upper limits $|m_{ee}| < 0.120$ eV from EXO-200 [61, 62] and KamLAND-ZEN [63] is shown by horizontal grey band. The vertical grey exclusion band represents the current bound coming from the cosmological data of $\sum m_i < 0.230$ eV at 95% confidence level obtained by the Planck collaboration [65].

As the residual flavor symmetry in the charged lepton sector is $G_l = \langle ac^s d^t \rangle$, the charged lepton diagonalization matrix is $U_l^{(3)}$ shown in table 2. Thus the lepton mixing matrix is determined to be

$$U^{III}_{\rm PMNS} = \frac{1}{\sqrt{3}} \begin{pmatrix} \cos\theta - e^{i\varphi_4}\sin\theta & 1 & \sin\theta + e^{i\varphi_4}\cos\theta \\ \omega\cos\theta - \omega^2 e^{i\varphi_4}\sin\theta & 1 & \omega\sin\theta + \omega^2 e^{i\varphi_4}\cos\theta \\ \omega^2\cos\theta - \omega e^{i\varphi_4}\sin\theta & 1 & \omega^2\sin\theta + \omega e^{i\varphi_4}\cos\theta \end{pmatrix} {\rm diag}(e^{i\varphi_5}, 1, e^{i\varphi_5}) Q_\nu \,, \tag{5.45}$$

where

$$\varphi_4 = \frac{2s - 6t - 3\delta}{9n}\pi, \qquad \varphi_5 = \frac{2s + 3\gamma - 3\delta}{9n}\pi \,. \tag{5.46}$$

Notice that φ_4 and φ_5 are not completely independent, and they can take the following discrete values:

$$\begin{aligned} &\varphi_4 \ (\text{mod}\ 2\pi) = 0, \frac{1}{9n}\pi, \frac{2}{9n}\pi, \ldots, \frac{18n-1}{9n}\pi \,, \\ &\varphi_4 - \varphi_5 \ (\text{mod}\ 2\pi) = 0, \frac{1}{3n}\pi, \frac{2}{3n}\pi, \ldots, \frac{6n-1}{3n}\pi \,. \end{aligned} \tag{5.47}$$

We easily see that one column of the PMNS matrix is $(1,1,1)^T/\sqrt{3}$ which can only be the second column vector in order to accommodate the experimental data of lepton mixing angles. The permutations of the PMNS matrix which leave the second column unchanged don't lead to physically different results. From Eq. (5.45) we can extract the mixing angles

$$\sin^2\theta_{13} = \frac{1}{3}\left[1 + \sin 2\theta \cos\varphi_4\right] \,,$$

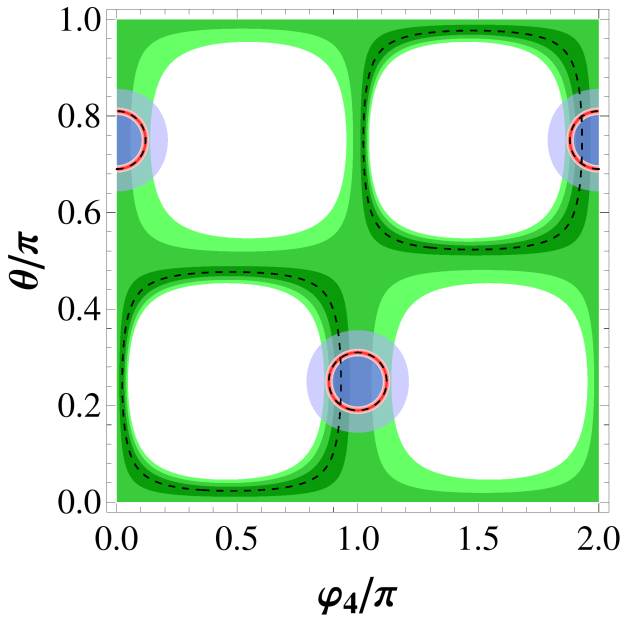

Figure 10: The contour regions of the three mixing angles in the case III. The red, blue and green areas denote the predictions for $\sin^2\theta_{13}$, $\sin^2\theta_{12}$ and $\sin^2\theta_{23}$ respectively. The allowed 1σ, 2σ and 3σ regions of each mixing angle are represented by different shadings. The best fit values of the mixing angles are indicated by dotted lines. Note that both the 1σ range and the best fit value of θ_{12} can not be achieved in this case because of the sum rule in Eq. (5.49a).

$$\begin{aligned}
\sin^2\theta_{12} &= \frac{1}{2-\sin 2\theta\cos\varphi_4}\,, \\
\sin^2\theta_{23} &= \frac{1-\sin 2\theta\sin\left(\varphi_4+\pi/6\right)}{2-\sin 2\theta\cos\varphi_4}\,.
\end{aligned} \tag{5.48}$$

Then we can derive the following sum rules among the mixing angles

$$3\sin^2\theta_{12}\cos^2\theta_{13} = 1, \tag{5.49a}$$

$$\left(1-3\sin^2\theta_{13}\right)\tan\varphi_4 + \sqrt{3}\cos^2\theta_{13}\cos 2\theta_{23} = 0\,. \tag{5.49b}$$

The correlation of Eq. (5.49a) yields $\sin^2\theta_{12} \simeq 0.341$ for the best fit value $\sin^2\theta_{13} = 0.0234$ [7]. Inputting the 3σ ranges of the atmospheric as well reactor mixing angles in Eq. (5.49b), we find the phase difference φ_4 should vary in the interval

$$\varphi_4 \in [0, 0.138\pi] \cup [0.862\pi, 1.138\pi] \cup [1.862\pi, 2\pi]\,. \tag{5.50}$$

As shown in Eq. (5.48), all the three mixing angles are expressed in terms of φ_4 and θ. The contour regions for $\sin^2\theta_{ij}$ in the plane of φ_4 and θ are displayed in figure 10. One can see that agreement with experimental data can be achieved for appropriate values of φ_4 and θ. Furthermore, the CP invariants are given by

$$\begin{aligned}
|J_{CP}| &= \frac{1}{6\sqrt{3}}\left|\cos 2\theta\right|\,, \\
|I_1| &= \frac{1}{9}\left|\cos^2\theta\sin 2\varphi_5 - \sin 2\theta\sin(\varphi_4+2\varphi_5) + \sin^2\theta\sin(2\varphi_4+2\varphi_5)\right|\,, \\
|I_2| &= \frac{1}{9}\left|\cos 2\theta\sin 2\varphi_4\right|\,.
\end{aligned} \tag{5.51}$$

Thus both δ_{CP} and α'_{31} only depend on φ_4 and θ while the Majorana phase α_{21} is dependent on all the three parameters φ_4, φ_5 and θ. The predictions for $|\sin\delta_{CP}|$ and $|\sin\alpha'_{31}|$ are shown in the plane θ versus φ_4 in figure 11. One can see that all values of the CP phases are possible in the regions where the lepton mixing angles are compatible with the experimental data at 3σ level. Moreover, the possible values of the mixing angles and CP phases for each $D^{(1)}_{9n,3n}$ group until $n = 50$ are plotted in figure 12.

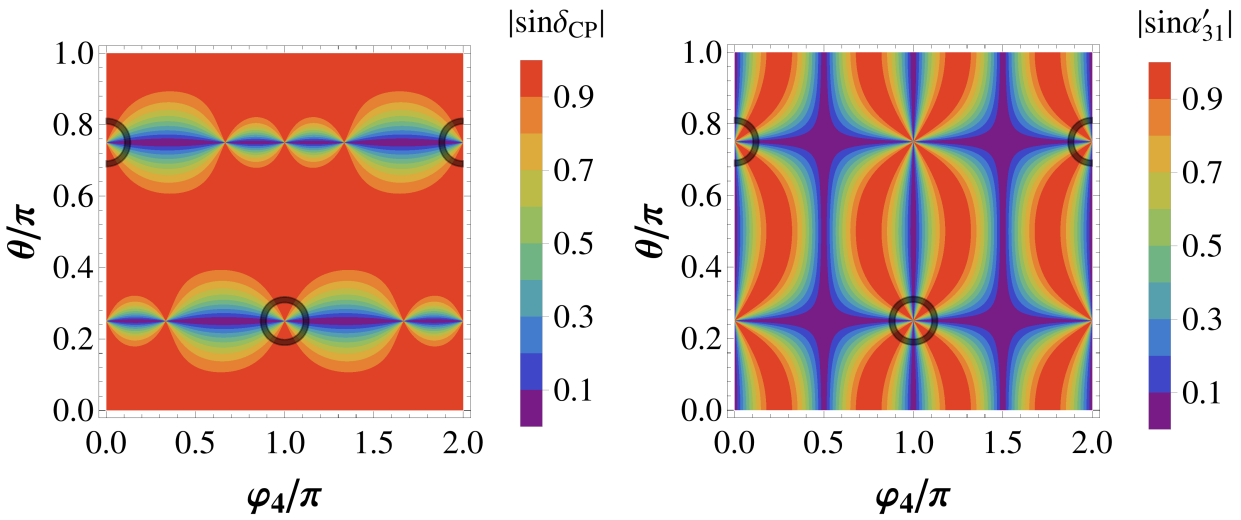

Figure 11: The contour plots of $|\sin\delta_{CP}|$ and $|\sin\alpha'_{31}|$ in the case III. The black areas represent the regions in which the lepton mixing angles are compatible with experimental data at 3σ level, and it can be read out from figure 10.

Then we proceed to study the phenomenologically viable mixing patterns which can be derived from the $D^{(1)}_{9n,3n}$ group with $n = 2$. Note that the index n has to be even in this case. We can check that the PMNS matrix given by Eq. (5.45) has the following symmetry properties

$$\begin{aligned} &U^{III}_{\rm PMNS}(\theta,\pi+\varphi_4,\varphi_5) = U^{III}_{\rm PMNS}(-\theta,\varphi_4,\varphi_5){\rm diag}(1,1,-1),\\ &U^{III}_{\rm PMNS}(\theta,\varphi_4,\pi/2+\varphi_5) = U^{III}_{\rm PMNS}(\theta,\varphi_4,\varphi_5){\rm diag}(i,1,i)\,, \end{aligned} \tag{5.52}$$

where the diagonal matrix on the right-handed side can be absorbed into Q_ν. That is to say, both $U^{III}_{\rm PMNS}(\theta,\pi+\varphi_4,\varphi_5)$ and $U^{III}_{\rm PMNS}(\theta,\varphi_4,\pi/2+\varphi_5)$ give rise to the same predictions for the lepton mixing parameters as $U^{III}_{\rm PMNS}(\theta,\varphi_4,\varphi_5)$ up to redefinition of the free parameter θ. Hence we can take the fundamental intervals of φ_4 and φ_5 to be $[0,\pi)$ and $[0,\pi/2)$ respectively. The allowed values of φ_4 are 0, $\pi/18$, $\pi/9$, ..., $17\pi/9$, $35\pi/18$. However, only φ_4 (mod π) $= 0$, $\pi/18$, $\pi/9$, $8\pi/9$ and $17\pi/18$ are within the range of Eq. (5.50) such that they can give a good fit to the experimental data. The results of the χ^2 analysis are summarized in table 9. Notice that the best fitting values of the mixing angles and $|\sin\delta_{CP}|$, $|\sin\alpha'_{31}|$ are dependent on φ_4 while the best fitting value of $|\sin\alpha_{21}|$ depends on φ_4 as well as φ_5. The mixing patterns with the same φ_4 but different φ_5 are expected to be distinguished by some rare processes which are sensitive to the Majorana phases such as the neutrinoless double decay and the radiative emission of neutrino pair in atoms [66]. In this case, the effective Majorana mass $|m_{ee}|$ is predicted to be

$$|m_{ee}| = \frac{1}{3}\left|m_1(\cos\theta - e^{i\varphi_4}\sin\theta)^2 + q_1 m_2 e^{-2i\varphi_5} + q_2 m_3(\sin\theta + e^{i\varphi_4}\cos\theta)^2\right|, \tag{5.53}$$

where $q_1, q_2 = \pm 1$. The numerical results are shown in figure 13.

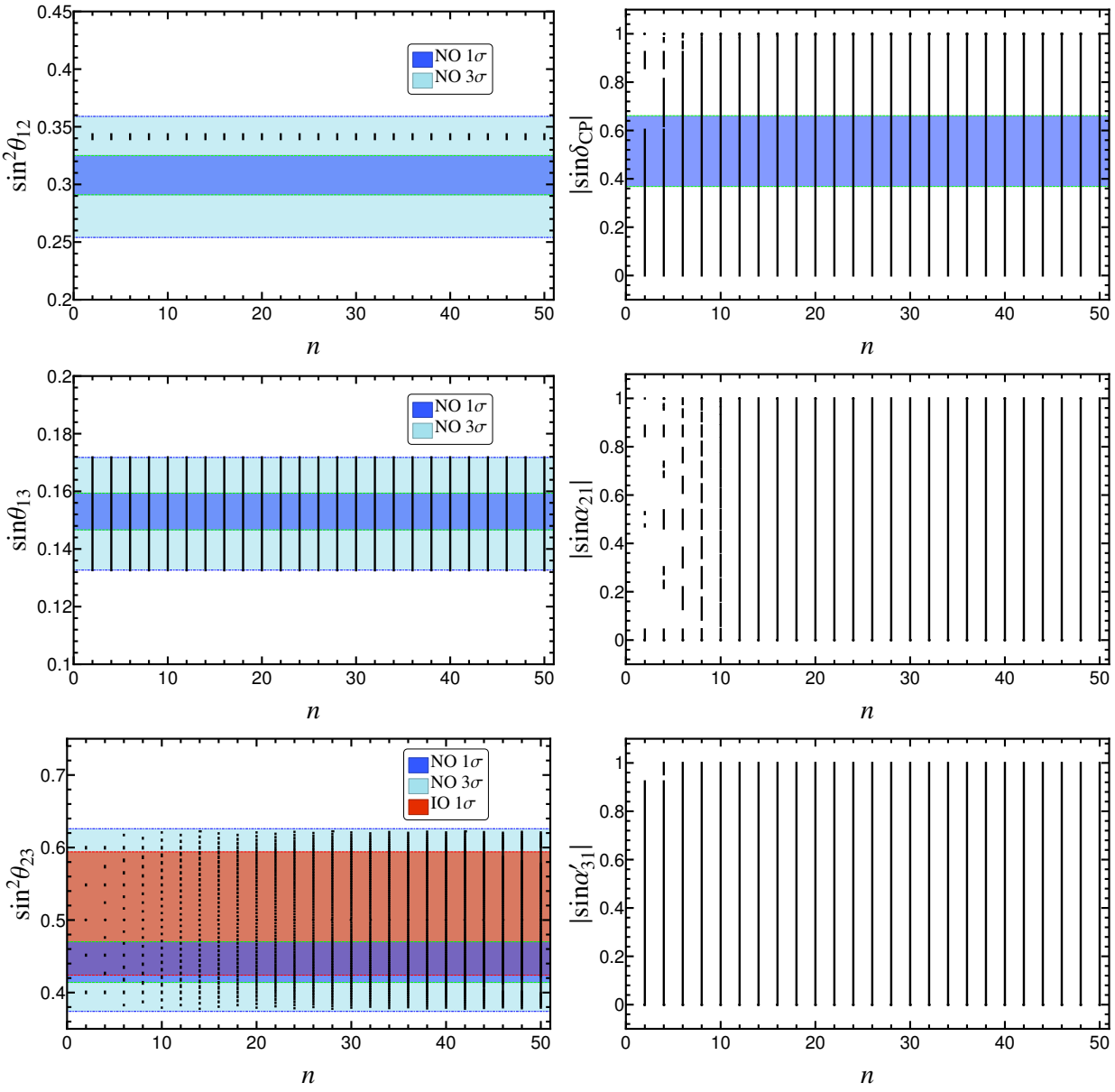

Figure 12: The possible values of $\sin^2\theta_{12}$, $\sin\theta_{13}$, $\sin^2\theta_{23}$, $|\sin\delta_{CP}|$, $|\sin\alpha_{21}|$ and $|\sin\alpha'_{31}|$ with respect to n for the mixing pattern $U^{III}_{\rm PMNS}$ in the case III, where the three lepton mixing angles are required to be within the experimentally preferred 3σ ranges. The 1σ and 3σ regions of the three neutrino mixing angles are adapted from global fit [7].

Case III									
$n=2$									
φ_4	φ_5	θ_{bf}	χ^2_{min}	$\sin^2\theta_{13}$	$\sin^2\theta_{12}$	$\sin^2\theta_{23}$	$\lvert\sin\delta_{CP}\rvert$	$\lvert\sin\alpha_{21}\rvert$	$\lvert\sin\alpha'_{31}\rvert$
0	$0, \frac{\pi}{6}, \frac{\pi}{3}$	2.168 (2.166)	7.480 (3.987)	0.0233 (0.0238)	0.341 (0.341)	0.5 (0.5)	1(1)	$\lvert\sin 2\varphi_5\rvert$ ($\lvert\sin 2\varphi_5\rvert$)	0 (0)
$\frac{\pi}{18}$	$\frac{\pi}{18}$	2.189 (2.186)	15.247 (4.334)	0.0233 (0.0238)	0.341 (0.341)	0.548 (0.548)	0.899 (0.902)	0.525 (0.526)	0.833 (0.827)
	$\frac{2\pi}{9}$							0.9996 (0.9996)	
	$\frac{7\pi}{18}$							0.474 (0.474)	
$\frac{17\pi}{18}$	$\frac{\pi}{9}$	0.953 (0.955)	4.029 (3.894)	0.0232 (0.0238)	0.341 (0.341)	0.452 (0.452)	0.899 (0.902)	0.474 (0.474)	0.834 (0.827)
	$\frac{5\pi}{18}$							0.9996 (0.9996)	
	$\frac{4\pi}{9}$							0.525 (0.526)	
$\frac{\pi}{9}$	$\frac{\pi}{9}$	2.429 (2.433)	28.249 (4.970)	0.0234 (0.0238)	0.341 (0.341)	0.600 (0.600)	0.400 (0.422)	0.853 (0.852)	0.685 (0.716)
	$\frac{5\pi}{18}$							0.879 (0.879)	
	$\frac{4\pi}{9}$							0.0255 (0.0272)	
$\frac{8\pi}{9}$	$\frac{\pi}{18}$	0.714 (0.708)	6.432 (7.023)	0.0233 (0.0239)	0.341 (0.341)	0.400 (0.400)	0.397 (0.424)	0.0253 (0.0274)	0.680 (0.719)
	$\frac{2\pi}{9}$							0.878 (0.879)	
	$\frac{7\pi}{18}$							0.853 (0.852)	

Table 9: Results of the χ^2 analysis for $n=2$ in the case III. The χ^2 function has a global minimum χ^2_{min} at the best fit value θ_{bf} for θ. We give the values of the mixing angles and CP violation phases for $\theta=\theta_{bf}$. The values given in parentheses denote the results for the IO neutrino mass spectrum. Notice that $\theta=\pi/2-\theta_{bf}$ gives rise to the same results for the mixing parameters except $|\sin\alpha_{21}|$, because the PMNS matrix $U^{III}_{\rm PMNS}$ fulfills $U^{III}_{\rm PMNS}(\theta,\varphi_4,\varphi_5)=[U^{III}_{\rm PMNS}(\pi/2-\theta,\varphi_4,-\varphi_4-\varphi_5)]^*$.

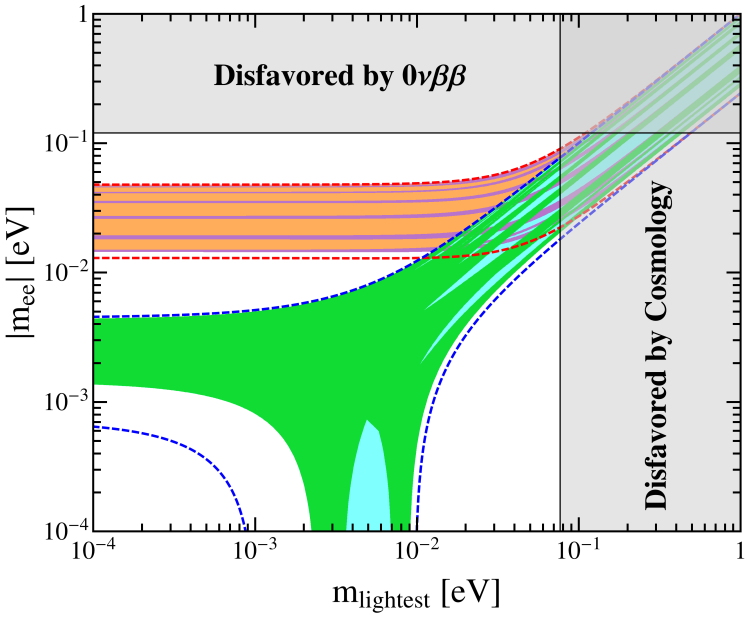

Figure 13: The possible values of the effective Majorana mass $|m_{ee}|$ as a function of the lightest neutrino mass in the case III. The red (blue) dashed lines indicate the most general allowed regions for IO (NO) neutrino mass spectrum obtained by varying the mixing parameters over the 3σ ranges [7]. The orange (cyan) areas denote the achievable values of $|m_{ee}|$ in the limit of $n \to \infty$ assuming IO (NO) spectrum. The purple and green regions are the theoretical predictions for the $D^{(1)}_{9n,3n}$ group with $n = 2$. Notice that the purple (green) region overlaps the orange (cyan) one. The present most stringent upper limits $|m_{ee}| < 0.120$ eV from EXO-200 [61, 62] and KamLAND-ZEN [63] is shown by horizontal grey band. The vertical grey exclusion band represents the current bound coming from the cosmological data of $\sum m_i < 0.230$ eV at 95% confidence level obtained by the Planck collaboration [65].

(IV) $G_l = \langle ac^s d^t \rangle$, $G_\nu = Z_2^{c^{9n/2}}$, $X_{\nu\mathbf{r}} = \{\rho_{\mathbf{r}}(a^2 b c^\gamma)\}$

This case differs from the case III in the residual CP transformation of the neutrino sector. The group index n has to be an even integer as well. In the same way, the neutrino mass matrix invariant under the assumed remnant symmetry is determined to be

$$m_\nu = \begin{pmatrix} m_{11} e^{-i\left(\theta + \frac{4\pi\gamma}{9n}\right)} & m_{12} e^{-\frac{2i\pi\gamma}{9n}} & 0 \\ m_{12} e^{-\frac{2i\pi\gamma}{9n}} & m_{11} e^{i\theta} & 0 \\ 0 & 0 & m_{33} e^{\frac{4i\pi\gamma}{9n}} \end{pmatrix} , \tag{5.54}$$

where m_{11}, m_{12}, m_{33} and θ are real parameters. The unitary transformation U_ν which diagonalizes m_ν is of the form

$$U_\nu = \frac{1}{\sqrt{2}} \begin{pmatrix} e^{i\left(\frac{\theta}{2} + \frac{2\pi\gamma}{9n}\right)} & e^{i\left(\frac{\theta}{2} + \frac{2\pi\gamma}{9n}\right)} & 0 \\ -e^{-i\frac{\theta}{2}} & e^{-i\frac{\theta}{2}} & 0 \\ 0 & 0 & \sqrt{2} e^{-\frac{2i\pi\gamma}{9n}} \end{pmatrix} Q_\nu \, . \tag{5.55}$$

The light neutrino masses are given by

$$m_1 = |m_{11} - m_{12}| \, , \quad m_2 = |m_{11} + m_{12}| \, , \quad m_3 = |m_{33}| \, . \tag{5.56}$$

Then we find that the PMNS matrix takes the form

$$U^{IV}_{\rm PMNS} = \frac{1}{\sqrt{3}} \begin{pmatrix} \sqrt{2} e^{i\varphi_7} \sin\left(\varphi_6 + \frac{\theta}{2}\right) & 1 & \sqrt{2} e^{i\varphi_7} \cos\left(\varphi_6 + \frac{\theta}{2}\right) \\ \sqrt{2} e^{i\varphi_7} \cos\left(\varphi_6 + \frac{\theta}{2} + \frac{\pi}{6}\right) & 1 & -\sqrt{2} e^{i\varphi_7} \sin\left(\varphi_6 + \frac{\theta}{2} + \frac{\pi}{6}\right) \\ -\sqrt{2} e^{i\varphi_7} \cos\left(\varphi_6 + \frac{\theta}{2} - \frac{\pi}{6}\right) & 1 & \sqrt{2} e^{i\varphi_7} \sin\left(\varphi_6 + \frac{\theta}{2} - \frac{\pi}{6}\right) \end{pmatrix} Q_\nu \, , \tag{5.57}$$

with

$$\varphi_6=\frac{\gamma-s+3t}{9n}\pi, \qquad \varphi_7=\frac{\gamma+s-t}{3n}\pi\,. \tag{5.58}$$

Obviously the second column of the PMNS matrix is $\left(1/\sqrt{3},1/\sqrt{3},1/\sqrt{3}\right)^T$ as well. The mixing parameters extracted from Eq. (5.57) are:

$$\begin{aligned}
&\sin^2\theta_{13}=\frac{1}{3}\left[1+\cos(\theta+2\varphi_6)\right], \quad \sin^2\theta_{12}=\frac{1}{2-\cos(\theta+2\varphi_6)}\,,\\
&\sin^2\theta_{23}=\frac{1+\sin\left(\theta+2\varphi_6-\pi/6\right)}{2-\cos(\theta+2\varphi_6)}\,,\\
&\sin\delta_{CP}=\sin\alpha_{31}=0, \qquad |\sin\alpha_{21}|=|\sin(2\varphi_7)|\,.
\end{aligned} \tag{5.59}$$

Notice that the mixing angles depend on the combination $\theta+2\varphi_6$ so that the values of the parameter φ_6 is irrelevant. Moreover, we can see that the mixing angles fulfill the following sum rules

$$3\cos^2\theta_{13}\sin^2\theta_{12}=1, \qquad 2\sin^2\theta_{23}=1\pm\tan\theta_{13}\sqrt{2-\tan^2\theta_{13}}\,. \tag{5.60}$$

The 3σ range of the reactor angle $0.0176\leq\sin^2\theta_{13}\leq 0.0295$ [7] can be reproduced for

$$\theta+2\varphi_6\in[0.865\pi,0.896\pi]\cup[1.104\pi,1.135\pi]\,. \tag{5.61}$$

Thus the solar and atmospheric mixing angles are determined to be within the intervals

$$\begin{aligned}
&0.339\leq\sin^2\theta_{12}\leq 0.343\,,\\
&0.378\leq\sin^2\theta_{23}\leq 0.406, \quad \text{or} \quad 0.594\leq\sin^2\theta_{23}\leq 0.622\,,
\end{aligned} \tag{5.62}$$

which are in accordance with the experimentally measured values. Note that the atmospheric angle θ_{23} deviates from maximal mixing. These predictions can be test by JUNO [53] and forthcoming long baseline neutrino oscillation experiments. As regards the CP violating phases, both Dirac phase δ_{CP} and the Majorana phase α_{31} are conserved while another Majorana phase α_{21} can take the discrete values of 0, $\frac{2}{3n}\pi$, $\frac{4}{3n}\pi$, ..., $\frac{6n-2}{3n}\pi$. In this case, the effective Majorana mass $|m_{ee}|$ takes a simple form,

$$|m_{ee}|=\frac{1}{3}\Big|2m_1\sin^2\left(\varphi_6+\theta/2\right)+q_1m_2e^{2i\varphi_7}+2q_2m_3\cos^2\left(\varphi_6+\theta/2\right)\Big|\,. \tag{5.63}$$

The predictions on $|m_{ee}|$ are plotted in figure 14. For the IO spectrum and $n=2$, we find $|m_{ee}|$ can take a few discrete values and these results can be tested in forthcoming $0\nu\beta\beta$ experiments.

6 Lepton mixing from a variant of semidirect approach

In contrast with semidirect approach discussed in section 5, we shall assume that the original symmetry $D^{(1)}_{9n,3n}\rtimes H_{CP}$ is broken down to $Z_2\times CP$ in the charged lepton sector, and the residual symmetry of the neutrino mass matrix is $K_4\rtimes H^{\nu}_{CP}$, where K_4 is a Klein subgroup of $D^{(1)}_{9n,3n}$. Since each order 2 element of the $D^{(1)}_{9n,3n}$ group is conjugate to either bd^x or $c^{9n/2}$, as shown in Eq. (5.4) and Eq. (5.5), it is sufficient to discuss the representative remnant symmetry $G_l=Z_2^{bd^x}, Z_2^{c^{9n/2}}$ and $G_\nu=K_4^{(c^{9n/2},d^{3n/2})}$, $K_4^{(d^{3n/2},bd^x)}$, $K_4^{(c^{9n/2}d^{3n/2},abc^{3y}d^y)}$ and $K_4^{(c^{9n/2},a^2bc^{3z}d^{2z})}$. In this variant of the semidirect approach, the PMNS matrix turns out

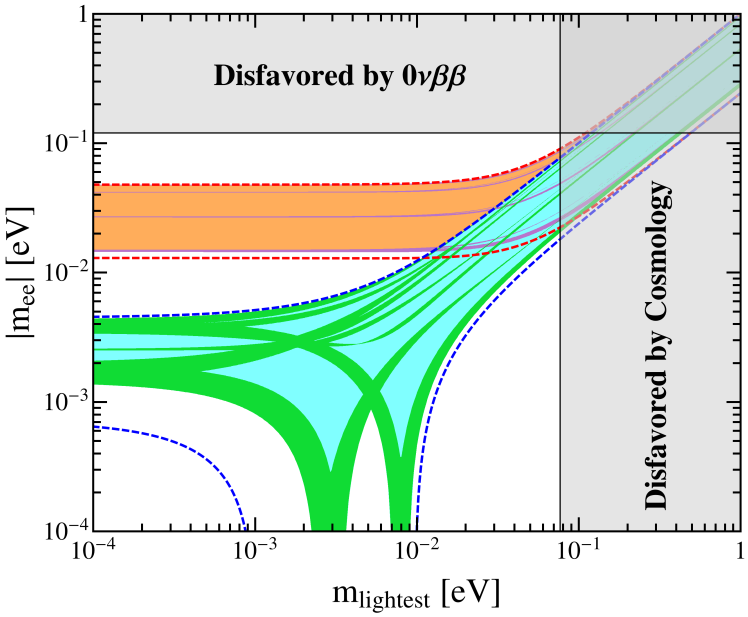

Figure 14: The possible values of the effective Majorana mass $|m_{ee}|$ as a function of the lightest neutrino mass in the case IV. The red (blue) dashed lines indicate the most general allowed regions for IO (NO) neutrino mass spectrum obtained by varying the mixing parameters over the 3σ ranges [7]. The orange (cyan) areas denote the achievable values of $|m_{ee}|$ in the limit of $n \to \infty$ assuming IO (NO) spectrum. The purple and green regions are the theoretical predictions for the $D^{(1)}_{9n,3n}$ group with $n = 2$. Notice that the purple (green) region overlaps the orange (cyan) one. The present most stringent upper limits $|m_{ee}| < 0.120$ eV from EXO-200 [61, 62] and KamLAND-ZEN [63] is shown by horizontal grey band. The vertical grey exclusion band represents the current bound coming from the cosmological data of $\sum m_i < 0.230$ eV at 95% confidence level obtained by the Planck collaboration [65].

to depend on only one real continuous parameter besides the discrete parameters specifying the remnant symmetries, and one row of the PMNS matrix would be completely fixed by the assumed remnant symmetries. The fixed row vectors for different representative residual flavor symmetries are listed in table 10. We find that essentially only one type of residual symmetry with $(G_\nu, G_l) = (K_4^{(c^{9n/2}, a^2bc^{3z}d^{2z})}, Z_2^{bd^{x'}})$ is phenomenologically viable in this scenario.

(V) $G_l = \{1, bd^x\}$, $X_{l\mathbf{r}} = \left\{\rho_{\mathbf{r}}(c^{2x+2\delta+3n\tau}d^\delta), \rho_{\mathbf{r}}(bc^{2x+2\delta+3n\tau}d^{x+\delta})\right\}$, $G_\nu = K_4^{(c^{9n/2}, a^2bc^{3z}d^{2z})}$ and $X_{\nu\mathbf{r}} = \{\rho_{\mathbf{r}}(c^\gamma d^{-2z}), \rho_{\mathbf{r}}(a^2bc^\gamma)\}$

Here we would like to recall that the residual CP transformations are determined by the restricted consistency conditions in Eqs. (3.3, 3.6). The parameter n should be even in order to have a residual Klein subgroup. The phenomenological constraints of the residual flavor symmetry $G_\nu = K_4^{(c^{9n/2}, a^2bc^{3z}d^{2z})}$ as well as the residual CP transformation $X_{\nu\mathbf{r}} = \{\rho_{\mathbf{r}}(c^\gamma d^{-2z}), \rho_{\mathbf{r}}(a^2bc^\gamma)\}$ has been studied in section 4. The light neutrino mass matrix m_ν and its diagonalization matrix U_ν are found to be given by Eq. (4.14) and Eq. (4.15) respectively. Then we proceed to the charged lepton sector. The invariance of the charged lepton mass matrix under the residual symmetry $G_l = \{1, bd^x\}$ and $X_{l\mathbf{r}} = \left\{\rho_{\mathbf{r}}(c^{2x+2\delta+3n\tau}d^\delta), \rho_{\mathbf{r}}(bc^{2x+2\delta+3n\tau}d^{x+\delta})\right\}$ implies that the hermitian matrix $m_l^\dagger m_l$ has to fulfill the invariant condition of Eq. (3.1), i.e.

$$\begin{aligned} \rho^\dagger_{\mathbf{3}}(bd^x) m_l^\dagger m_l \rho_{\mathbf{3}}(bd^x) &= m_l^\dagger m_l, \\ \rho^\dagger_{\mathbf{3}}(c^{2x+2\delta+3n\tau}d^\delta) m_l^\dagger m_l \rho_{\mathbf{3}}(c^{2x+2\delta+3n\tau}d^\delta) &= \left(m_l^\dagger m_l\right)^*, \end{aligned} \tag{6.1}$$

	$G_l = Z_2^{bd^{x'}}$	$G_l = Z_2^{c^{9n/2}}$
$G_\nu = K_4^{(c^{9n/2}, d^{3n/2})}$	$\frac{1}{\sqrt{2}}\begin{pmatrix} 0 \\ -1 \\ 1 \end{pmatrix}^T$ ✗	$\begin{pmatrix} 0 \\ 0 \\ 1 \end{pmatrix}^T$ ✗
$G_\nu = K_4^{(d^{3n/2}, bd^x)}$	$\begin{pmatrix} 0 \\ \cos\left(\frac{x+x'}{3n}\pi\right) \\ -i\sin\left(\frac{x+x'}{3n}\pi\right) \end{pmatrix}^T$ ✗	$\frac{1}{\sqrt{2}}\begin{pmatrix} 0 \\ 1 \\ 1 \end{pmatrix}^T$ ✗
$G_\nu = K_4^{(c^{9n/2}d^{3n/2}, abc^{3y}d^y)}$	$\frac{1}{2}\begin{pmatrix} -\sqrt{2} \\ 1 \\ 1 \end{pmatrix}^T$ ✓	$\frac{1}{\sqrt{2}}\begin{pmatrix} 0 \\ 1 \\ 1 \end{pmatrix}^T$ ✗
$G_\nu = K_4^{(c^{9n/2}, a^2bc^{3z}d^{2z})}$	$\frac{1}{2}\begin{pmatrix} -\sqrt{2} \\ 1 \\ 1 \end{pmatrix}^T$ ✓	$\begin{pmatrix} 1 \\ 0 \\ 0 \end{pmatrix}^T$ ✗

Table 10: The column vector of the PMNS matrix determined by the residual flavor symmetries G_ν and G_l, where $x, x', y, z = 0, 1, \ldots, 3n-1$. If one (or two) element of the fixed column is vanishing, we would use the notation "✗" to indicate that it is disfavored by the present experimental data otherwise the notation "✓" is labelled to indicate that agreement with the experimental data could be achieved. Because two pair of subgroups $(G_\nu, G_l) = (K_4^{(c^{9n/2}d^{3n/2}, abc^{3y}d^y)}, Z_2^{bd^{x'}})$ and $(K_4^{(c^{9n/2}, a^2bc^{3z}d^{2z})}, Z_2^{bd^{x'}})$ with $z = x' + y$ are conjugate to each other under the action of the element $bd^{x'}$, they lead to the same results for the PMNS matrix after all the admissible residual CP transformations are considered.

which lead to

$$m_l^\dagger m_l = \begin{pmatrix} \widetilde{\mathfrak{m}}_{11} & \widetilde{\mathfrak{m}}_{12} e^{i\pi\frac{\delta}{3n}} & \widetilde{\mathfrak{m}}_{12} e^{i\pi\frac{2x+\delta}{3n}} \\ \widetilde{\mathfrak{m}}_{12} e^{-i\pi\frac{\delta}{3n}} & \widetilde{\mathfrak{m}}_{22} & \widetilde{\mathfrak{m}}_{23} e^{i\pi\frac{2x}{3n}} \\ \widetilde{\mathfrak{m}}_{12} e^{-i\pi\frac{2x+\delta}{3n}} & \widetilde{\mathfrak{m}}_{23} e^{-i\pi\frac{2x}{3n}} & \widetilde{\mathfrak{m}}_{22} \end{pmatrix} , \tag{6.2}$$

where $\widetilde{\mathfrak{m}}_{11}$, $\widetilde{\mathfrak{m}}_{12}$, $\widetilde{\mathfrak{m}}_{22}$ and $\widetilde{\mathfrak{m}}_{23}$ are real, and they have dimension of squared mass. It can be diagonalized by the unitary matrix

$$U_l = \frac{1}{\sqrt{2}} \begin{pmatrix} 0 & -\sqrt{2}\sin\theta & \sqrt{2}\cos\theta \\ -e^{i\pi\frac{2x}{3n}} & e^{-i\pi\frac{\delta}{3n}}\cos\theta & e^{-i\pi\frac{\delta}{3n}}\sin\theta \\ 1 & e^{-i\pi\frac{2x+\delta}{3n}}\cos\theta & e^{-i\pi\frac{2x+\delta}{3n}}\sin\theta \end{pmatrix} , \tag{6.3}$$

with the angle θ satisfying

$$\tan 2\theta = \frac{2\sqrt{2}\,\widetilde{\mathfrak{m}}_{12}}{\widetilde{\mathfrak{m}}_{11} - \widetilde{\mathfrak{m}}_{22} - \widetilde{\mathfrak{m}}_{23}} . \tag{6.4}$$

The squared charged lepton masses are determined to be of the form

$$\begin{aligned} m_{l_1}^2 &= \widetilde{\mathfrak{m}}_{22} - \widetilde{\mathfrak{m}}_{23} , \\ m_{l_2}^2 &= \frac{1}{2}\left[\widetilde{\mathfrak{m}}_{11} + \widetilde{\mathfrak{m}}_{22} + \widetilde{\mathfrak{m}}_{23} - \frac{\widetilde{\mathfrak{m}}_{11} - \widetilde{\mathfrak{m}}_{22} - \widetilde{\mathfrak{m}}_{23}}{\cos 2\theta}\right] , \\ m_{l_3}^2 &= \frac{1}{2}\left[\widetilde{\mathfrak{m}}_{11} + \widetilde{\mathfrak{m}}_{22} + \widetilde{\mathfrak{m}}_{23} + \frac{\widetilde{\mathfrak{m}}_{11} - \widetilde{\mathfrak{m}}_{22} - \widetilde{\mathfrak{m}}_{23}}{\cos 2\theta}\right] . \end{aligned} \tag{6.5}$$

Notice that the order of the masses $m_{l_1}^2$, $m_{l_2}^2$ and $m_{l_3}^2$ can not be pinned down by remnant symmetry, therefore the matrix U_l in Eq. (6.3) is determined up to permutations and phases

of its column vectors. The lepton flavor mixing originates from the mismatch between the unitary transformations U_l in Eq. (6.3) and U_ν in Eq. (4.15), and the PMNS matrix can take the form

$$U^{V,1}_{\rm PMNS} = \frac{1}{2}\begin{pmatrix} \sin\theta+\sqrt{2}e^{i\varphi_8}\cos\theta & \sin\theta-\sqrt{2}e^{i\varphi_8}\cos\theta & \sqrt{2}e^{i\varphi_9}\sin\theta \\ 1 & 1 & -\sqrt{2}e^{i\varphi_9} \\ \cos\theta-\sqrt{2}e^{i\varphi_8}\sin\theta & \cos\theta+\sqrt{2}e^{i\varphi_8}\sin\theta & \sqrt{2}e^{i\varphi_9}\cos\theta \end{pmatrix} , \tag{6.6}$$

or

$$U^{V,2}_{\rm PMNS} = \frac{1}{2}\begin{pmatrix} \sin\theta+\sqrt{2}e^{i\varphi_8}\cos\theta & \sin\theta-\sqrt{2}e^{i\varphi_8}\cos\theta & \sqrt{2}e^{i\varphi_9}\sin\theta \\ \cos\theta-\sqrt{2}e^{i\varphi_8}\sin\theta & \cos\theta+\sqrt{2}e^{i\varphi_8}\sin\theta & \sqrt{2}e^{i\varphi_9}\cos\theta \\ 1 & 1 & -\sqrt{2}e^{i\varphi_9} \end{pmatrix} , \tag{6.7}$$

where

$$\varphi_8 = -\frac{2z+\delta}{3n}\pi, \qquad \varphi_9 = \frac{2x-4z-\gamma}{3n}\pi \, . \tag{6.8}$$

Obviously the values of both φ_8 and φ_9 are integer multiple of $\frac{\pi}{3n}$, i.e.

$$\varphi_8, \varphi_9 \ (\text{mod}\ 2\pi) = 0, \frac{1}{3n}\pi, \frac{2}{3n}\pi, \ldots, \frac{6n-1}{3n}\pi \, . \tag{6.9}$$

The mixing patterns $U^{V,1}_{\rm PMNS}$ and $U^{V,2}_{\rm PMNS}$ are related through the exchange of the second and third rows in the PMNS mixing matrix. Other permutations of rows and columns don't lead to new patterns consistent with experimental data. We can extract the following results for the mixing angles,

$$\begin{aligned} &\sin^2\theta_{13} = \frac{1}{2}\sin^2\theta, \qquad \sin^2\theta_{12} = \frac{1}{2} - \frac{\sqrt{2}\sin 2\theta\cos\varphi_8}{3+\cos 2\theta}, \\ &\sin^2\theta_{23} = \frac{2}{3+\cos 2\theta} \ \text{ for } \ U^{V,1}_{\rm PMNS}, \qquad \sin^2\theta_{23} = \frac{1+\cos 2\theta}{3+\cos 2\theta} \ \text{ for } \ U^{V,2}_{\rm PMNS} \, . \end{aligned} \tag{6.10}$$

The 3σ range of $\sin^2\theta_{13}$ can be reproduced for

$$\theta \in [0.060\pi, 0.078\pi] \cup [0.922\pi, 0.940\pi] \ . \tag{6.11}$$

We can check that the mixing angles fulfill the following sum rules,

$$\cos 2\theta_{12} = \pm 2\tan\theta_{13}\sqrt{1-\tan^2\theta_{13}}\cos\varphi_8 \, , \tag{6.12a}$$

$$2\cos^2\theta_{13}\sin^2\theta_{23} = 1, \quad \text{or} \quad 2\cos^2\theta_{13}\sin^2\theta_{23} = \cos 2\theta_{13} \, , \tag{6.12b}$$

where the "+" and "−" signs are valid for $0 < \theta < \pi/2$ and $\pi/2 < \theta < \pi$ respectively. In order to accommodate the experimental data on solar and reactor mixing angles, the first sum rule of Eq. (6.12a) implies that the parameter φ_8 should vary in the interval

$$\varphi_8 \in [0, 0.193\pi] \cup [0.807\pi, 1.193\pi] \cup [1.807\pi, 2\pi] \, . \tag{6.13}$$

From the correlation of Eq. (6.12b), we can derive

$$0.509 \leq \sin^2\theta_{23} \leq 0.515, \ \text{ or } \ 0.485 \leq \sin^2\theta_{23} \leq 0.491 \, . \tag{6.14}$$

The contour plots for $\sin^2\theta_{ij}$ is shown in figure 15. Since both reactor angle θ_{13} and the atmospheric angle θ_{23} only depend on the parameter θ, the corresponding contour regions

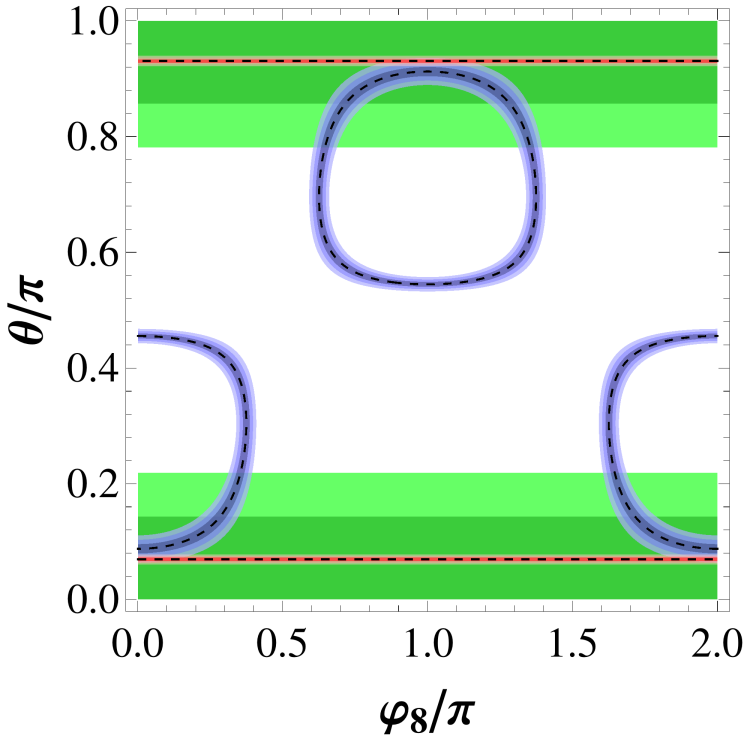

Figure 15: The contour regions of the three mixing angles in the case V. The red, blue and green areas denote the predictions for $\sin^2\theta_{13}$, $\sin^2\theta_{12}$ and $\sin^2\theta_{23}$ respectively. The allowed 1σ, 2σ and 3σ regions of each mixing angle are represented by different shadings. The best fit values of the mixing angles are indicated by dotted lines. In this case the atmospheric angle θ_{23} is predicted to be in the interval of Eq. (6.14) such that neither the 1σ range nor its best fit value can be achieved.

are horizontal bands. There exist three small regions in which all the three mixing angles are within the experimentally preferred 3σ ranges. Furthermore, we find the following expressions for the CP invariants,

$$|J_{CP}| = \frac{1}{8\sqrt{2}}\left|\sin 2\theta \sin\varphi_8\right| , \qquad |I_1| = \frac{1}{8\sqrt{2}}\left|(1+3\cos 2\theta)\sin 2\theta \sin\varphi_8\right| ,$$
$$|I_2| = \frac{\sin^2\theta}{8}\left|\sqrt{2}\sin 2\theta \sin(2\varphi_9-\varphi_8) + 2\cos^2\theta \sin 2(\varphi_9-\varphi_8) + \sin^2\theta \sin 2\varphi_9\right| , \quad (6.15)$$

from which we know that both δ_{CP} and α_{21} are only dependent on θ and φ_8 while the value of α'_{31} depends on three parameters θ, φ_8 and φ_9. We display the predictions for $|\sin\delta_{CP}|$ and $|\sin\alpha_{21}|$ in the $\varphi_8-\theta$ plane in figure 16. One can see that both δ_{CP} and α_{21} can not be maximal if the three mixing angles are required to be consistent with the experimental data. In analogy to previous cases, we numerically study the possible values of the mixing parameters for each $D^{(1)}_{9n,3n}$ group. We can read from figure 17 that a bit larger θ_{12} (still in the 3σ range) is favored with $0.328 \leq \sin^2\theta_{12} \leq 0.359$, and the atmospheric angle $\sin^2\theta_{23}$ is predicted to be around 0.487 and 0.513. These results can be testable at forthcoming neutrino oscillation facilities. The same conclusions on CP phases are reached as those from figure 16. We find the upper bounds of $|\sin\delta_{CP}|$ and $|\sin\alpha_{21}|$ are $|\sin\delta_{CP}| \leq 0.594$ and $|\sin\alpha_{21}| \leq 0.399$ respectively. On the other hand, any value of the Majorana phase α_{31} is possible for large value of n.

Now we discuss the lepton mixing patterns which can be obtained from the $D^{(1)}_{9n,3n}$ group with $n = 2$. Note that the smallest $D^{(1)}_{9n,3n}$ group for $n = 1$ doesn't comprise the required

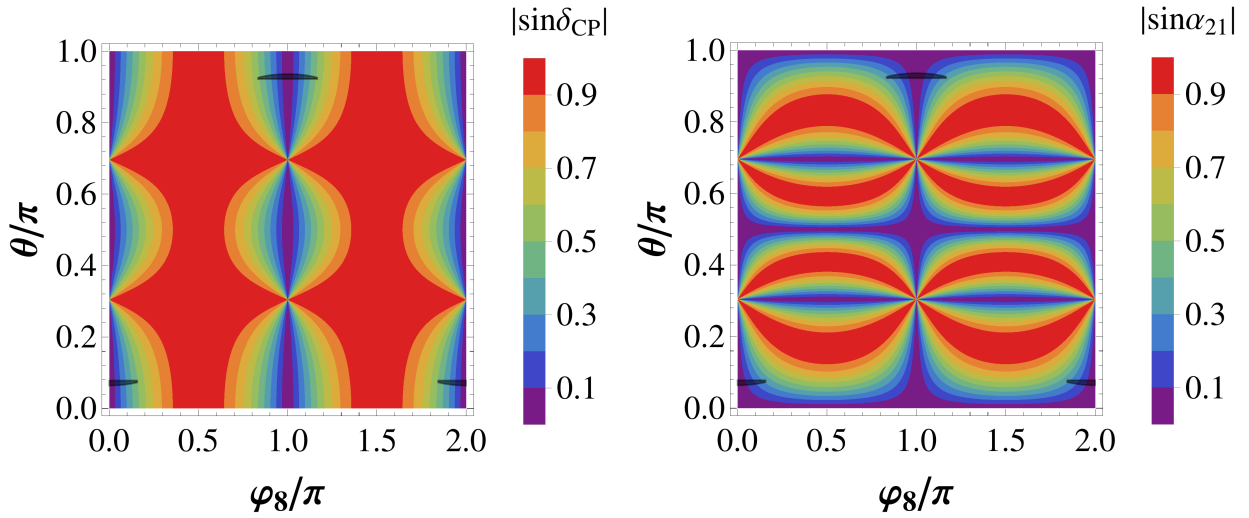

Figure 16: The contour plots of $|\sin\delta_{CP}|$ and $|\sin\alpha_{21}|$ in the case V. The black areas represent the regions in which the lepton mixing angles are compatible with experimental data at 3σ level, and it can be read out from figure 15.

Klein subgroup. The PMNS matrices $U^{V,1}_{\rm PMNS}$ and $U^{V,2}_{\rm PMNS}$ fulfill the following relations

$$U^{V}_{\rm PMNS}(\theta,\varphi_8+\pi,\varphi_9)=\text{diag}(-1,1,1)U^{V}_{\rm PMNS}(-\theta,\varphi_8,\varphi_9), \tag{6.16a}$$
$$U^{V}_{\rm PMNS}(\theta,\varphi_8,\varphi_9+\pi/2)=U^{V}_{\rm PMNS}(\theta,\varphi_8,\varphi_9)\text{diag}(1,1,i), \tag{6.16b}$$
$$U^{V}_{\rm PMNS}(\theta,\pi-\varphi_8,\varphi_9)=\text{diag}(-1,1,1)[U^{V}_{\rm PMNS}(-\theta,\varphi_8,-\varphi_9)]^{*}\,, \tag{6.16c}$$

where $U^{V}_{\rm PMNS}$ refers to $U^{V,1}_{\rm PMNS}$ and $U^{V,2}_{\rm PMNS}$. The diagonal matrices on the left-handed and right-handed sides can be absorbed by the charged lepton fields and Q_ν respectively. Therefore the shifts of φ_8 into $\varphi_8+\pi$ and φ_9 into $\varphi_9+\pi/2$ don't lead to physically new results. For $n=2$ the values of φ_8 and φ_9 can be 0, $\pi/6$, $\pi/3$, ..., $11\pi/6$. Considering the constraint on the parameter φ_8 given by Eq. (6.13), we find only $\varphi_8\ (\text{mod}\ \pi)=0$, $\pi/6$ and $5\pi/6$ can describe the data on lepton mixing. The results of our χ^2 analysis are displayed in table 11. Since the mixing angles $\sin^2\theta_{ij}$ and the CP invariants J_{CP} and I_1 are expressed in terms of θ and φ_8, and the parameter φ_9 only enters into the expression of I_2, the relation in Eq. (6.16c) implies that φ_8 and $\pi-\varphi_8$ give rise to the same best fitting values of mixing parameters except $|\sin\alpha'_{31}|$. This is exactly the reason why the numerical results for $\varphi_8=\pi/6$ and $\varphi_8=5\pi/6$ are only different in the values of $|\sin\alpha'_{31}|$. Finally we plot the predictions for the effective mass $|m_{ee}|$ with respect to the lightest neutrino mass in figure 18. One sees that the values of $|m_{ee}|$ are rather close to the lower or upper boundary of the 3σ region for IO.

7 Conclusions

The type D finite subgroup of $SU(3)$ has two independent series: $D^{(0)}_{n,n}\cong\Delta(6n^2)$ and $D^{(1)}_{9n,3n}\cong(Z_{9n}\times Z_{3n})\rtimes S_3$. The $\Delta(6n^2)$ flavor symmetry with or without CP symmetry and its predictions for the lepton flavor mixing has been discussed in the literature. In the present work, we have performed a comprehensive analysis of the mixing patterns which can be derived from another type D group series $D^{(1)}_{9n,3n}$ and the generalized CP. The phenomenological consequence of the "direct" approach, "semidirect" approach and "variant of semidirect" approach are studied in a model independent way. The three approaches differ in the residual symmetries preserved by the neutrino and charged lepton sectors.

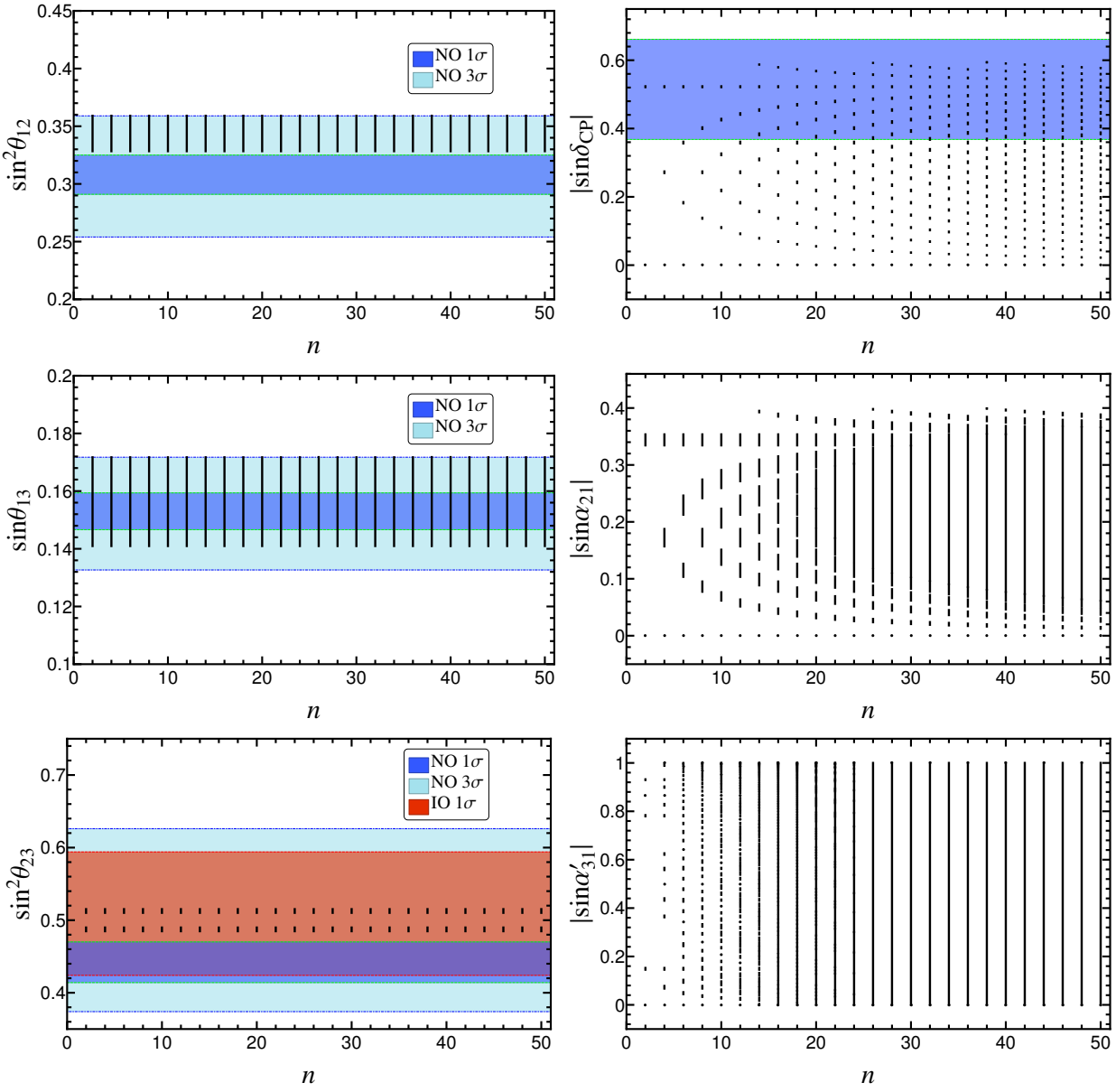

Figure 17: The possible values of $\sin^2\theta_{12}$, $\sin\theta_{13}$, $\sin^2\theta_{23}$, $|\sin\delta_{CP}|$, $|\sin\alpha_{21}|$ and $|\sin\alpha'_{31}|$ with respect to n for the mixing pattern $U^{V,1}_{\rm PMNS}$ and $U^{V,2}_{\rm PMNS}$ in the case V, where the three lepton mixing angles are required to be within the experimentally preferred 3σ ranges. The 1σ and 3σ regions of the three neutrino mixing angles are adapted from global fit [7]. Note that the group index n should be even in this case.

The mathematical structure of $D^{(1)}_{9n,3n}$ has been investigated. Using the method of induced representations, we find all the irreducible representations of $D^{(1)}_{9n,3n}$ group and its character table for arbitrary n. We have derived the Kronecker products and constructed the Clebsch-Gordan coefficients. These details would be necessary and particularly useful for model builders aiming at construction of flavor models based on the group $D^{(1)}_{9n,3n}$. Furthermore, we have identified the class-inverting automorphisms of the $D^{(1)}_{9n,3n}$ group, and show that the corresponding CP transformations are of the same form as the flavor symmetry transformations in our working basis.

In the "direct" approach, the original symmetry $D^{(1)}_{9n,3n} \rtimes H_{CP}$ is broken down to $K_4 \times H^{\nu}_{CP}$ in the neutrino sector and to $G_l \rtimes H^{l}_{CP}$ in the charged lepton sector, where G_l is an abelian subgroup which allows to distinguish the three generations of leptons. In this scenario, all

Case V										
$n = 2$										
s	φ_8	φ_9	θ_{bf}	χ^2_{min}	$\sin^2\theta_{13}$	$\sin^2\theta_{12}$	$\sin^2\theta_{23}$	$\lvert\sin\delta_{CP}\rvert$	$\lvert\sin\alpha_{21}\rvert$	$\lvert\sin\alpha'_{31}\rvert$
$U^{V,1}_{\rm PMNS}$	0	0	0.224 (0.227)	9.890 (4.409)	0.0248 (0.0253)	0.343 (0.341)	0.513 (0.513)	0 (0)	0 (0)	0 (0)
		$\frac{\pi}{6}$								0.866 (0.866)
		$\frac{\pi}{3}$								0.866 (0.866)
	$\frac{\pi}{6}$	0	0.227 (0.229)	16.405 (10.772)	0.0253 (0.0258)	0.362 (0.361)	0.513 (0.513)	0.520 (0.521)	0.326 (0.329)	0.786 (0.785)
		$\frac{\pi}{6}$								0.142 (0.144)
		$\frac{\pi}{3}$								0.928 (0.929)
	$\frac{5\pi}{6}$	0	2.915 (2.913)	16.405 (10.772)	0.0253 (0.0258)	0.362 (0.361)	0.513 (0.513)	0.520 (0.521)	0.326 (0.329)	0.786 (0.785)
		$\frac{\pi}{6}$								0.928 (0.929)
		$\frac{\pi}{3}$								0.142 (0.144)
$U^{V,2}_{\rm PMNS}$	0	0	0.225 (0.227)	6.938 (4.288)	0.0250 (0.0253)	0.342 (0.341)	0.487 (0.487)	0 (0)	0 (0)	0 (0)
		$\frac{\pi}{6}$								0.866 (0.866)
		$\frac{\pi}{3}$								0.866 (0.866)
	$\frac{\pi}{6}$	0	0.228 (0.229)	13.389 (10.649)	0.0255 (0.0258)	0.362 (0.361)	0.487 (0.487)	0.520 (0.521)	0.328 (0.330)	0.786(0.785)
		$\frac{\pi}{6}$								0.143 (0.144)
		$\frac{\pi}{3}$								0.929 (0.929)
	$\frac{5\pi}{6}$	0	2.914 (2.913)	13.389 (10.649)	0.0255 (0.0258)	0.362 (0.361)	0.487 (0.487)	0.520 (0.521)	0.328 (0.330)	0.786 (0.785)
		$\frac{\pi}{6}$								0.929 (0.929)
		$\frac{\pi}{3}$								0.143 (0.144)

Table 11: Results of the χ^2 analysis for $n = 2$ in the case V. The χ^2 function has a global minimum χ^2_{min} at the best fit value θ_{bf} for θ. We give the values of the mixing angles and CP violation phases for $\theta = \theta_{bf}$. The values given in parentheses denote the results for the IO neutrino mass spectrum. Because of the symmetry relations in Eq. (6.16), only the results for $0 \leq \varphi_8 < \pi$ and $0 \leq \varphi_9 < \pi/2$ are shown here.

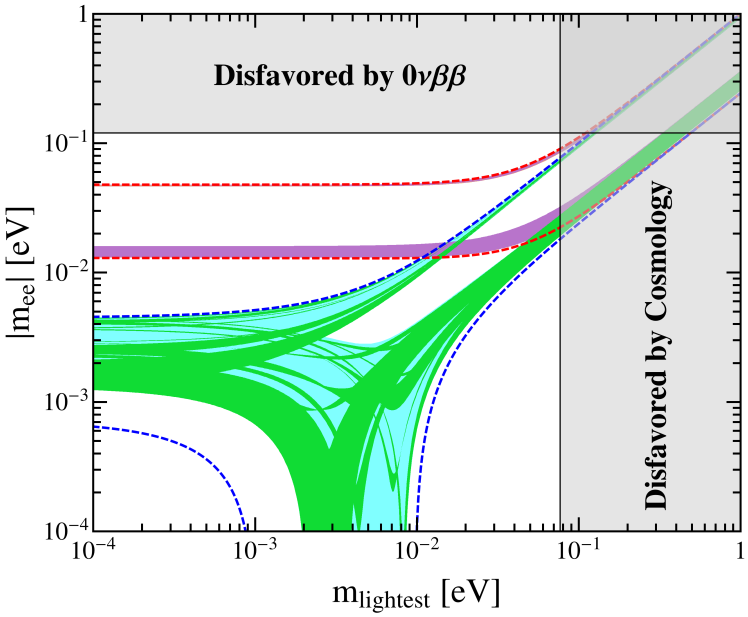

Figure 18: The possible values of the effective Majorana mass $|m_{ee}|$ as a function of the lightest neutrino mass in the case V. The red (blue) dashed lines indicate the most general allowed regions for IO (NO) neutrino mass spectrum obtained by varying the mixing parameters over the 3σ ranges [7]. The orange (cyan) areas denote the achievable values of $|m_{ee}|$ in the limit of $n \to \infty$ assuming IO (NO) spectrum. The purple and green regions are the theoretical predictions for the $D^{(1)}_{9n,3n}$ group with $n = 2$. Notice that the purple (green) region overlaps the orange (cyan) one. The present most stringent upper limits $|m_{ee}| < 0.120$ eV from EXO-200 [61, 62] and KamLAND-ZEN [63] is shown by horizontal grey band. The vertical grey exclusion band represents the current bound coming from the cosmological data of $\sum m_i < 0.230$ eV at 95% confidence level obtained by the Planck collaboration [65].

the lepton mixing parameters including the Majorana CP phases are completely fixed by the residual symmetries. We have considered all the possible residual subgroups K_4, G_l and the residual CP transformations that can be consistently combined. We find that the lepton mixing matrices compatible with the data are of the trimaximal form. Both Dirac phase δ_{CP} and the Majorana phase α_{31} are predicted to be conserved, and the values of the Majorana phase α_{21} are 0, $\frac{2}{3n}\pi$, $\frac{4}{3n}\pi$, ..., $\frac{6n-2}{3n}\pi$.

In contrast with the "direct" approach, the residual symmetry preserved by the neutrino mass matrix is $Z_2 \times H^{\nu}_{CP}$ in the "semidirect" approach. Since the remnant flavor symmetry of the neutrino sector is Z_2 instead of K_4, it would fix only one column of the PMNS matrix. Taking into account the remnant CP transformations further, all the lepton mixing angles as well as the CP violating phases would be predicted in terms of a continuous free parameter θ besides the parameters characterizing the residual symmetries. We find that only four types of mixing patterns named as cases I, II, III and IV can accommodate the experimental data on lepton mixing angles for certain values of the continuous parameter θ and the discrete parameter φ_i determined by the postulated residual symmetries. For cases III and IV, the residual Z_2 subgroup is chosen to be generated by the element $c^{9n/2}$ such that the group index n has to be even. We have performed a detailed analytical and numerical analysis. It is remarkable that either the solar mixing angle θ_{12} or the atmospheric mixing angle θ_{23} is bounded within certain intervals for arbitrary n. As a consequence, these predictions can be testable by the next generation of reactor neutrino experiments and long baseline experiments. The admissible values of the mixing angles and CP phases for each $D^{(1)}_{9n,3n}$ group until $n = 50$ have been studied. Interestingly enough, the first two smallest $D^{(1)}_{9n,3n}$ groups with $n = 1, 2$ already allow a good fit to the data on lepton mixing angles, and the CP violating phases can be conserved, maximal or some other irregular values. Moreover, the phenomenological predictions for the neutrinoless double beta decay are exploited.

In the so-called "variant of semidirect" approach, the remnant symmetries of the neutrino and the charged lepton mass matrices are assumed to be $K_4 \times H^{\nu}_{CP}$ and $Z_2 \times H^{l}_{CP}$ respectively. We find only one type of mixing pattern named as case V is phenomenologically viable in this scenario. One row of the PMNS matrix is determined to be $(1/2, 1/2, -e^{i\varphi_9}/\sqrt{2})$. The solar mixing angle is predicted to lie in the interval $0.328 \leq \sin^2\theta_{12} \leq 0.359$, and the atmospheric angle is in the range of $0.510 \leq \sin^2\theta_{23} \leq 0.515$ or $0.485 \leq \sin^2\theta_{23} \leq 0.490$. Moreover, both Dirac phase and the Majorana phase α_{21} are bounded from above $|\sin\delta_{CP}| \leq 0.594$ and $|\sin\alpha_{21}| \leq 0.399$ respectively.

In our framework, the obtained results for lepton flavor mixing only depend on the structure of flavor symmetry group and the postulated residual symmetries, and they are independent of the breaking mechanism that how the required vacuum alignment needed to achieve the remnant symmetries is dynamically realized. It would be interesting to construct concrete models in which the breaking of the symmetry group to the residual symmetries are spontaneous due to the non-vanishing vacuum expectation values of some flavon fields.

Acknowledgements

This work is supported by the National Natural Science Foundation of China under Grant Nos. 11275188, 11179007 and 11522546.

Appendix

A Group theory of $D^{(1)}_{9n,3n} \cong (Z_{9n} \times Z_{3n}) \rtimes S_3$

The group $D^{(1)}_{9n,3n}$ for a generic integer n is a non-Abelian finite subgroup of $SU(3)$ of type D [45]. Its order is $162n^2$. It is isomorphic to the semidirect product of the S_3, the smallest non-Abelian finite group, with $(Z_{9n} \times Z_{3n})$, i.e. $D^{(1)}_{9n,3n} \cong (Z_{9n} \times Z_{3n}) \rtimes S_3$. The $D^{(1)}_{9n,3n}$ group can be defined in terms of four generators a, b, c and d fulfilling the following relations [14, 45]:

$$\begin{aligned} a^3 = b^2 = (ab)^2 = c^{9n} = d^{3n} = 1, \quad cd = dc, \\ aca^{-1} = cd, \quad ada^{-1} = c^{-3}d^{-2}, \quad bcb^{-1} = cd, \quad bdb^{-1} = d^{-1}\,. \end{aligned} \tag{A.1}$$

One can see that a and b generate S_3, and c and d generate the Z_{9n} and Z_{3n} subgroups respectively. Any group element $g \in D^{(1)}_{9n,3n}$ can be written as a product of powers of the generators a, b, c and d,

$$g = a^\alpha b^\beta c^\gamma d^\delta\,, \tag{A.2}$$

with $\alpha = 0, 1, 2$, $\beta = 0, 1$, $\gamma = 0, 1, \ldots, 9n-1$ and $\delta = 0, 1, \ldots, 3n-1$. From the multiplication rules in Eq. (A.1), the following useful relations can be obtained,

$$\begin{aligned} &ca = ac^{-2}d^{-1}, \qquad da = ac^3 d, \qquad ba = a^2 b, \quad ca^2 = a^2 cd, \\ &da^2 = a^2 c^{-3} d^{-2}, \qquad ba^2 = ab, \qquad cb = bcd, \qquad db = bd^{-1}\,. \end{aligned} \tag{A.3}$$

Utilizing Eqs. (A.2, A.3), we find that the elements of $D^{(1)}_{9n,3n}$ group belong to the following conjugacy classes:

$$\begin{aligned} 1 &: 1\mathcal{C}_1 = \{1\}\,, \\ 2 &: 1\mathcal{C}_1^{(\nu)} = \{c^\nu\}\,, \quad \nu = 3n, 6n, \\ 9n-3 &: 3\mathcal{C}_1^{(\rho)} = \left\{c^\rho, c^\rho d^\rho, c^{-2\rho} d^{-\rho}\right\}, \quad \rho \neq 0, 3n, 6n, \\ \frac{27n(n-1)+6}{6} &: 6\mathcal{C}_1^{(\rho,\sigma)} = \left\{c^\rho d^\sigma, c^{\rho-3\sigma} d^{\rho-2\sigma}, c^{3\sigma-2\rho} d^{\sigma-\rho}, c^\rho d^{\rho-\sigma}, c^{3\sigma-2\rho} d^{2\sigma-\rho}, c^{\rho-3\sigma} d^{-\sigma}\right\}, \\ 3 &: 18n^2\mathcal{C}_2^{(\tau)} = \{ac^{\tau+3x}d^y, a^2 c^{\tau+3x} d^{\tau+3x-y} |\ x, y = 0, 1, \ldots, 3n-1\},\ \tau = 0, 1, 2 \\ 9n &: 9n\mathcal{C}_3^{(\rho)} = \left\{bc^\rho d^x, a^2 bc^{\rho-3x} d^{\rho-2x}, abc^{\rho-3x} d^{-x} | x = 0, 1, \ldots, 3n-1\right\}, \rho = 0, 1, \ldots, 9n-1\,, \end{aligned}$$

where the quantity on the left of the colon denotes the number of classes and the quantity on the right of the colon refers to the number of elements contained in the classes. The parameters ρ and σ in the conjugacy class $6\mathcal{C}_1^{(\rho,\sigma)}$ can take the values $\rho = 0, 1, \ldots, 9n-1$, $\sigma = 0, 1, \ldots, 3n-1$, and the following possibilities are excluded,

$$\rho - 2\sigma = 0 \bmod(3n), \qquad \rho - \sigma = 0 \bmod(3n), \qquad \sigma = 0\,. \tag{A.4}$$

As a result, the $D^{(1)}_{9n,3n}$ group totally has $1+2+(9n-3)+\frac{27n(n-1)+6}{6}+3+9n = (3n+1)(3n+8)/2$ different conjugacy classes. Furthermore, we can check that the center of the $D^{(1)}_{9n,3n}$ group is $Z(D^{(1)}_{9n,3n}) = \{1, c^{3n}, c^{6n}\}$.

A.1 Irreducible representations of $D^{(1)}_{9n,3n}$ group

Now we proceed to construct all the irreducible representations of the $D^{(1)}_{9n,3n}$ group. Firstly we concentrate on the one-dimensional representations in which all generators are

represented by pure numbers and they are commutable with each other. From Eq. (A.1), we see that

$$a = d = 1, \quad b^2 = 1, \quad c^3 = 1\,. \tag{A.5}$$

Hence $D^{(1)}_{9n,3n}$ group has six singlet representations given by

$$\begin{aligned}
&\mathbf{1_{0,0}} : a = b = c = d = 1\,,\\
&\mathbf{1_{0,1}} : a = b = d = 1, \quad c = \omega\,,\\
&\mathbf{1_{0,2}} : a = b = d = 1, \quad c = \omega^2\,,\\
&\mathbf{1_{1,0}} : a = c = d = 1, \quad b = -1\,,\\
&\mathbf{1_{1,1}} : a = d = 1, \quad b = -1, \quad c = \omega\,,\\
&\mathbf{1_{1,2}} : a = d = 1, \quad b = -1, \quad c = \omega^2\,,
\end{aligned} \tag{A.6}$$

for any integer n, where $\omega \equiv e^{2\pi i/3}$. These one-dimensional representations differ in the values of the generators b and c, and they can be neatly written as

$$\mathbf{1}_{i,j} \;:\; a = d = 1, \quad b = (-1)^i, \quad c = \omega^j, \;\; \text{with} \;\; i = 0, 1, \; j = 0, 1, 2\,. \tag{A.7}$$

As far as we know, the representations of the $D^{(1)}_{9n,3n}$ group has not been worked out in the literature. It is a nontrivial task. In the following, we shall use the method of induced representations to build the remaining irreducible representations. The induced representation can be commonly found in the literature. In the following, we first briefly review the basic idea of the induced representation. Let $\mathcal{G}$ be a finite group and $\mathcal{H}$ any subgroup of $\mathcal{G}$ with index n. The index of $\mathcal{H}$ in $\mathcal{G}$ is the number of cosets of $\mathcal{H}$ in $\mathcal{G}$, i.e. $n = |\mathcal{G}|/|\mathcal{H}|$ where $|\mathcal{G}|$ and $|\mathcal{H}|$ denote the order of $\mathcal{G}$ and $\mathcal{H}$ respectively. We denote x_1, x_2, ..., x_n as a full set of representatives in $\mathcal{G}$ of the cosets in $\mathcal{G}/\mathcal{H}$, i.e.

$$\mathcal{G}/\mathcal{H} = x_1(x_1 \equiv 1)\mathcal{H} \;\oplus\; x_2\mathcal{H} \;\oplus\; \cdots \;\oplus\; x_n\mathcal{H}\,. \tag{A.8}$$

Furthermore, let ϱ be a d-dimensional irreducible representation of $\mathcal{H}$ with $\varrho : H \to GL(V)$, where V is the representation space of dimension d and $GL(V)$ is the group of non-singular linear maps on V. Supposing $\{e_1, \ldots, e_d\}$ is a basis of the vector space V, the action of any element $h \in \mathcal{H}$ on the basis vector e_i is

$$h : \; e_i \;\mapsto\; \varrho(h)_{ji} e_j\,. \tag{A.9}$$

The induced representation can be thought of as acting on the following space:

$$W = \bigoplus_{i=1}^{n} x_i V\,, \tag{A.10}$$

where each $x_i V$ is an isomorphic copy of the vector space V. The basis vector of the space W can be taken to be

$$x_k e_i \equiv e_{k,i}\,, \quad \text{with} \quad k = 1, 2, \ldots, n, \;\; i = 1, 2, \ldots, d\,. \tag{A.11}$$

According to the definition of coset, any $g \in \mathcal{G}$ will then send each x_k to a unique $x_m h$ with $h \in \mathcal{H}$ such that $g x_k = x_m h$ where $k, m = 1, 2, \ldots, n$. In the induced representation, an element $g \in \mathcal{G}$ acts on the vector space W as follows

$$g : \; e_{k,i} \;\mapsto\; g e_{k,i} = g x_k e_i = x_m h e_i = \varrho(h)_{ji} x_m e_j = \varrho(h)_{ji} e_{m,j}\,. \tag{A.12}$$

Thus we see that $\mathcal{G}$ acts linearly on W, and its action is thus represented by a $(dn \times dn)$ matrix. Notice that the induced representation is not necessarily irreducible.

We now apply this method to the group $D^{(1)}_{9n,3n} = \mathcal{G}$, and take the subgroup to be $\mathcal{H} = Z_{9n} \times Z_{3n}$. The index of $\mathcal{H}$ in $\mathcal{G}$ is $n = 6$. Since $\mathcal{H}$ is an abelian subgroup, its irreducible representations ϱ can only be one-dimensional. e_1 is the basis for the representation space of $\mathcal{H}$, the generators c and d act on e_1 as follows

$$ce_1 = \eta^l e_1, \qquad de_1 = \eta^{-3k} e_1\,, \tag{A.13}$$

where $\eta = e^{\frac{2\pi i}{9n}}$, the values of the parameters l and k are $l = 0, 1, \ldots, 9n-1$ and $k = 0, 1, \ldots, 3n-1$. The six representative elements of the coset $\mathcal{G}/\mathcal{H}$ can be chosen to be

$$x_1 = 1, \quad x_2 = a^2, \quad x_3 = a, \quad x_4 = b, \quad x_5 = ab, \quad x_6 = a^2 b\,. \tag{A.14}$$

As a consequence, we can obtain the basis of the vector space W on which the induced representation is defined,

$$\begin{aligned} &e_1 \equiv x_1 e_1 = e_1, \quad e_2 \equiv x_2 e_1 = a^2 e_1, \quad e_3 \equiv x_3 e_1 = a e_1, \\ &e_4 \equiv x_4 e_1 = b e_1, \quad e_5 \equiv x_5 e_1 = ab e_1, \quad e_6 \equiv x_6 e_1 = a^2 b e_1\,. \end{aligned} \tag{A.15}$$

According to Eq. (A.12), the actions of the generators a, b, c and d on the above six basis vectors can be straightforwardly derived by utilizing the useful identities in Eq. (A.3) :

$$\begin{array}{lll} ae_1 = e_3, & ae_2 = e_1, & ae_3 = e_2, \\ ae_4 = e_5, & ae_5 = e_6, & ae_6 = e_4, \\ be_1 = e_4, & be_2 = e_5, & be_3 = e_6, \\ be_4 = e_1, & be_5 = e_2, & be_6 = e_3, \\ ce_1 = \eta^l e_1, & ce_2 = \eta^{l-3k} e_2, & ce_3 = \eta^{-2l+3k} e_3, \\ ce_4 = \eta^{l-3k} e_4, & ce_5 = \eta^{-2l+3k} e_5, & ce_6 = \eta^l e_6, \\ de_1 = \eta^{-3k} e_1, & de_2 = \eta^{-3l+6k} e_2, & de_3 = \eta^{3l-3k} e_3, \\ de_4 = \eta^{3k} e_4, & de_5 = \eta^{3l-6k} e_5, & de_6 = \eta^{-3l+3k} e_6\,. \end{array} \tag{A.16}$$

Then we can read out the representation matrices as follows

$$\mathbf{6}_{(l,k)}: \quad a = \begin{pmatrix} a_1 & 0 \\ 0 & a_2 \end{pmatrix}, \qquad b = \begin{pmatrix} 0 & \mathbb{1}_3 \\ \mathbb{1}_3 & 0 \end{pmatrix}, \qquad c = \begin{pmatrix} c_1 & 0 \\ 0 & c_2 \end{pmatrix}, \qquad d = \begin{pmatrix} d_1 & 0 \\ 0 & d_2 \end{pmatrix}, \tag{A.17}$$

where $\mathbb{1}_3$ refers to a 3×3 unit matrix, and the different submatrices are given by

$$\begin{aligned} a_1 &= \begin{pmatrix} 0 & 1 & 0 \\ 0 & 0 & 1 \\ 1 & 0 & 0 \end{pmatrix}, \qquad a_2 = \begin{pmatrix} 0 & 0 & 1 \\ 1 & 0 & 0 \\ 0 & 1 & 0 \end{pmatrix}, \\ c_1 &= \begin{pmatrix} \eta^l & 0 & 0 \\ 0 & \eta^{l-3k} & 0 \\ 0 & 0 & \eta^{-2l+3k} \end{pmatrix}, \qquad c_2 = \begin{pmatrix} \eta^{l-3k} & 0 & 0 \\ 0 & \eta^{-2l+3k} & 0 \\ 0 & 0 & \eta^{l} \end{pmatrix}, \\ d_1 &= \begin{pmatrix} \eta^{-3k} & 0 & 0 \\ 0 & \eta^{-3l+6k} & 0 \\ 0 & 0 & \eta^{3l-3k} \end{pmatrix}, \qquad d_2 = d_1^{-1} = \begin{pmatrix} \eta^{3k} & 0 & 0 \\ 0 & \eta^{3l-6k} & 0 \\ 0 & 0 & \eta^{-3l+3k} \end{pmatrix}. \end{aligned} \tag{A.18}$$

The above different representations labelled by (l, k) may be equivalent. If we perform the similarity transformations generated by

$$S = \begin{pmatrix} a_1 & 0 \\ 0 & a_1 \end{pmatrix}, \qquad T = \begin{pmatrix} 0 & t \\ t & 0 \end{pmatrix}, \qquad S^3 = T^2 = (ST)^2 = 1\,, \tag{A.19}$$

where

$$t = \begin{pmatrix} 0 & 0 & 1 \\ 0 & 1 & 0 \\ 1 & 0 & 0 \end{pmatrix} , \tag{A.20}$$

the representations matrices for a and b are kept intact while the diagonal elements of both c and d are interchanged. As a result, the same representation is labeled in six different ways

$$\begin{pmatrix} l \\ k \end{pmatrix}, \ \begin{pmatrix} l-3k \\ l-2k \end{pmatrix}, \ \begin{pmatrix} -2l+3k \\ -l+k \end{pmatrix}, \ \begin{pmatrix} l \\ l-k \end{pmatrix}, \ \begin{pmatrix} -2l+3k \\ -l+2k \end{pmatrix}, \ \begin{pmatrix} l-3k \\ -k \end{pmatrix} . \tag{A.21}$$

The six pairs above can be compactly written into the form

$$M_s^p \begin{pmatrix} l \\ k \end{pmatrix} , \tag{A.22}$$

where

$$M_s^p = \begin{pmatrix} 1 & -3 \\ 1 & -2 \end{pmatrix}^p \begin{pmatrix} 1 & 0 \\ 1 & -1 \end{pmatrix}^s , \quad \text{with} \quad p = 0, 1, 2, \ s = 0, 1 . \tag{A.23}$$

Now we proceed to study whether the six-dimensional representations constructed by the induced representation method are irreducible or not by the famous **Mackey theorem** in math [67–69]. If any one of them is reducible, we further decompose it into the direct sum of the irreducible representations of $D^{(1)}_{9n,3n}$ group.

Theorem (Mackey's Irreducibility Criterion): Let $\mathcal{H} \subset \mathcal{G}$ and ϱ be a representation of $\mathcal{H}$. For $s \in \mathcal{G}$, we define

$$\mathcal{H}_s \equiv \mathcal{H} \cap s\mathcal{H}s^{-1}, \qquad \varrho^s(h) \equiv \varrho(s^{-1}hs) \tag{A.24}$$

for $h \in \mathcal{H}_s$ such that ϱ^s is a representation of $\mathcal{H}_s$. Then the induced representation $\mathrm{Ind}^{\mathcal{G}}_{\mathcal{H}}(\varrho)$ is irreducible if and only if

(1) ϱ is irreducible.

(2) For all $s \in \mathcal{G} \setminus \mathcal{H}$, ϱ^s and $\mathrm{Res}^{\mathcal{H}_s}_{\mathcal{H}}(\varrho)$ are disjoint.

Here $\mathrm{Ind}^{\mathcal{G}}_{\mathcal{H}}(\varrho)$ denotes a representation of G and it is induced from a representation ϱ on a subgroup $\mathcal{H}$. $\mathrm{Res}^{\mathcal{H}_s}_{\mathcal{H}}(\varrho)$ is the restriction of the representation ϱ on $\mathcal{H}$ to $\mathcal{H}_s$. The notation $\mathcal{G} \setminus \mathcal{H}$ denotes the group elements in $\mathcal{G}$ but not in $\mathcal{H}$. Two representations ϱ and ϱ' of a group are said to be disjoint if and only if they contain no equivalent subrepresentations, equivalently if and only if their characters are orthogonal. From this theorem, it is easy to further obtain a useful corollary.

Corollary: Suppose $\mathcal{H}$ is a normal subgroup of $\mathcal{G}$, then we have $\mathcal{H}_s = \mathcal{H}$ and $\mathrm{Res}^{\mathcal{H}_s}_{\mathcal{H}}(\varrho) = \varrho$. In order that $\mathrm{Ind}^{\mathcal{G}}_{\mathcal{H}}(\varrho)$ be irreducible, it is necessary and sufficient that ϱ is irreducible and not isomorphic to any of its conjugate ρ^s for $s \notin H$.

This implies that the representation $\mathrm{Ind}^{\mathcal{G}}_{\mathcal{H}}(\varrho)$ would be reducible if there is a $s \in \mathcal{G} \setminus \mathcal{H}$ leading to $\varrho^s(\mathcal{H}) \cong \varrho(\mathcal{H})$ for normal subgroup $\mathcal{H}$. The corollary can be exploited to determine whether the six-dimensional representations $\mathbf{6}_{(l,k)}$ of the $D^{(1)}_{9n,3n}$ group in Eq. (A.17) are reducible or not. The subgroup $\mathcal{H} = Z_{9n} \times Z_{3n}$ is a normal subgroup of $D^{(1)}_{9n,3n}$, and it is abelian such that its irreducible representation ϱ is one-dimensional and specified by Eq. (A.13). From the above corollary of the Mackey theorem, we know that the six-dimensional representation $\mathbf{6}_{(l,k)}$ is reducible if and only if $\varrho^s(\mathcal{H})$ and $\varrho(\mathcal{H})$ are equivalent representations for an element $s \in D^{(1)}_{9n,3n} \setminus \mathcal{H}$. In order to obtain the conditions in which the six-dimensional representations $\mathbf{6}_{(l,k)}$ is reducible, we only need to consider the value of s is b, ab, a^2b, a and a^2 respectively. The results are collected in table 12.

s	$\varrho^s(\mathcal{H}) \cong \varrho(\mathcal{H})$	Reducible conditions
b	$\varrho(b^{-1}cb) = \varrho(c),\ \varrho(b^{-1}db) = \varrho(d)$	$3k = 0\ (\mathrm{mod}\ 9n)$
ab	$\varrho((ab)^{-1}c(ab)) = \varrho(c),\ \varrho((ab)^{-1}d(ab)) = \varrho(d)$	$3l - 3k = 0\ \mathrm{mod}(9n)$
a^2b	$\varrho\left((a^2b)^{-1}c(a^2b)\right) = \varrho(c),\ \varrho((a^2b)^{-1}d(a^2b)) = \varrho(d)$	$3l - 6k = 0\ \mathrm{mod}(9n)$
$a(a^2)$	$\varrho(a^{-1}ca) = \varrho(c),\ \varrho(a^{-1}da) = \varrho(d)$	$3k = 0,\ 3l = 0\ \mathrm{mod}(9n)$

Table 12: The reducible conditions for the six-dimensional representations $\mathbf{6}_{(l,k)}$. The one-dimensional representation ϱ of $\mathcal{H}$ is given by Eq. (A.13), i.e. $\varrho(c) = \eta^l$ and $\varrho(d) = \eta^{-3k}$. The values of parameters l and k are $l = 0, 1, \cdots, 9n-1$ and $k = 0, 1, \cdots, 3n-1$.

- **Six-dimensional representations**

  Six-dimensional representations of the $D^{(1)}_{9n,3n}$ group have been constructed by the method of induced representation, as shown in Eq. (A.17) and Eq. (A.18). From table 12, we find that the induced representation $\mathbf{6}_{(l,k)}$ in Eq. (A.17) would be reducible when any of the following conditions are met

$$\begin{cases} 9n & : \quad k = 0, \quad l = 0, 1, \ldots, 9n-1, \\ 9n-3 & : \quad 3l - 3k = 0\ \mathrm{mod}(9n), \quad k \neq 0 \\ 9n-3 & : \quad 3l - 6k = 0\ \mathrm{mod}(9n), \quad k \neq 0 \end{cases} , \tag{A.25}$$

  where the quantity on the left of the colon is the number of (l, k) values of the properties on the right of the colon. Excluding these values for l and k, there should be $9n \times 3n - 9n - (9n-3) - (9n-3) = 27n(n-1) + 6$ different pairs of (l, k). Furthermore, taking into account the over counting issue shown in Eq. (A.21), we essentially have $\frac{27n(n-1)+6}{6}$ six-dimensional irreducible representations, and the representation matrices of the generators are given in Eq. (A.17).

- **Three-dimensional representations**

  Once the conditions $3k = 0$, $3l - 3k = 0\ \mathrm{mod}(9n)$ or $3l - 6k = 0\ \mathrm{mod}(9n)$ are fulfilled, the six-dimensional induced representation $6_{(l,k)}$ could be decomposed into the direct sum of three and two-dimensional representations. Firstly we concentrate on the case of $3k = 0$ or equivalently $k = 0$. From Eq. (A.16) we see that the eigenvalues of c on the three pairs of basis vectors (e_1, e_4), (e_2, e_6) and (e_3, e_5) are η^l, η^l and η^{-2l} respectively, and the eigenvalues of d on the three pairs vectors (e_1, e_4), (e_2, e_6) and (e_3, e_5) are 1, η^{-3l} and η^{3l} respectively. Hence we recombine the six vectors $e_1, \ldots, e_6$ into

$$e'_1 = x_1 e_1 + y_1 e_4, \quad e'_2 = x_2 e_2 + y_2 e_6, \quad e'_3 = x_3 e_3 + y_3 e_5\,. \tag{A.26}$$

  In the case of $3k = 0$ and $l \neq 0, 3n, 6n$, the three vectors e'_1, e'_2 and e'_3 can be distinguished from each other by the actions of c and d, and they must be closed under the action of a and b. Considering the effect of a, we find

$$a e'_1 = e'_3, \quad a e'_2 = e'_1, \quad a e'_3 = e'_2\,, \tag{A.27}$$

  which yields

$$x_1 = x_2 = x_3 \equiv x, \qquad y_1 = y_2 = y_3 \equiv y\,. \tag{A.28}$$

  Furthermore, closeness under the action of b implies

$$b e'_1 = \pm e'_1, \quad b e'_2 = \pm e'_3, \quad b e'_3 = \pm e'_2\,. \tag{A.29}$$

In the case of $be'_1 = e'_1$, i.e. $x = y$, then the normalized basis vectors of a three-dimensional subspace can be chosen to be

$$e'_1 = \frac{1}{\sqrt{2}}(e_1 + e_4), \quad e'_2 = \frac{1}{\sqrt{2}}(e_2 + e_6) = a^2 e'_1, \quad e'_3 = \frac{1}{\sqrt{2}}(e_3 + e_5) = a e'_1 \,. \tag{A.30}$$

In the case of $be'_1 = -e'_1$, i.e. $x = -y$, we define the three normalized orthogonal vectors as

$$e'_4 = \frac{1}{\sqrt{2}}(e_1 - e_4), \quad e'_5 = \frac{1}{\sqrt{2}}(e_2 - e_6) = a^2 e'_4, \quad e'_6 = \frac{1}{\sqrt{2}}(e_3 - e_5) = a e'_4 \,. \tag{A.31}$$

It is easy to check that e'_4, e'_5 and e'_6 span another three-dimensional subspace. The basis transformation matrix from e_i to e'_i is denoted by Ω, i.e.

$$e'_i = \sum_{j=1}^{6} e_j \Omega_{ji} \,, \tag{A.32}$$

where the similarity transformation Ω reads

$$\Omega = \frac{1}{\sqrt{2}} \begin{pmatrix} \mathbb{1}_3 & \mathbb{1}_3 \\ \varpi & -\varpi \end{pmatrix}, \qquad \varpi = \begin{pmatrix} 1 & 0 & 0 \\ 0 & 0 & 1 \\ 0 & 1 & 0 \end{pmatrix}, \tag{A.33}$$

In the new basis, the representation matrices of the generators are of the following form

$$\begin{aligned} a' &\equiv \Omega^{-1} a \Omega = \begin{pmatrix} a_{\mathbf{3}_{l,0}} & 0 \\ 0 & a_{\mathbf{3}_{l,1}} \end{pmatrix}, \qquad b' \equiv \Omega^{-1} b \Omega = \begin{pmatrix} b_{\mathbf{3}_{l,0}} & 0 \\ 0 & b_{\mathbf{3}_{l,1}} \end{pmatrix}, \\ c' &\equiv \Omega^{-1} c \Omega = \begin{pmatrix} c_{\mathbf{3}_{l,0}} & 0 \\ 0 & c_{\mathbf{3}_{l,1}} \end{pmatrix}, \qquad d' \equiv \Omega^{-1} d \Omega = \begin{pmatrix} d_{\mathbf{3}_{l,0}} & 0 \\ 0 & d_{\mathbf{3}_{l,1}} \end{pmatrix}, \end{aligned} \tag{A.34}$$

where

$$\begin{aligned} &a_{\mathbf{3}_{l,0}} = \begin{pmatrix} 0 & 1 & 0 \\ 0 & 0 & 1 \\ 1 & 0 & 0 \end{pmatrix}, \; b_{\mathbf{3}_{l,0}} = \begin{pmatrix} 1 & 0 & 0 \\ 0 & 0 & 1 \\ 0 & 1 & 0 \end{pmatrix}, \; c_{\mathbf{3}_{l,0}} = \begin{pmatrix} \eta^l & 0 & 0 \\ 0 & \eta^l & 0 \\ 0 & 0 & \eta^{-2l} \end{pmatrix}, \; d_{\mathbf{3}_{l,0}} = \begin{pmatrix} 1 & 0 & 0 \\ 0 & \eta^{-3l} & 0 \\ 0 & 0 & \eta^{3l} \end{pmatrix}, \\ &a_{\mathbf{3}_{l,1}} = a_{\mathbf{3}_{l,0}}, \qquad b_{\mathbf{3}_{l,1}} = -b_{\mathbf{3}_{l,0}}, \qquad c_{\mathbf{3}_{l,1}} = c_{\mathbf{3}_{l,0}}, \qquad d_{\mathbf{3}_{l,1}} = d_{\mathbf{3}_{l,0}} \,. \end{aligned} \tag{A.35}$$

This means that the six-dimensional representation $\mathbf{6}_{l,0}$ breaks up into two three-dimensional irreducible representation $\mathbf{3}_{l,0}$ and $\mathbf{3}_{l,1}$ which differ in the overall sign of b. Notice that the values of $l = 0,\, 3n,\, 6n$ should be excluded, since both triplet representations $\mathbf{3}_{l,0}$ and $\mathbf{3}_{l,1}$ then could be decomposed into one-dimensional and two-dimensional representation.

Next we proceed to consider the case of $3l - 3k = 0 \mod(9n)$ and $l \neq 0, 3n, 6n$. We can construct the eigenstates of the generators c and d as follows

$$e'_1 = x_1 e_1 + y_1 e_5, \quad e'_2 = x_2 e_2 + y_2 e_4, \quad e'_3 = x_3 e_3 + y_3 e_6 \,. \tag{A.36}$$

Note that e'_1, e'_2 and e'_3 are mapped into each other under the action of a and b, Taking into account the normalization condition further, we have $x_1 = x_2 = x_3 = y_1 = y_2 = y_3 = 1/\sqrt{2}$ such that

$$e'_1 = \frac{1}{\sqrt{2}}(e_1 + e_5), \quad e'_2 = \frac{1}{\sqrt{2}}(e_2 + e_4) = a^2 e'_1, \quad e'_3 = \frac{1}{\sqrt{2}}(e_3 + e_6) = a e'_1 \,, \tag{A.37}$$

or $x_1 = x_2 = x_3 = -y_1 = -y_2 = y_3 = -1/\sqrt{2}$ which leads to

$$e'_4 = \frac{1}{\sqrt{2}}(e_1 - e_5), \quad e'_5 = \frac{1}{\sqrt{2}}(e_2 - e_4) = a^2 e'_4, \qquad e'_6 = \frac{1}{\sqrt{2}}(e_3 - e_6) = a e'_4 \,. \quad \text{(A.38)}$$

It is straightforward to check the following equations are fulfilled

$$\begin{aligned}
&be'_1 = e'_2, \quad be'_2 = e'_1, \quad be'_3 = e'_3, \quad ce'_1 = \eta^l e'_1, \quad ce'_2 = \eta^{-2l} e'_2, \quad ce'_3 = \eta^l e'_3, \\
&de'_1 = \eta^{-3l} e'_1, \quad de'_2 = \eta^{3l} e'_2, \quad de'_3 = e'_3, \quad be'_4 = -e'_5, \quad be'_5 = -e'_4, \quad be'_6 = -e'_6, \\
&ce'_4 = \eta^l e'_4, \quad ce'_5 = \eta^{-2l} e'_5, \quad ce'_6 = \eta^l e'_6, \quad de'_4 = \eta^{-3l} e'_4, \quad de'_5 = \eta^{3l} e'_5, \quad de'_6 = e'_6 \,. \quad \text{(A.39)}
\end{aligned}$$

As a result, the induced representation $\mathbf{6}_{l,\,l \bmod (3n)}$ for $l \neq 0,\ 3n,\ 6n$ can be split into two three-dimensional representations. The unitary transformation from the e_i basis to the e'_i basis is

$$e'_i = \sum_{j=1}^{6} \Omega_{ji} e_j \,, \quad \text{(A.40)}$$

with

$$\Omega = \frac{1}{\sqrt{2}} \begin{pmatrix} \mathbb{1}_3 & \mathbb{1}_3 \\ \varpi & -\varpi \end{pmatrix}, \qquad \varpi = \begin{pmatrix} 0 & 1 & 0 \\ 1 & 0 & 0 \\ 0 & 0 & 1 \end{pmatrix} . \quad \text{(A.41)}$$

Performing the similarity transformation Ω, the representation matrices in the new basis are given by

$$\begin{aligned}
a' &= \Omega^{-1} a \Omega = \begin{pmatrix} a_{\mathbf{3}_{l,2}} & 0 \\ 0 & a_{\mathbf{3}_{l,3}} \end{pmatrix}, \qquad b' = \Omega^{-1} b \Omega = \begin{pmatrix} b_{\mathbf{3}_{l,2}} & 0 \\ 0 & b_{\mathbf{3}_{l,3}} \end{pmatrix}, \\
c' &= \Omega^{-1} c \Omega = \begin{pmatrix} c_{\mathbf{3}_{l,2}} & 0 \\ 0 & c_{\mathbf{3}_{l,3}} \end{pmatrix}, \qquad d' = \Omega^{-1} d \Omega = \begin{pmatrix} d_{\mathbf{3}_{l,2}} & 0 \\ 0 & d_{\mathbf{3}_{l,3}} \end{pmatrix} ,
\end{aligned} \quad \text{(A.42)}$$

where

$$\begin{aligned}
&a_{\mathbf{3}_{l,2}} = \begin{pmatrix} 0 & 1 & 0 \\ 0 & 0 & 1 \\ 1 & 0 & 0 \end{pmatrix}, \ b_{\mathbf{3}_{l,2}} = \begin{pmatrix} 0 & 1 & 0 \\ 1 & 0 & 0 \\ 0 & 0 & 1 \end{pmatrix}, \ c_{\mathbf{3}_{l,2}} = \begin{pmatrix} \eta^l & 0 & 0 \\ 0 & \eta^{-2l} & 0 \\ 0 & 0 & \eta^l \end{pmatrix}, \ d_{\mathbf{3}_{l,2}} = \begin{pmatrix} \eta^{-3l} & 0 & 0 \\ 0 & \eta^{3l} & 0 \\ 0 & 0 & 1 \end{pmatrix}, \\
&a_{\mathbf{3}_{l,3}} = a_{\mathbf{3}_{l,2}}, \qquad b_{\mathbf{3}_{l,3}} = -b_{\mathbf{3}_{l,2}}, \qquad c_{\mathbf{3}_{l,3}} = c_{\mathbf{3}_{l,2}}, \qquad d_{\mathbf{3}_{l,3}} = d_{\mathbf{3}_{l,2}} \,.
\end{aligned} \quad \text{(A.43)}$$

Therefore $\mathbf{6}_{l,\,l \bmod (3n)}$ for $l \neq 0,\ 3n,\ 6n$ is the direct sum of three-dimensional irreducible representations $\mathbf{3}_{l,3}$ and $\mathbf{3}_{l,4}$.

Finally we consider the case of $3l - 6k = 0 \bmod (9n)$ with $k \neq 0$ and $l \neq 0, 3n, 6n$. In the same fashion as previous cases, we first recombine the basis vectors into

$$e'_1 = x_1 e_1 + y_1 e_6, \quad e'_2 = x_2 e_2 + y_2 e_5, \quad e'_3 = x_3 e_3 + y_3 e_4 \,, \quad \text{(A.44)}$$

which are eigenstates of both c and d and fulfill

$$ce'_1 = \eta^{-2l'} e'_1, \ ce'_2 = \eta^{l'} e'_2, \ ce'_3 = \eta^{l'} e'_3, \ de'_1 = \eta^{3l'} e'_1, \ de'_2 = e'_2, \ de'_3 = \eta^{-3l'} e'_3 \,, \quad \text{(A.45)}$$

for any values of x_i and y_i $(i = 1, 2, 3)$, where $l' = l - 3k = 3n - k, 6n - k, 9n - k$ with $k = 0, 1, \ldots, 3n - 1$ such that the value of l' can be $0, 1, \ldots, 9n - 1$. Taking

into account the action of the remaining two generators a and b, we find two three-dimensional subspaces would be generated. The basis of the first subspace can be chosen to be

$$e'_1=\frac{1}{\sqrt{2}}(e_1+e_6),\quad e'_2=\frac{1}{\sqrt{2}}(e_2+e_5)=a^2e'_1,\quad e'_3=\frac{1}{\sqrt{2}}(e_3+e_4)=ae'_1\,, \tag{A.46}$$

The basis vectors of the second three-dimensional subspace are

$$e'_4=\frac{1}{\sqrt{2}}(e_1-e_6),\quad e'_5=\frac{1}{\sqrt{2}}(e_2-e_5)=a^2e'_4,\quad e'_6=\frac{1}{\sqrt{2}}(e_3-e_4)=ae'_4\,, \tag{A.47}$$

We can read out the unitary basis transformation

$$\Omega=\frac{1}{\sqrt{2}}\begin{pmatrix}\mathbb{1}_3 & \mathbb{1}_3\\ \varpi & -\varpi\end{pmatrix},\qquad \varpi=\begin{pmatrix}0&0&1\\0&1&0\\1&0&0\end{pmatrix}. \tag{A.48}$$

The representation matrices for the generators a, b, c and d transform as

$$\begin{aligned}
a'&=\Omega^{-1}a\Omega=\begin{pmatrix}a_{\mathbf{3}_{l',4}} & 0\\ 0 & a_{\mathbf{3}_{l',5}}\end{pmatrix},\qquad b'=\Omega^{-1}b\Omega=\begin{pmatrix}b_{\mathbf{3}_{l',4}} & 0\\ 0 & b_{\mathbf{3}_{l',5}}\end{pmatrix},\\
c'&=\Omega^{-1}c\Omega=\begin{pmatrix}c_{\mathbf{3}_{l',4}} & 0\\ 0 & c_{\mathbf{3}_{l',5}}\end{pmatrix},\qquad d'=\Omega^{-1}d\Omega=\begin{pmatrix}d_{\mathbf{3}_{l',4}} & 0\\ 0 & d_{\mathbf{3}_{l',5}}\end{pmatrix},
\end{aligned} \tag{A.49}$$

where

$$\begin{aligned}
&a_{\mathbf{3}_{l',4}}=\begin{pmatrix}0&1&0\\0&0&1\\1&0&0\end{pmatrix},\ b_{\mathbf{3}_{l',4}}=\begin{pmatrix}0&0&1\\0&1&0\\1&0&0\end{pmatrix},\ c_{\mathbf{3}_{l',4}}=\begin{pmatrix}\eta^{-2l'}&0&0\\0&\eta^{l'}&0\\0&0&\eta^{l'}\end{pmatrix},\ d_{\mathbf{3}_{l',4}}=\begin{pmatrix}\eta^{3l'}&0&0\\0&1&0\\0&0&\eta^{-3l'}\end{pmatrix},\\
&a_{\mathbf{3}_{l',5}}\ =\ a_{\mathbf{3}_{l',4}},\qquad b_{\mathbf{3}_{l',5}}\ =\ -\,b_{\mathbf{3}_{l',4}},\qquad c_{\mathbf{3}_{l',5}}\ =\ c_{\mathbf{3}_{l',4}},\qquad d_{\mathbf{3}_{l',5}}\ =\ d_{\mathbf{3}_{l',4}}\,.
\end{aligned} \tag{A.50}$$

Note that both triplet representations $\mathbf{3}_{l',4}$ and $\mathbf{3}_{l',5}$ would be reducible for $l'=0,3n,6n$.

So far we have obtained six three-dimensional irreducible representations $\mathbf{3}_{l,0}$, $\mathbf{3}_{l,1}$, $\mathbf{3}_{l,2}$, $\mathbf{3}_{l,3}$, $\mathbf{3}_{l,4}$, $\mathbf{3}_{l,5}$. However, only two of them are inequivalent because they are related with each other by similarity transformations as follows :

$$\begin{aligned}
&a_{\mathbf{3}_{l,2}}=U^\dagger a_{\mathbf{3}_{l,0}}U,\quad b_{\mathbf{3}_{l,2}}=U^\dagger b_{\mathbf{3}_{l,0}}U,\quad c_{\mathbf{3}_{l,2}}=U^\dagger c_{\mathbf{3}_{l,0}}U,\quad d_{\mathbf{3}_{l,2}}=U^\dagger d_{\mathbf{3}_{l,0}}U,\\
&a_{\mathbf{3}_{l,3}}=U^\dagger a_{\mathbf{3}_{l,1}}U,\quad b_{\mathbf{3}_{l,3}}=U^\dagger b_{\mathbf{3}_{l,1}}U,\quad c_{\mathbf{3}_{l,3}}=U^\dagger c_{\mathbf{3}_{l,1}}U,\quad d_{\mathbf{3}_{l,3}}=U^\dagger d_{\mathbf{3}_{l,1}}U,\\
&a_{\mathbf{3}_{l,4}}=U a_{\mathbf{3}_{l,0}}U^\dagger,\quad b_{\mathbf{3}_{l,4}}=U b_{\mathbf{3}_{l,0}}U^\dagger,\quad c_{\mathbf{3}_{l,4}}=U c_{\mathbf{3}_{l,0}}U^\dagger,\quad d_{\mathbf{3}_{l,4}}=U d_{\mathbf{3}_{l,0}}U^\dagger,\\
&a_{\mathbf{3}_{l,5}}=U a_{\mathbf{3}_{l,1}}U^\dagger,\quad b_{\mathbf{3}_{l,5}}=U b_{\mathbf{3}_{l,1}}U^\dagger,\quad c_{\mathbf{3}_{l,5}}=U c_{\mathbf{3}_{l,1}}U^\dagger,\quad d_{\mathbf{3}_{l,5}}=U d_{\mathbf{3}_{l,1}}U^\dagger\,,
\end{aligned} \tag{A.51}$$

where the unitary transformation U is

$$U=\begin{pmatrix}0&0&1\\1&0&0\\0&1&0\end{pmatrix}. \tag{A.52}$$

Hence we conclude that the $D^{(1)}_{9n,3n}$ group totally has $2(9n-3)$ inequivalent three-dimensional irreducible representations which can be chosen to be $\mathbf{3}_{l,0}$ and $\mathbf{3}_{l,1}$ with $l\neq 0,3n,6n$.

- **Two-dimensional representations**

In the following, we shall show that both triplet representations $\mathbf{3}_{l,0}$ and $\mathbf{3}_{l,1}$ for $l = 0, 3n, 6n$ would be reduced into the direct sum of one-dimensional representation and two-dimensional representation. Firstly we concentrate on $\mathbf{3}_{l,0}$. In this case, the three basis vectors e'_1, e'_2 and e'_3 in Eq. (A.30) can not be distinguished by the actions of c and d, the eigenstates of the generator a are

$$e''_1 = \frac{1}{\sqrt{3}}(e'_1+e'_2+e'_3), \quad e''_2 = \frac{1}{\sqrt{3}}(e'_1+\omega e'_2+\omega^2 e'_3), \quad e''_3 = \frac{1}{\sqrt{3}}(e'_1+\omega^2 e'_2+\omega e'_3)\,, \tag{A.53}$$

with $ae''_1 = e''_1$, $ae''_2 = \omega e''_2$ and $ae''_3 = \omega^2 e''_3$. Under the action of the generator b, e''_1 is mapped into itself and e''_2 and e''_3 are interchanged. Therefore the representation space of $\mathbf{3}_{l,0}$ is split into one-dimensional subspace proportional to e''_1 and two-dimensional invariant subspaces spanned by e''_2 and e''_3. However, the representation matrix for b is off-diagonal in the two-dimensional representation. In the present work, we would like to work in a basis where the representation matrix of b is diagonal in the doublet representation such that all the relevant clebsch-gordan coefficients are real, as shown in Appendix A.2. Consequently we choose the basis vectors as follows

$$\begin{aligned}
e'''_1 &= e''_1 = \frac{1}{\sqrt{3}}(e'_1 + e'_2 + e'_3), \\
e'''_2 &= \frac{1}{\sqrt{2}}(e''_2 + e''_3) = \frac{1}{\sqrt{6}}(2e'_1 - e'_2 - e'_3), \\
e'''_3 &= \frac{i}{\sqrt{2}}(e''_2 - e''_3) = \frac{-1}{\sqrt{2}}(e'_2 - e'_3)\,.
\end{aligned} \tag{A.54}$$

Then we can read out the unitary basis transformation matrix as

$$\mathcal{S} = \frac{1}{\sqrt{6}}\begin{pmatrix} \sqrt{2} & 2 & 0 \\ \sqrt{2} & -1 & -\sqrt{3} \\ \sqrt{2} & -1 & \sqrt{3} \end{pmatrix}\,, \tag{A.55}$$

with $e'''_i = \sum_{j=1}^{3} e'_j \mathcal{S}_{ji}$. In this set of new basis, the representation matrices for the generators a, b, c and d are

$$\begin{aligned}
a'' &= \mathcal{S}^{-1} a_{\mathbf{3}_{l,0}} \mathcal{S} = \begin{pmatrix} 1 & 0 \\ 0 & a_{\mathbf{2}_0} \end{pmatrix}, \qquad & b'' &= \mathcal{S}^{-1} b_{\mathbf{3}_{l,0}} \mathcal{S} = \begin{pmatrix} 1 & 0 \\ 0 & b_{\mathbf{2}_0} \end{pmatrix}, \\
c'' &= \mathcal{S}^{-1} c_{\mathbf{3}_{l,0}} \mathcal{S} = \eta^l \mathbb{1}_3, & d'' &= \mathcal{S}^{-1} d_{\mathbf{3}_{l,0}} \mathcal{S} = \mathbb{1}_3,
\end{aligned} \tag{A.56}$$

with

$$a_{\mathbf{2}_0} = \frac{1}{2}\begin{pmatrix} -1 & -\sqrt{3} \\ \sqrt{3} & -1 \end{pmatrix}, \quad b_{\mathbf{2}_0} = \begin{pmatrix} 1 & 0 \\ 0 & -1 \end{pmatrix}\,, \tag{A.57}$$

Note that $\eta^l = 1, \omega, \omega^2$ for $l = 0, 3n, 6n$ respectively.

Now we turn to another set of reducible triplet representations $\mathbf{3}_{l,1}$ with $l = 0, 3n, 6n$. In the same way as previous case, the new basis vectors are taken to be

$$e''_4 = \frac{1}{\sqrt{3}}(e'_4 + e'_5 + e'_6)\,, \quad e''_5 = \frac{i}{\sqrt{2}}(e'_5 - e'_6)\,, \quad e''_6 = \frac{i}{\sqrt{6}}(2e'_4 - e'_5 - e'_6)\,, \tag{A.58}$$

where e'_4, e'_5 and e'_6 are specified by Eq. (A.31). The unitary transformation for this basis change is

$$\mathcal{S} = \frac{1}{\sqrt{6}}\begin{pmatrix} \sqrt{2} & 0 & 2i \\ \sqrt{2} & i\sqrt{3} & -i \\ \sqrt{2} & -i\sqrt{3} & -i \end{pmatrix}\,. \tag{A.59}$$

The corresponding representation matrices are given by

$$\begin{aligned} a'' &= \mathcal{S}^{-1} a_{\mathbf{3}_{l,1}} \mathcal{S} = \begin{pmatrix} 1 & 0 \\ 0 & a_{\mathbf{2}_0} \end{pmatrix}, \qquad b'' = \mathcal{S}^{-1} b_{\mathbf{3}_{l,1}} \mathcal{S} = \begin{pmatrix} -1 & 0 \\ 0 & b_{\mathbf{2}_0} \end{pmatrix}, \\ c'' &= \mathcal{S}^{-1} c_{\mathbf{3}_{l,1}} \mathcal{S} = \eta^l \mathbb{1}_3, \qquad\qquad d'' = \mathcal{S}^{-1} d_{\mathbf{3}_{l,1}} \mathcal{S} = \mathbb{1}_3 \,, \end{aligned} \tag{A.60}$$

where $a_{\mathbf{2}_0}$ and $b_{\mathbf{2}_0}$ are shown in Eq. (A.57). Hence by performing similarity transformation on the reducible triplet representations $\mathbf{3}_{l,0}$ and $\mathbf{3}_{l,1}$ for $l = 0, 3n, 6n$, we can obtain three inequivalent two-dimensional irreducible representations and six one-dimensional representations given in Eq. (A.6). The three two-dimensional representations differ in the representation matrix of c:

$$\begin{aligned} & a_{\mathbf{2}_0} = \frac{1}{2} \begin{pmatrix} -1 & -\sqrt{3} \\ \sqrt{3} & -1 \end{pmatrix}, \quad b_{\mathbf{2}_0} = \begin{pmatrix} 1 & 0 \\ 0 & -1 \end{pmatrix}, \quad c_{\mathbf{2}_0} = d_{\mathbf{2}_0} = \mathbb{1}_2, \\ & a_{\mathbf{2}_1} = a_{\mathbf{2}_0}, \quad b_{\mathbf{2}_1} = b_{\mathbf{2}_0}, \quad c_{\mathbf{2}_1} = \omega \mathbb{1}_2, \quad d_{\mathbf{2}_1} = \mathbb{1}_2, \\ & a_{\mathbf{2}_2} = a_{\mathbf{2}_0}, \quad b_{\mathbf{2}_2} = b_{\mathbf{2}_0}, \quad c_{\mathbf{2}_2} = \omega^2 \mathbb{1}_2, \quad d_{\mathbf{2}_2} = \mathbb{1}_2 \,, \end{aligned} \tag{A.61}$$

which can also be sententiously written as

$$a_{\mathbf{2}_i} = \frac{1}{2} \begin{pmatrix} -1 & -\sqrt{3} \\ \sqrt{3} & -1 \end{pmatrix}, \; b_{\mathbf{2}_i} = \begin{pmatrix} 1 & 0 \\ 0 & -1 \end{pmatrix}, \; c_{\mathbf{2}_i} = \omega^i \mathbb{1}_2, \; d_{\mathbf{2}_i} = \mathbb{1}_2, \; i = 0, 1, 2 \,. \tag{A.62}$$

There are no more irreducible representations as we see that the number of irreducible representations is already equal to the number of conjugacy classes:

$$\frac{27n(n-1)+6}{6} + 2(9n-3) + 3 + 6 = 1 + 2 + (9n-3) + \frac{27n(n-1)+6}{6} + 3 + 9n \,. \tag{A.63}$$

Furthermore, we find that the sum of the squares of the dimensions of the irreducible representations is really equal to the order of the group, i.e.

$$\frac{27n(n-1)+6}{6} \times 6^2 + 2(9n-3) \times 3^2 + 3 \times 2^2 + 6 \times 1^2 = 162n^2 \,. \tag{A.64}$$

We can derive the $D^{(1)}_{9n,3n}$ character table by taking traces over the relevant representation matrices. The results are displayed in table 13, where $\tilde{M}^p_s$ refers to

$$\tilde{M}^p_s \equiv \begin{pmatrix} 1 & 1 \\ -3 & -2 \end{pmatrix}^p \begin{pmatrix} 1 & 0 \\ -3 & -1 \end{pmatrix}^s, \quad \text{with} \;\; p = 0, 1, 2, \quad s = 0, 1, \tag{A.65}$$

With the character table, it is easy to calculate the Kronecker products of two irreducible representations of the $D^{(1)}_{9n,3n}$ group as follows:

$$\begin{aligned} & \mathbf{1}_{i,j} \otimes \mathbf{1}_{p,q} = \mathbf{1}_{f,g}, \quad \mathbf{1}_{i,j} \otimes \mathbf{2}_q = \mathbf{2}_g, \quad \mathbf{1}_{i,j} \otimes \mathbf{3}_{l,p} = \mathbf{3}_{l+3nj,f}, \quad \mathbf{1}_{i,j} \otimes \mathbf{6}_{(l,k)} = \mathbf{6}_{(l+3nj,k)}, \\ & \mathbf{2}_j \otimes \mathbf{2}_q = \mathbf{1}_{0,g} \oplus \mathbf{1}_{1,g} \oplus \mathbf{2}_g, \quad \mathbf{2}_j \otimes \mathbf{3}_{l,i} = \mathbf{3}_{l+3nj,0} \oplus \mathbf{3}_{l+3nj,1}, \\ & \mathbf{2}_j \otimes \mathbf{6}_{(l,k)} \;\; = \mathbf{6}_{(l+3nj,k)} \oplus \mathbf{6}_{(l+3nj,k)}, \qquad \mathbf{3}_{l,i} \otimes \mathbf{3}_{l',p} \;\; = \mathbf{3}_{l+l',f} \oplus \mathbf{6}_{(l+l',l')} \end{aligned}$$

	$1\mathcal{C}_1$	$1\mathcal{C}_1^{(\nu)}$	$3\mathcal{C}_1^{(\rho)}$	$6\mathcal{C}_1^{(\rho,\sigma)}$	$18n^2\mathcal{C}_2^{(\tau)}$	$9n\mathcal{C}_3^{(\rho)}$
$\mathbf{1_{0,0}}$	1	1	1	1	1	1
$\mathbf{1_{0,1}}$	1	1	ω^{ρ}	ω^{ρ}	ω^{τ}	ω^{ρ}
$\mathbf{1_{0,2}}$	1	1	$\omega^{2\rho}$	$\omega^{2\rho}$	$\omega^{2\tau}$	$\omega^{2\rho}$
$\mathbf{1_{1,0}}$	1	1	1	1	1	-1
$\mathbf{1_{1,1}}$	1	1	ω^{ρ}	ω^{ρ}	ω^{τ}	$-\omega^{\rho}$
$\mathbf{1_{1,2}}$	1	1	$\omega^{2\rho}$	$\omega^{2\rho}$	$\omega^{2\tau}$	$-\omega^{2\rho}$
$\mathbf{2_0}$	2	2	2	2	-1	0
$\mathbf{2_1}$	2	2	$2\omega^{\rho}$	$2\omega^{\rho}$	$-\omega^{\tau}$	0
$\mathbf{2_2}$	2	2	$2\omega^{2\rho}$	$2\omega^{2\rho}$	$-\omega^{2\tau}$	0
$\mathbf{3}_{l,0}$	3	$3\eta^{l\nu}$	$\sum_p \eta^{(\rho,0)\tilde{M}_0^p\binom{l}{0}}$	$\sum_p \eta^{(\rho,\sigma)\tilde{M}_0^p\binom{l}{0}}$	0	$\eta^{l\rho}$
$\mathbf{3}_{l,1}$	3	$3\eta^{l\nu}$	$\sum_p \eta^{(\rho,0)\tilde{M}_0^p\binom{l}{0}}$	$\sum_p \eta^{(\rho,\sigma)\tilde{M}_0^p\binom{l}{0}}$	0	$-\eta^{l\rho}$
$\mathbf{6}_{(l,k)}$	6	$6\eta^{l\nu}$	$\sum_{p,s} \eta^{(\rho,0)\tilde{M}_s^p\binom{l}{-3k}}$	$\sum_{p,s} \eta^{(\rho,\sigma)\tilde{M}_s^p\binom{l}{-3k}}$	0	0

Table 13: The character table of the $D_{9n,3n}^{(1)}$ group. The different conjugacy classes are presented in Eq. (A.4). The notation $\tilde{M}_s^p$ is explained in Eq. (A.65).

A.2 Clebsch-Gordan Coefficients of the $D_{9n,3n}^{(1)}$ group

In the following, we shall decompose the product of two irreducible representations into a sum of irreducible representations of $D_{9n,3n}^{(1)}$. Under the action of the generators a, b and c, different $D_{9n,3n}^{(1)}$ vector multiplets transform as follows:

$$
\begin{aligned}
\mathbf{6}_{(l,k)}:&\quad \begin{pmatrix}\alpha_1\\ \alpha_2\\ \alpha_3\\ \alpha_4\\ \alpha_5\\ \alpha_6\end{pmatrix} \overset{a}{\mapsto} \begin{pmatrix}\alpha_2\\ \alpha_3\\ \alpha_1\\ \alpha_6\\ \alpha_4\\ \alpha_5\end{pmatrix}, \quad \overset{b}{\mapsto} \begin{pmatrix}\alpha_4\\ \alpha_5\\ \alpha_6\\ \alpha_1\\ \alpha_2\\ \alpha_3\end{pmatrix}, \quad \overset{c}{\mapsto} \begin{pmatrix}\eta^{l}\alpha_1\\ \eta^{l-3k}\alpha_2\\ \eta^{3k-2l}\alpha_3\\ \eta^{l-3k}\alpha_4\\ \eta^{3k-2l}\alpha_5\\ \eta^{l}\alpha_6\end{pmatrix},\\
\mathbf{3}_{l,0}:&\quad \begin{pmatrix}\alpha_1\\ \alpha_2\\ \alpha_3\end{pmatrix} \overset{a}{\mapsto} \begin{pmatrix}\alpha_2\\ \alpha_3\\ \alpha_1\end{pmatrix}, \quad \overset{b}{\mapsto} \begin{pmatrix}\alpha_1\\ \alpha_3\\ \alpha_2\end{pmatrix}, \quad \overset{c}{\mapsto} \begin{pmatrix}\eta^{l}\alpha_1\\ \eta^{l}\alpha_2\\ \eta^{-2l}\alpha_3\end{pmatrix},\\
\mathbf{3}_{l,1}:&\quad \begin{pmatrix}\alpha_1\\ \alpha_2\\ \alpha_3\end{pmatrix} \overset{a}{\mapsto} \begin{pmatrix}\alpha_2\\ \alpha_3\\ \alpha_1\end{pmatrix}, \quad \overset{b}{\mapsto} \begin{pmatrix}-\alpha_1\\ -\alpha_3\\ -\alpha_2\end{pmatrix}, \quad \overset{c}{\mapsto} \begin{pmatrix}\eta^{l}\alpha_1\\ \eta^{l}\alpha_2\\ \eta^{-2l}\alpha_3\end{pmatrix},\\
\mathbf{2_0}:&\quad \begin{pmatrix}\alpha_1\\ \alpha_2\end{pmatrix} \overset{a}{\mapsto} \frac{1}{2}\begin{pmatrix}-\alpha_1-\sqrt{3}\alpha_2\\ \sqrt{3}\alpha_1-\alpha_2\end{pmatrix}, \quad \overset{b}{\mapsto} \begin{pmatrix}\alpha_1\\ -\alpha_2\end{pmatrix}, \quad \overset{c}{\mapsto} \begin{pmatrix}\alpha_1\\ \alpha_2\end{pmatrix},\\
\mathbf{2_1}:&\quad \begin{pmatrix}\alpha_1\\ \alpha_2\end{pmatrix} \overset{a}{\mapsto} \frac{1}{2}\begin{pmatrix}-\alpha_1-\sqrt{3}\alpha_2\\ \sqrt{3}\alpha_1-\alpha_2\end{pmatrix}, \quad \overset{b}{\mapsto} \begin{pmatrix}\alpha_1\\ -\alpha_2\end{pmatrix}, \quad \overset{c}{\mapsto} \omega\begin{pmatrix}\alpha_1\\ \alpha_2\end{pmatrix},\\
\mathbf{2_2}:&\quad \begin{pmatrix}\alpha_1\\ \alpha_2\end{pmatrix} \overset{a}{\mapsto} \frac{1}{2}\begin{pmatrix}-\alpha_1-\sqrt{3}\alpha_2\\ \sqrt{3}\alpha_1-\alpha_2\end{pmatrix}, \quad \overset{b}{\mapsto} \begin{pmatrix}\alpha_1\\ -\alpha_2\end{pmatrix}, \quad \overset{c}{\mapsto} \omega^2\begin{pmatrix}\alpha_1\\ \alpha_2\end{pmatrix},
\end{aligned}
\tag{A.66}
$$

where the action of the generator d is not considered because it can be expressed in terms of a, b and c, as shown in Eq. (A.1). Starting from these set of transformations rules, we can build a set of terms which define a space of an irreducible representation. Henceforth all Clebsch-Gordan (CG) coefficients would be reported in the form of $\alpha \otimes \beta$. We shall use α_i

to denote the elements of first representation and β_i stands for the elements of the second representation of the tensor product. Moreover, we shall denote $f \equiv i + p \pmod 2$ and $g \equiv j + q \pmod 3$ for simplicity of notation.

- $\mathbf{1}_{i,j} \otimes \mathbf{1}_{p,q} = \mathbf{1}_{f,g}$

$$\mathbf{1}_{f,g} \sim \alpha\beta\,. \tag{A.67}$$

- $\mathbf{1}_{i,j} \otimes \mathbf{2}_{q} = \mathbf{2}_{g}$

$$i=0\ :\ \mathbf{2}_g \sim \begin{pmatrix} \alpha\beta_1 \\ \alpha\beta_2 \end{pmatrix}, \qquad i=1\ :\ \mathbf{2}_g \sim \begin{pmatrix} \alpha\beta_2 \\ -\alpha\beta_1 \end{pmatrix}. \tag{A.68}$$

- $\mathbf{1}_{i,j} \otimes \mathbf{3}_{l,p} = \mathbf{3}_{l+3nj,f}$

$$\mathbf{3}_{l+3nj,f} \sim \begin{pmatrix} \alpha\beta_1 \\ \alpha\beta_2 \\ \alpha\beta_3 \end{pmatrix}. \tag{A.69}$$

- $\mathbf{1}_{i,j} \otimes \mathbf{6}_{(l,k)} = \mathbf{6}_{(l+3nj,k)}$

$$\mathbf{6}_{(l+3nj,k)} \sim \begin{pmatrix} \alpha\beta_1 \\ \alpha\beta_2 \\ \alpha\beta_3 \\ (-1)^i\alpha\beta_4 \\ (-1)^i\alpha\beta_5 \\ (-1)^i\alpha\beta_6 \end{pmatrix}. \tag{A.70}$$

- $\mathbf{2}_{j} \otimes \mathbf{2}_{q} = \mathbf{1}_{0,g} \oplus \mathbf{1}_{1,g} \oplus \mathbf{2}_{g}$

$$\mathbf{1}_{0,g} \sim \alpha_1\beta_1 + \alpha_2\beta_2, \qquad \mathbf{1}_{1,g} \sim \alpha_1\beta_2 - \alpha_2\beta_1, \qquad \mathbf{2}_g \sim \begin{pmatrix} \alpha_1\beta_1 - \alpha_2\beta_2 \\ -\alpha_1\beta_2 - \alpha_2\beta_1 \end{pmatrix}. \tag{A.71}$$

- $\mathbf{2}_{j} \otimes \mathbf{3}_{l,i} = \mathbf{3}_{l+3nj,i} \oplus \mathbf{3}_{l+3nj,m}$, where $m = i + 1 \pmod 2$

$$\mathbf{3}_{l+3nj,i} \sim \begin{pmatrix} 2\alpha_1\beta_1 \\ -(\alpha_1 + \sqrt{3}\alpha_2)\beta_2 \\ (-\alpha_1 + \sqrt{3}\alpha_2)\beta_3 \end{pmatrix}, \qquad \mathbf{3}_{l+3nj,m} \sim \begin{pmatrix} 2\alpha_2\beta_1 \\ (\sqrt{3}\alpha_1 - \alpha_2)\beta_2 \\ -(\sqrt{3}\alpha_1 + \alpha_2)\beta_3 \end{pmatrix}. \tag{A.72}$$

- $\mathbf{2}_{j} \otimes \mathbf{6}_{(l,k)} = \mathbf{6}_{(l+3nj,k)} \oplus \mathbf{6}_{(l+3nj,k)}$

$$\mathbf{6}_{(l+3nj,k)} \sim \begin{pmatrix} 2\alpha_1\beta_1 \\ -(\alpha_1 + \sqrt{3}\alpha_2)\beta_2 \\ (-\alpha_1 + \sqrt{3}\alpha_2)\beta_3 \\ 2\alpha_1\beta_4 \\ (-\alpha_1 + \sqrt{3}\alpha_2)\beta_5 \\ -(\alpha_1 + \sqrt{3}\alpha_2)\beta_6 \end{pmatrix}, \qquad \mathbf{6}_{(l+3nj,k)} \sim \begin{pmatrix} 2\alpha_2\beta_1 \\ (\sqrt{3}\alpha_1 - \alpha_2)\beta_2 \\ -(\sqrt{3}\alpha_1 + \alpha_2)\beta_3 \\ -2\alpha_2\beta_4 \\ (\sqrt{3}\alpha_1 + \alpha_2)\beta_5 \\ -(\sqrt{3}\alpha_1 - \alpha_2)\beta_6 \end{pmatrix}. \tag{A.73}$$

- $\mathbf{3}_{l,i} \otimes \mathbf{3}_{l',p} = \mathbf{3}_{l+l',f} \oplus \mathbf{6}_{(l+l',l')}$

$$\mathbf{3}_{l+l',f} \sim \begin{pmatrix} \alpha_1\beta_1 \\ \alpha_2\beta_2 \\ \alpha_3\beta_3 \end{pmatrix}, \qquad \mathbf{6}_{(l+l',l')} \sim \begin{pmatrix} \alpha_1\beta_2 \\ \alpha_2\beta_3 \\ \alpha_3\beta_1 \\ (-1)^{i-p}\alpha_1\beta_3 \\ (-1)^{i-p}\alpha_3\beta_2 \\ (-1)^{i-p}\alpha_2\beta_1 \end{pmatrix}. \tag{A.74}$$

- $\mathbf{3}_{l,i} \otimes \mathbf{6}_{(l',k')} = \mathbf{6}_{(l+l',k')} \oplus \mathbf{6}_{(l+l'-3k',l'-2k')} \oplus \mathbf{6}_{(l-2l'+3k',k'-l')}$

$$\mathbf{6}_{(l+l',k')} \sim \begin{pmatrix} \alpha_1\beta_1 \\ \alpha_2\beta_2 \\ \alpha_3\beta_3 \\ (-1)^i\alpha_1\beta_4 \\ (-1)^i\alpha_3\beta_5 \\ (-1)^i\alpha_2\beta_6 \end{pmatrix}, \quad \mathbf{6}_{(l+l'-3k',l'-2k')} \sim \begin{pmatrix} \alpha_1\beta_2 \\ \alpha_2\beta_3 \\ \alpha_3\beta_1 \\ (-1)^i\alpha_1\beta_5 \\ (-1)^i\alpha_3\beta_6 \\ (-1)^i\alpha_2\beta_4 \end{pmatrix}, \quad \mathbf{6}_{(l-2l'+3k',k'-l')} \sim \begin{pmatrix} \alpha_1\beta_3 \\ \alpha_2\beta_1 \\ \alpha_3\beta_2 \\ (-1)^i\alpha_1\beta_6 \\ (-1)^i\alpha_3\beta_4 \\ (-1)^i\alpha_2\beta_5 \end{pmatrix}.$$

- $\mathbf{6}_{(l,k)} \otimes \mathbf{6}_{(l',k')} = \mathbf{6}_{(l+l',k+k')} \oplus \mathbf{6}_{(l+l'-3k',k-2k'+l')} \oplus \mathbf{6}_{(l-2l'+3k',k+k'-l')}$
$\oplus \mathbf{6}_{(l+l'-3k',k-k')} \oplus \mathbf{6}_{(l-2l'+3k',k+2k'-l')} \oplus \mathbf{6}_{(l+l',k-k'+l')}$

$$\mathbf{6}_{(l+l',k+k')} \sim \begin{pmatrix} \alpha_1\beta_1 \\ \alpha_2\beta_2 \\ \alpha_3\beta_3 \\ \alpha_4\beta_4 \\ \alpha_5\beta_5 \\ \alpha_6\beta_6 \end{pmatrix}, \qquad \mathbf{6}_{(l+l'-3k',k-2k'+l')} \sim \begin{pmatrix} \alpha_1\beta_2 \\ \alpha_2\beta_3 \\ \alpha_3\beta_1 \\ \alpha_4\beta_5 \\ \alpha_5\beta_6 \\ \alpha_6\beta_4 \end{pmatrix}, \quad \mathbf{6}_{(l-2l'+3k',k+k'-l')} \sim \begin{pmatrix} \alpha_1\beta_3 \\ \alpha_2\beta_1 \\ \alpha_3\beta_2 \\ \alpha_4\beta_6 \\ \alpha_5\beta_4 \\ \alpha_6\beta_5 \end{pmatrix},$$

$$\mathbf{6}_{(l+l'-3k',k-k')} \sim \begin{pmatrix} \alpha_1\beta_4 \\ \alpha_2\beta_6 \\ \alpha_3\beta_5 \\ \alpha_4\beta_1 \\ \alpha_5\beta_3 \\ \alpha_6\beta_2 \end{pmatrix}, \mathbf{6}_{(l-2l'+3k',k+2k'-l')} \sim \begin{pmatrix} \alpha_1\beta_5 \\ \alpha_2\beta_4 \\ \alpha_3\beta_6 \\ \alpha_4\beta_2 \\ \alpha_5\beta_1 \\ \alpha_6\beta_3 \end{pmatrix}, \mathbf{6}_{(l+l',k-k'+l')} \sim \begin{pmatrix} \alpha_1\beta_6 \\ \alpha_2\beta_5 \\ \alpha_3\beta_4 \\ \alpha_4\beta_3 \\ \alpha_5\beta_2 \\ \alpha_6\beta_1 \end{pmatrix}. \tag{A.75}$$

We would like to point out that certain three-dimensional and six-dimensional representations in the above tensor product decompositions may be reducible, and accordingly it should be reduced into smaller irreducible representations of the $D^{(1)}_{9n,3n}$ group. The reducible conditions and corresponding reduction formulae are summarized in table 14.

References

[1] K. Abe *et al.* [T2K Collaboration], Phys. Rev. Lett. **107**, 041801 (2011) doi:10.1103/PhysRevLett.107.041801 [arXiv:1106.2822 [hep-ex]].

[2] P. Adamson *et al.* [MINOS Collaboration], Phys. Rev. Lett. **107**, 181802 (2011) doi:10.1103/PhysRevLett.107.181802 [arXiv:1108.0015 [hep-ex]].

[3] Y. Abe *et al.* [Double Chooz Collaboration], Phys. Rev. Lett. **108**, 131801 (2012) doi:10.1103/PhysRevLett.108.131801 [arXiv:1112.6353 [hep-ex]]; Phys. Rev. D **86**, 052008 (2012) doi:10.1103/PhysRevD.86.052008 [arXiv:1207.6632 [hep-ex]].

	$l \pmod{9n} = 3n\lambda,\ \lambda = 0,1,2$		
	$\mathbf{3}_{l,i} \cong \mathbf{1}_{i,\lambda} \oplus \mathbf{2}_\lambda$		
$\mathbf{3}_{l,i} \sim \begin{pmatrix}\gamma_1\\ \gamma_2\\ \gamma_3\end{pmatrix}$	$\mathbf{1}_{i,\lambda} \sim \gamma_1+\gamma_2+\gamma_3$ $\mathbf{2}_\lambda \sim \begin{pmatrix}-2\gamma_1+\gamma_2+\gamma_3\\ \sqrt{3}\gamma_2-\sqrt{3}\gamma_3\end{pmatrix}$, for $i=0$ $\mathbf{2}_\lambda \sim \begin{pmatrix}\sqrt{3}\gamma_2-\sqrt{3}\gamma_3\\ 2\gamma_1-\gamma_2-\gamma_3\end{pmatrix}$, for $i=1$		
	$\begin{cases}3k=0 \pmod{9n}\\ l\neq 0 \pmod{3n}\end{cases}$	$\begin{cases}3l-3k=0 \pmod{9n}\\ l\neq 0 \pmod{3n}\end{cases}$	$\begin{cases}3l-6k=0 \pmod{9n}\\ l,k\neq 0 \pmod{3n}\end{cases}$
	$\mathbf{6}_{(l,k)} \cong \mathbf{3}_{l,0} \oplus \mathbf{3}_{l,1}$	$\mathbf{6}_{(l,k)} \cong \mathbf{3}_{l,0} \oplus \mathbf{3}_{l,1}$	$\mathbf{6}_{(l,k)} \cong \mathbf{3}_{l-3k,0} \oplus \mathbf{3}_{l-3k,1}$
$\mathbf{6}_{(l,k)} \sim \begin{pmatrix}\gamma_1\\ \gamma_2\\ \gamma_3\\ \gamma_4\\ \gamma_5\\ \gamma_6\end{pmatrix}$	$\mathbf{3}_{l,0} \sim \begin{pmatrix}\gamma_1+\gamma_4\\ \gamma_2+\gamma_6\\ \gamma_3+\gamma_5\end{pmatrix}$ $\mathbf{3}_{l,1} \sim \begin{pmatrix}\gamma_1-\gamma_4\\ \gamma_2-\gamma_6\\ \gamma_3-\gamma_5\end{pmatrix}$	$\mathbf{3}_{l,0} \sim \begin{pmatrix}\gamma_3+\gamma_6\\ \gamma_1+\gamma_5\\ \gamma_2+\gamma_4\end{pmatrix}$ $\mathbf{3}_{l,1} \sim \begin{pmatrix}\gamma_3-\gamma_6\\ \gamma_1-\gamma_5\\ \gamma_2-\gamma_4\end{pmatrix}$	$\mathbf{3}_{l-3k,0} \sim \begin{pmatrix}\gamma_2+\gamma_5\\ \gamma_3+\gamma_4\\ \gamma_1+\gamma_6\end{pmatrix}$ $\mathbf{3}_{l-3k,1} \sim \begin{pmatrix}\gamma_2-\gamma_5\\ \gamma_3-\gamma_4\\ \gamma_1-\gamma_6\end{pmatrix}$
	$k \pmod{3n} = 0,\quad l \pmod{9n} = 3n\lambda,\ \lambda = 0,1,2$		
	$\mathbf{6}_{(l,k)} \cong \mathbf{1}_{0,\lambda} \oplus \mathbf{1}_{1,\lambda} \oplus \mathbf{2}_\lambda \oplus \mathbf{2}_\lambda$		
$\mathbf{6}_{(l,k)} \sim \begin{pmatrix}\gamma_1\\ \gamma_2\\ \gamma_3\\ \gamma_4\\ \gamma_5\\ \gamma_6\end{pmatrix}$	$\mathbf{1}_{0,\lambda} \sim \gamma_1+\gamma_2+\gamma_3+\gamma_4+\gamma_5+\gamma_6$, $\mathbf{1}_{1,\lambda} \sim \gamma_1+\gamma_2+\gamma_3-\gamma_4-\gamma_5-\gamma_6$, $\mathbf{2}_\lambda \sim \begin{pmatrix}-2\gamma_1+\gamma_2+\gamma_3-2\gamma_4+\gamma_5+\gamma_6\\ \sqrt{3}\,(\gamma_2-\gamma_3-\gamma_5+\gamma_6)\end{pmatrix}$, $\mathbf{2}_\lambda \sim \begin{pmatrix}\sqrt{3}\,(\gamma_2-\gamma_3+\gamma_5-\gamma_6)\\ 2\gamma_1-\gamma_2-\gamma_3-2\gamma_4+\gamma_5+\gamma_6\end{pmatrix}$		

Table 14: The reducible conditions for $\mathbf{3}_{l,0}$, $\mathbf{3}_{l,1}$ and $\mathbf{6}_{(l,k)}$, and the decomposition of reducible three-dimensional and six-dimensional representations into smaller irreducible representations of $D^{(1)}_{9n,3n}$. Notice that the expression for the doublet vector $\mathbf{2}_\lambda$ is not unique in the decomposition of $\mathbf{6}_{(3n\lambda,0)} \cong \mathbf{1}_{0,\lambda} \oplus \mathbf{1}_{1,\lambda} \oplus \mathbf{2}_\lambda \oplus \mathbf{2}_\lambda$.

[4] F. P. An *et al.* [Daya Bay Collaboration], Phys. Rev. Lett. **108**, 171803 (2012) doi:10.1103/PhysRevLett.108.171803 [arXiv:1203.1669 [hep-ex]]; Chin. Phys. C **37**, 011001 (2013) doi:10.1088/1674-1137/37/1/011001 [arXiv:1210.6327 [hep-ex]].

[5] J. K. Ahn *et al.* [RENO Collaboration], Phys. Rev. Lett. **108**, 191802 (2012) doi:10.1103/PhysRevLett.108.191802 [arXiv:1204.0626 [hep-ex]].

[6] K. Abe *et al.* [T2K Collaboration], Phys. Rev. D **91**, no. 7, 072010 (2015) doi:10.1103/PhysRevD.91.072010 [arXiv:1502.01550 [hep-ex]].

[7] F. Capozzi, G. L. Fogli, E. Lisi, A. Marrone, D. Montanino and A. Palazzo, Phys. Rev. D **89**, 093018 (2014) doi:10.1103/PhysRevD.89.093018 [arXiv:1312.2878 [hep-ph]].

[8] D. V. Forero, M. Tortola and J. W. F. Valle, Phys. Rev. D **90**, no. 9, 093006 (2014) doi:10.1103/PhysRevD.90.093006 [arXiv:1405.7540 [hep-ph]].

[9] M. C. Gonzalez-Garcia, M. Maltoni and T. Schwetz, JHEP **1411**, 052 (2014) doi:10.1007/JHEP11(2014)052 [arXiv:1409.5439 [hep-ph]].

[10] G. Altarelli and F. Feruglio, Rev. Mod. Phys. **82**, 2701 (2010) doi:10.1103/RevModPhys.82.2701 [arXiv:1002.0211 [hep-ph]].

[11] H. Ishimori, T. Kobayashi, H. Ohki, Y. Shimizu, H. Okada and M. Tanimoto, Prog. Theor. Phys. Suppl. **183**, 1 (2010) doi:10.1143/PTPS.183.1 [arXiv:1003.3552 [hep-th]].

[12] S. F. King and C. Luhn, Rept. Prog. Phys. **76**, 056201 (2013) doi:10.1088/0034-4885/76/5/056201 [arXiv:1301.1340 [hep-ph]]; S. F. King, A. Merle, S. Morisi, Y. Shimizu and M. Tanimoto, New J. Phys. **16**, 045018 (2014) doi:10.1088/1367-2630/16/4/045018 [arXiv:1402.4271 [hep-ph]]; S. F. King, J. Phys. G **42**, 123001 (2015) doi:10.1088/0954-3899/42/12/123001 [arXiv:1510.02091 [hep-ph]].

[13] R. M. Fonseca and W. Grimus, JHEP **1409**, 033 (2014) doi:10.1007/JHEP09(2014)033 [arXiv:1405.3678 [hep-ph]].

[14] C. Y. Yao and G. J. Ding, Phys. Rev. D **92**, no. 9, 096010 (2015) doi:10.1103/PhysRevD.92.096010 [arXiv:1505.03798 [hep-ph]].

[15] P. Chen, C. C. Li and G. J. Ding, Phys. Rev. D **91**, 033003 (2015) doi:10.1103/PhysRevD.91.033003 [arXiv:1412.8352 [hep-ph]].

[16] P. Chen, C. Y. Yao and G. J. Ding, Phys. Rev. D **92**, no. 7, 073002 (2015) doi:10.1103/PhysRevD.92.073002 [arXiv:1507.03419 [hep-ph]].

[17] L. L. Everett, T. Garon and A. J. Stuart, JHEP **1504**, 069 (2015) doi:10.1007/JHEP04(2015)069 [arXiv:1501.04336 [hep-ph]].

[18] P. F. Harrison and W. G. Scott, Phys. Lett. B **535**, 163 (2002) doi:10.1016/S0370-2693(02)01753-7 [hep-ph/0203209]; P. F. Harrison and W. G. Scott, Phys. Lett. B **547**, 219 (2002) doi:10.1016/S0370-2693(02)02772-7 [hep-ph/0210197]; P. F. Harrison and W. G. Scott, Phys. Lett. B **594**, 324 (2004) doi:10.1016/j.physletb.2004.05.039 [hep-ph/0403278].

[19] W. Grimus and L. Lavoura, Phys. Lett. B **579**, 113 (2004) doi:10.1016/j.physletb.2003.10.075 [hep-ph/0305309]; W. Grimus and L. Lavoura, Fortsch. Phys. **61**, 535 (2013) doi:10.1002/prop.201200118 [arXiv:1207.1678 [hep-ph]].

[20] Y. Farzan and A. Y. Smirnov, JHEP **0701**, 059 (2007) doi:10.1088/1126-6708/2007/01/059 [hep-ph/0610337].

[21] P. Chen, G. J. Ding, F. Gonzalez-Canales and J. W. F. Valle, arXiv:1512.01551 [hep-ph].

[22] F. Feruglio, C. Hagedorn and R. Ziegler, JHEP **1307**, 027 (2013) doi:10.1007/JHEP07(2013)027 [arXiv:1211.5560 [hep-ph]].

[23] M. Holthausen, M. Lindner and M. A. Schmidt, JHEP **1304**, 122 (2013) doi:10.1007/JHEP04(2013)122 [arXiv:1211.6953 [hep-ph]].

[24] G. Ecker, W. Grimus and W. Konetschny, Nucl. Phys. B **191**, 465 (1981) doi:10.1016/0550-3213(81)90309-6; G. Ecker, W. Grimus and H. Neufeld, Nucl. Phys. B **247**, 70 (1984) doi:10.1016/0550-3213(84)90373-0; J. Bernabeu, G. C. Branco and M. Gronau, Phys. Lett. B **169**, 243 (1986) doi:10.1016/0370-2693(86)90659-3; G. Ecker, W. Grimus and H. Neufeld, J. Phys. A **20**, L807 (1987) doi:10.1088/0305-4470/20/12/010; H. Neufeld, W. Grimus and G. Ecker, Int. J. Mod. Phys. A **3**, 603 (1988) doi:10.1142/S0217751X88000254.

[25] W. Grimus and M. N. Rebelo, Phys. Rept. **281**, 239 (1997) doi:10.1016/S0370-1573(96)00030-0 [hep-ph/9506272].

[26] M. C. Chen, M. Fallbacher, K. T. Mahanthappa, M. Ratz and A. Trautner, Nucl. Phys. B **883**, 267 (2014) doi:10.1016/j.nuclphysb.2014.03.023 [arXiv:1402.0507 [hep-ph]].

[27] G. J. Ding, S. F. King and A. J. Stuart, JHEP **1312**, 006 (2013) doi:10.1007/JHEP12(2013)006 [arXiv:1307.4212 [hep-ph]].

[28] G. J. Ding, S. F. King, C. Luhn and A. J. Stuart, JHEP **1305**, 084 (2013) doi:10.1007/JHEP05(2013)084 [arXiv:1303.6180 [hep-ph]].

[29] F. Feruglio, C. Hagedorn and R. Ziegler, Eur. Phys. J. C **74**, 2753 (2014) doi:10.1140/epjc/s10052-014-2753-2 [arXiv:1303.7178 [hep-ph]].

[30] C. Luhn, Nucl. Phys. B **875**, 80 (2013) doi:10.1016/j.nuclphysb.2013.07.003 [arXiv:1306.2358 [hep-ph]].

[31] C. C. Li and G. J. Ding, Nucl. Phys. B **881**, 206 (2014) doi:10.1016/j.nuclphysb.2014.02.002 [arXiv:1312.4401 [hep-ph]].

[32] C. C. Li and G. J. Ding, JHEP **1508**, 017 (2015) doi:10.1007/JHEP08(2015)017 [arXiv:1408.0785 [hep-ph]].

[33] G. C. Branco, I. de Medeiros Varzielas and S. F. King, Nucl. Phys. B **899**, 14 (2015) doi:10.1016/j.nuclphysb.2015.07.024 [arXiv:1505.06165 [hep-ph]]; G. C. Branco, I. de Medeiros Varzielas and S. F. King, Phys. Rev. D **92**, no. 3, 036007 (2015) doi:10.1103/PhysRevD.92.036007 [arXiv:1502.03105 [hep-ph]].

[34] G. J. Ding and Y. L. Zhou, Chin. Phys. C **39**, no. 2, 021001 (2015) doi:10.1088/1674-1137/39/2/021001 [arXiv:1312.5222 [hep-ph]]; G. J. Ding and Y. L. Zhou, JHEP **1406**, 023 (2014) doi:10.1007/JHEP06(2014)023 [arXiv:1404.0592 [hep-ph]].

[35] C. C. Li and G. J. Ding, JHEP **1505**, 100 (2015) doi:10.1007/JHEP05(2015)100 [arXiv:1503.03711 [hep-ph]].

[36] A. Di Iura, C. Hagedorn and D. Meloni, JHEP **1508**, 037 (2015) doi:10.1007/JHEP08(2015)037 [arXiv:1503.04140 [hep-ph]].

[37] P. Ballett, S. Pascoli and J. Turner, Phys. Rev. D **92**, no. 9, 093008 (2015) doi:10.1103/PhysRevD.92.093008 [arXiv:1503.07543 [hep-ph]].

[38] G. J. Ding and S. F. King, Phys. Rev. D **89**, no. 9, 093020 (2014) doi:10.1103/PhysRevD.89.093020 [arXiv:1403.5846 [hep-ph]].

[39] C. Hagedorn, A. Meroni and E. Molinaro, Nucl. Phys. B **891**, 499 (2015) doi:10.1016/j.nuclphysb.2014.12.013 [arXiv:1408.7118 [hep-ph]].

[40] G. J. Ding and S. F. King, arXiv:1510.03188 [hep-ph].

[41] G. J. Ding, S. F. King and T. Neder, JHEP **1412**, 007 (2014) doi:10.1007/JHEP12(2014)007 [arXiv:1409.8005 [hep-ph]].

[42] S. F. King and T. Neder, Phys. Lett. B **736**, 308 (2014) doi:10.1016/j.physletb.2014.07.043 [arXiv:1403.1758 [hep-ph]].

[43] G.A. Miller, H.F. Blichfeldt and L.E. Dickson, *Theory and applications of finite groups* (John Wiley & Sons, New York, 1916).

[44] W. Grimus and P. O. Ludl, J. Phys. A **43**, 445209 (2010) doi:10.1088/1751-8113/43/44/445209 [arXiv:1006.0098 [hep-ph]].

[45] W. Grimus and P. O. Ludl, J. Phys. A **47**, no. 7, 075202 (2014) doi:10.1088/1751-8113/47/7/075202 [arXiv:1310.3746 [math-ph]].

[46] W. Grimus and P. O. Ludl, J. Phys. A **45**, 233001 (2012) doi:10.1088/1751-8113/45/23/233001 [arXiv:1110.6376 [hep-ph]].

[47] S. F. King, T. Neder and A. J. Stuart, Phys. Lett. B **726**, 312 (2013) doi:10.1016/j.physletb.2013.08.052 [arXiv:1305.3200 [hep-ph]].

[48] J. A. Escobar and C. Luhn, J. Math. Phys. **50**, 013524 (2009) doi:10.1063/1.3046563 [arXiv:0809.0639 [hep-th]].

[49] The GAP Group, *GAP – Groups, Algorithms, and Programming, Version 4.4.12*, 2008. `http://www.gap-system.org`.

[50] C. S. Lam, Phys. Lett. B **656**, 193 (2007) doi:10.1016/j.physletb.2007.09.032 [arXiv:0708.3665 [hep-ph]].

[51] G. Altarelli, F. Feruglio and L. Merlo, JHEP **0905**, 020 (2009) doi:10.1088/1126-6708/2009/05/020 [arXiv:0903.1940 [hep-ph]].

[52] K. A. Olive *et al.* [Particle Data Group Collaboration], Chin. Phys. C **38**, 090001 (2014). doi:10.1088/1674-1137/38/9/090001

[53] F. An *et al.* [JUNO Collaboration], arXiv:1507.05613 [physics.ins-det].

[54] S. B. Kim, Nucl. Part. Phys. Proc. **265-266**, 93 (2015) doi:10.1016/j.nuclphysbps.2015.06.024 [arXiv:1412.2199 [hep-ex]].

[55] C. Adams *et al.* [LBNE Collaboration], arXiv:1307.7335 [hep-ex]; M. Bass *et al.* [LBNE Collaboration], Phys. Rev. D **91**, no. 5, 052015 (2015) doi:10.1103/PhysRevD.91.052015 [arXiv:1311.0212 [hep-ex]].

[56] S. K. Agarwalla *et al.* [LAGUNA-LBNO Collaboration], JHEP **1405**, 094 (2014) doi:10.1007/JHEP05(2014)094 [arXiv:1312.6520 [hep-ph]]; L. Agostino *et al.*, arXiv:1409.4405 [physics.ins-det]; S. K. Agarwalla *et al.* [LAGUNA-LBNO Collaboration], arXiv:1412.0593 [hep-ph]; S. K. Agarwalla *et al.* [LAGUNA-LBNO Collaboration], arXiv:1412.0804 [hep-ph].

[57] E. Kearns *et al.* [Hyper-Kamiokande Working Group Collaboration], arXiv:1309.0184 [hep-ex].

[58] E. Baussan, M. Dracos, T. Ekelof, E. F. Martinez, H. Ohman and N. Vassilopoulos, arXiv:1212.5048 [hep-ex]; E. Baussan *et al.* [ESSnuSB Collaboration], Nucl. Phys. B **885**, 127 (2014) doi:10.1016/j.nuclphysb.2014.05.016 [arXiv:1309.7022 [hep-ex]].

[59] S. Geer, Phys. Rev. D **57**, 6989 (1998) [Phys. Rev. D **59**, 039903 (1999)] doi:10.1103/PhysRevD.57.6989, 10.1103/PhysRevD.59.039903 [hep-ph/9712290]; A. De Rujula, M. B. Gavela and P. Hernandez, Nucl. Phys. B **547**, 21 (1999) doi:10.1016/S0550-3213(99)00070-X [hep-ph/9811390]; A. Bandyopadhyay *et al.* [ISS Physics Working Group Collaboration], Rept. Prog. Phys. **72**, 106201 (2009) doi:10.1088/0034-4885/72/10/106201 [arXiv:0710.4947 [hep-ph]].

[60] M. Agostini *et al.* [GERDA Collaboration], Phys. Rev. Lett. **111**, no. 12, 122503 (2013) doi:10.1103/PhysRevLett.111.122503 [arXiv:1307.4720 [nucl-ex]].

[61] M. Auger *et al.* [EXO-200 Collaboration], Phys. Rev. Lett. **109**, 032505 (2012) doi:10.1103/PhysRevLett.109.032505 [arXiv:1205.5608 [hep-ex]].

[62] J. B. Albert *et al.* [EXO-200 Collaboration], Nature **510**, 229 (2014) doi:10.1038/nature13432 [arXiv:1402.6956 [nucl-ex]].

[63] A. Gando *et al.* [KamLAND-Zen Collaboration], Phys. Rev. Lett. **110**, no. 6, 062502 (2013) doi:10.1103/PhysRevLett.110.062502 [arXiv:1211.3863 [hep-ex]].

[64] F. Piquemal, Nucl. Phys. Proc. Suppl. **235-236**, 273 (2013). doi:10.1016/j.nuclphysbps.2013.04.022

[65] P. A. R. Ade *et al.* [Planck Collaboration], Astron. Astrophys. **571**, A16 (2014) doi:10.1051/0004-6361/201321591 [arXiv:1303.5076 [astro-ph.CO]].

[66] M. Yoshimura, Phys. Rev. D **75**, 113007 (2007) doi:10.1103/PhysRevD.75.113007 [hep-ph/0611362].

[67] G. W. Mackey, Amer. J. Math. **73**, 576 (1951); G. W. Mackey, Acta Math. **99**, 265 (1958); L. Corwing, Proc. Amer. Math. Soc. **47**, 279 (1975);

[68] B. Simon, *Representations of finite and compact groups*, (American Mathematical Soc., 1996).

[69] J. -P. Serre, *Linear representations of finite groups*, (Springer Science & Business Media, 2012).